1941

Report of crane girder tests, Iron and Steel Engineer, Vol.18 (1941), p. 47, Reprint No. 54 (41-2)

I. E. Madsen

Report of

CRANE GIRDER TESTS

Report of CRANE GIRDER TESTS

By J. Madsen

Assistant Research Engineer
Fritz Engineering Laboratories
LEHIGH UNIVERSITY
BETHLEHEM, PENNSYLVANIA

REPRINTED FROM NOVEMBER, 1941, IRON AND STEEL ENGINEER

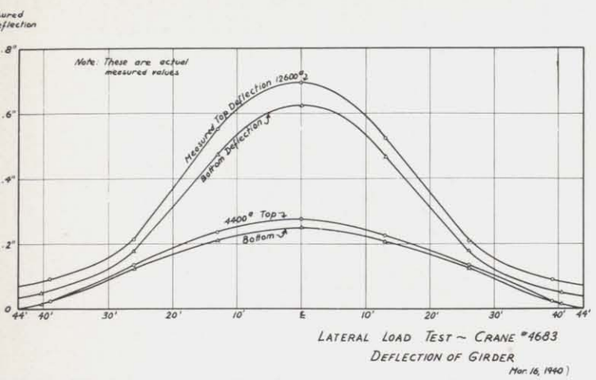

Figure 2

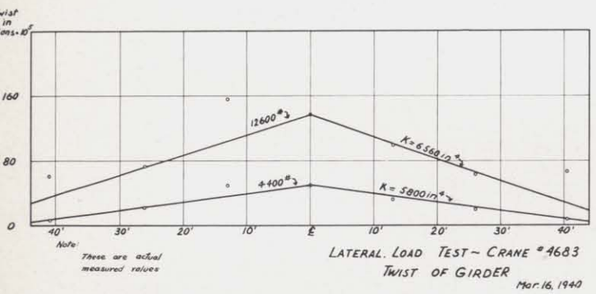

Figure 3

▲

Figure 4

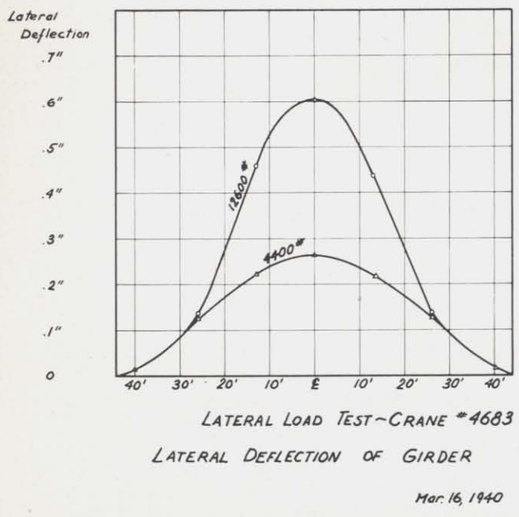

between these two readings gives the strain in the member due to the applied load. The results are generally accurate to plus or minus 300 lb. per sq. in.

The lateral deflection of the girders was found by measuring the change in distance between the adjacent flanges of the two girders. This was done on the top and bottom flanges at seven sections using a 0.001 in. Federal dial. The difference between the readings of the zero load and final load gave the total movement of both flanges. The difference between the lateral deflection of the top flange and bottom flange at the same section divided by the distance between the flange reading points gave the twist of the girder at that section in radian units. Since the twist curves are computed from the difference of measured differences, the plotted points for the twist curves show some scatter. Knowing the twist, one can determine the average lateral deflection of the girder.

The load was applied by tightening a turnbuckle fastened to the two girders. A calibrated spring was interposed in the system and its closure was measured by 0.001 in. Ames dials. The closure was a measure of the actual load. This loading simulated the manner in which the braking and accelerating forces load an actual crane, except that in the actual crane both girders are deflected in the same direction, and in the mill tests the girders were bent in opposite directions.

TEST RESULTS

Crane No. 4683—The deflections as measured were the combined deflections of both girders. In Figure 2 are plotted the average deflection of each girder or the total measured deflection divided by 2. These deflections are plotted along the length of the girder and the center line mark denotes the center of the girder span. It should be noted that the deflection at the end tie is not zero for the 12,600 lb. load but is about 0.07 in. at the top flange and 0.035 in. for the bottom flange due to slip in the end connection.

The measured twist of the girder is shown in Figure 3. Some initial slip is also present. The torsional constants K, as computed from the curves, are marked on the corresponding curves. They are fairly close to the theoretical value of 6300 in.^{4}, as computed from Bredt's theory.*

The lateral deflection corrected for the initial slip noted in Figure 2, and also for the twist shown in Figure 3, is plotted in Figure 4. The slip correction was made by adding or subtracting a value to the measured deflection of the top flange so that the deflection of the end would be zero. This was also done for the bottom flange. These corrections were only a small percentage of the total deflection and are made because the elastic twist and deflections at the ends of the girder are zero. The curves for the different loads have a somewhat different type of curvature due to the greater end fixity of the girders when the 12,600 lb. load was on the girder.

The stresses were measured on the idler girder. Readings were taken on seven sections along the girder. At each section a number of readings were taken. On the top cover plate, readings were taken at the edge and 5 in. from the edge. They were also taken at the center line of the web and at distances 10 and 20 in. above and below the center line. Readings were also taken on the bottom flange angle 1 in. in from the edge of the angle.

Figure 5 shows the stress distribution at the center section and also shows the location of the gauge lines. The stress is plotted from the adjacent side of the box section as an origin.

In Figure 6 is shown the variation of the stress along the girder on the inside and outside edges of the top cover plate. The corresponding stresses along the bottom flange are shown in Figure 7. They are seen to be quite similar. The theoretical stresses shown are computed on the basis that the whole girder section resists lateral load. The fact that the measured stress closely approximates the theoretical stress shows that the girder acts very nearly as a unit under the action of the lateral load. At the center of the span it will be noted that the measured stresses on the top flange are a little larger than the theoretical, whereas on the bottom flange they are a little smaller. This is probably due to secondary torsional stresses at the center of the crane. Since the direction of twist reverses at the bridge center there can be no warping due to twist at this section. It is not likely that the stress variation is due to the top flange taking an appreciably greater proportion of the lateral load than the bottom flange, because the difference between the deflections of the top and bottom flanges (corrected for slip) is a smaller percentage than the measured variation in stresses. This is further substantiated by the fact that except at the center, the measured stress values lie very close to the theoretical values.

Figure 8 shows the variation in the average web stress along the girder. It should be remembered that the stresses in these tests are measured only on the outside of the girders since it is impossible to get inside the girder. Therefore the measured stresses represent the average stress of the members only when they are fairly straight in comparison with their thickness. This is substantially true for flange members, but not neces-

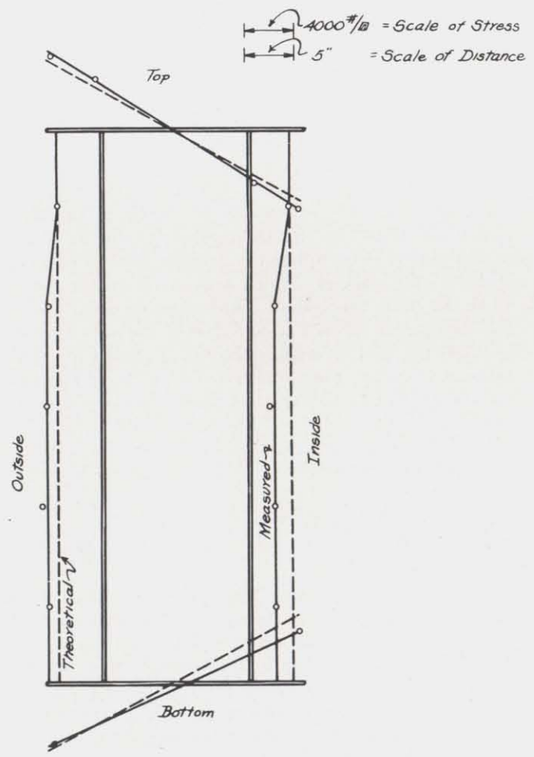

Figure 5

LATERAL LOAD TEST ~ CRANE #4683
STRESS DISTRIBUTION AT CENTER OF GIRDER
March 16, 1940

▲

Figure 6

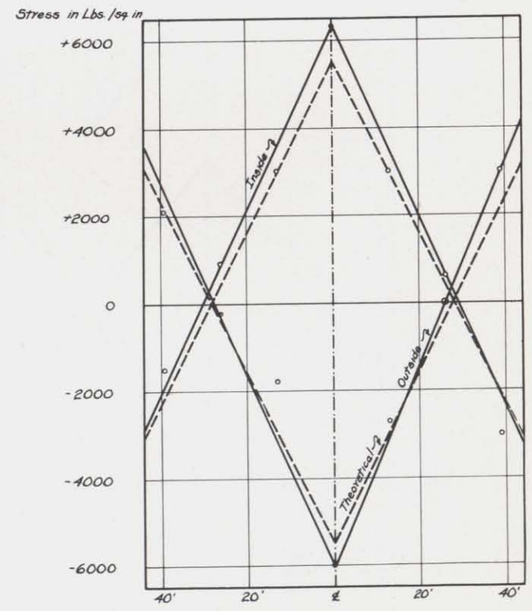

LATERAL LOAD TEST
CRANE #4683
TOP COVERPLATE STRESSES
Mar. 14, 1940

*Rudolph Bredt. *Kritische Bemerkungen zur Drehungselastizitat Zeitschrift des Vereines deutscher Ingenieure*, July 1896, p. 785.

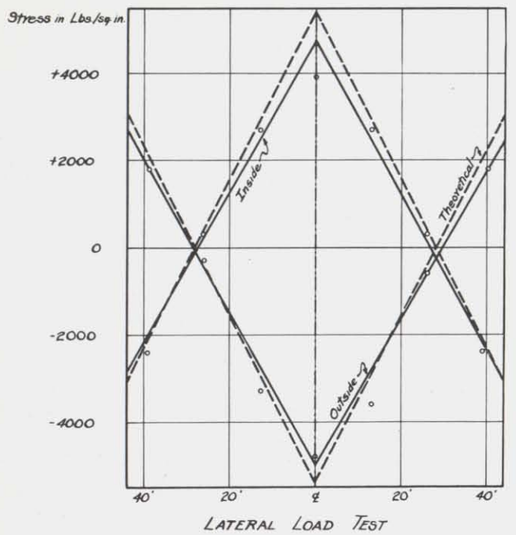

LATERAL LOAD TEST
CRANE #4683
BOTTOM FLANGE STRESSES

March 16, 1940

Figure 7

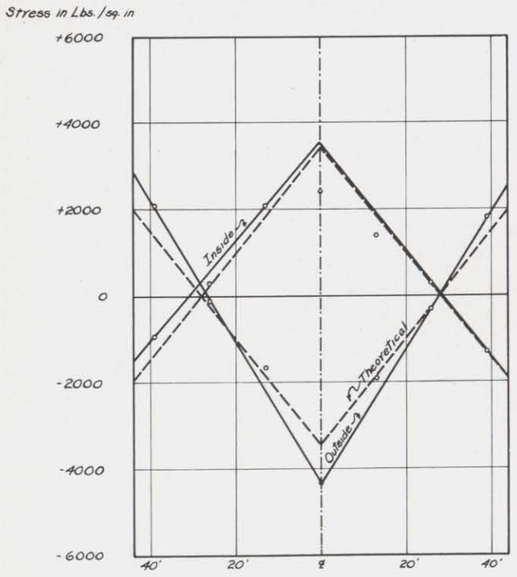

LATERAL LOAD TEST
CRANE #4683
WEB STRESSES

Mar. 16, 1940

Figure 8

sarily true for web members; therefore the measured stress curves for the webs may not give the average stress, particularly when the web is thin.

In the stress curves for this crane the point of zero stress is seen to be at an average distance of 16 ft. from the ends of the girder. A point of contraflexure shows that some fixity is present. In this case the location of the point of zero stress corresponds to a partial fixity of 73 per cent. The statement 73 per cent partial fixity means that the moment at the end of the girder is 73 per cent of that which would be present if the girder were acting as a fully fixed beam.

The slip which occurred in the joint reduced the fixity. In addition, it is impossible to get 100 per cent fixity, since the elastic deflection due to the stress in the end carriage reduces the maximum possible end fixity to a value below 100 per cent. The fixity of the two girders varies due to the stiffening effect of the walkway. The 73 per cent fixity factor given above applies to both girders normally only when they have the same lateral moments of inertia. However, the stiffness factor of the end tie (moment of inertia divided by the length) is enough larger than that of the bridge girders so that there is no great difference between the points of contraflexure of the bridge girders. Therefore the 73 per cent fixity factor is a fair approximation. It should be remembered that no attempt is usually made to compute or allow for end fixity in design, in which case the end fixity is usually an added factor of safety. The theoretical stresses shown in the diagrams were computed using an end fixity of 73 per cent and a value of 4850 in.^{4} for the gross horizontal moment of inertia. The check is seen to be very close.

As an additional check the deflection was computed using 4850 in.^{4} for the moment of inertia of the idler girder and 17,540 in.^{4} for the moment of inertia of the motor girder. The difference between the two values is due to the walkway which was on the motor girder when the crane was tested. The computed deflection of the idler girder is 0.972 in. and that of the motor girder is 0.268 in. The average deflection is 0.620 in. The measured average lateral deflection as shown in Figure 4 is 0.605 in., and provides a good check. As stated before, the partial fixity factor of 73 per cent could be used for both girders only because they had approximately the same point of contraflexure. The influence of the walkway upon the lateral deflection of the motor girder should be noted as it reduces the deflection of this girder to 0.275 times the value it would have had, were the walkway not there.

No stress readings were taken at the 4400 lb. load but the deflections were measured. The deflection of 0.262 in. corresponds to a partial fixity of 60 per cent. The fixity at the higher load is greater than at the lower load. This is probably due to the fact that at the higher load, enough deformation had occurred to increase the number of bolts in bearing in the end tie, thus increasing the restraint.

It should be remembered that the design lateral load is about 1900 lb. However, this load in the test would have resulted in stresses too low to measure. The fixity will vary somewhat with the load. At very low loads the friction of the bolts carries the moment. As the load increases, there is a slip which reduces the fixity but as the bolts start to bear, the fixity increases. This is shown by the increase in end fixity between the 4400 lb. and 12,600 lb. loads. The section acting to resist the lateral load does not vary with the load.

The theoretical deflections were computed by the following formula:

$$d=\frac{wl^3}{48EI}-\frac{Ml^2}{8EI}$$

M is the end moment as found from the measured stresses, w is the center load, l is the span length, I is the moment of inertia, and E is the modulus of elasticity.

The twist was computed by the formula:

$$\Theta=\frac{M_t l}{GK}$$

where Θ is the total angle of twist, G is the shear modulus, and K is the torsional constant. The torsion constant as computed from Bredt's formula is equal to the relation:

$$K=\frac{4A^2}{\int\frac{ds}{t}}$$

which, for a box section gives:

$$K=\frac{2b^2d^2t\,t_1}{bt_1+dt}$$

where b and d are the width and depth respectively, t_1 equals the web thickness, and t is the average of the top and bottom flange thicknesses. In this crane, the torsional stiffness factors of both girders are practically alike, since, although the walkway changes the lateral moment of inertia markedly, it changes the torsion constant less than 1 per cent.

The results of the tests on riveted crane No. 4683 can be summarized as follows:

1. The whole section of the girder resisted the lateral moment.

2. Partial end fixity due to slip was present between the bridge girder and end tie. Its value varied from 60 to 73 per cent as the load varied.

3. The twist of this riveted girder could be computed by Bredt's theory showing that there was no appreciable rivet slip to reduce the torsional rigidity. It should be noticed that the shearing stress due to torsion was only about 300 lb. per sq. in.

4. Secondary direct stresses due to torsion were present at the center of the girder. They were of small magnitude.

5. The walkway along the motor girder reduced the lateral deflection of this girder 75 per cent as compared with the deflection of the idler girder. Its effectiveness may be due to the fact that it was fastened to the web for its whole length and thus acted integrally as a stiffener on the girder.

Crane No. 8441—The tests on welded crane No. 8441 were similar to those on No. 4683 and the discussion in this section will be devoted primarily to those points which differ from crane No. 4683.

Crane No. 8441 (see Figure 9) had no walkways on it during the tests. The girders were first tested with no gusset plates between the end tie and bridge girder and the lateral deflection curves are shown in Figure 10. Similar curves for the tests in which gusset plates were used are shown in Figure 11. The deflection of the girder with the gusset plates is less than the girder

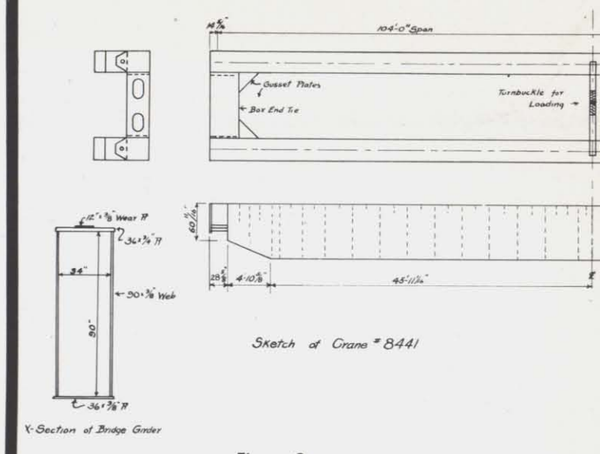

Sketch of Crane #8441

Y-Section at Bridge Girder

Figure 9

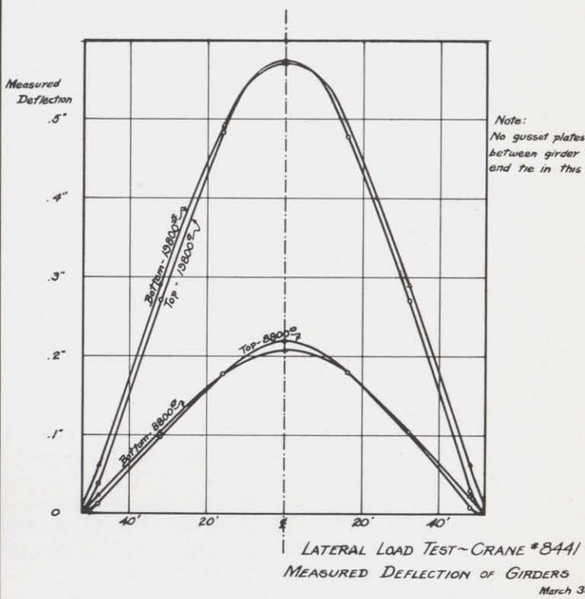

LATERAL LOAD TEST ~ CRANE #8441
MEASURED DEFLECTION OF GIRDERS

March 3

Figure 10

▲

Figure 11

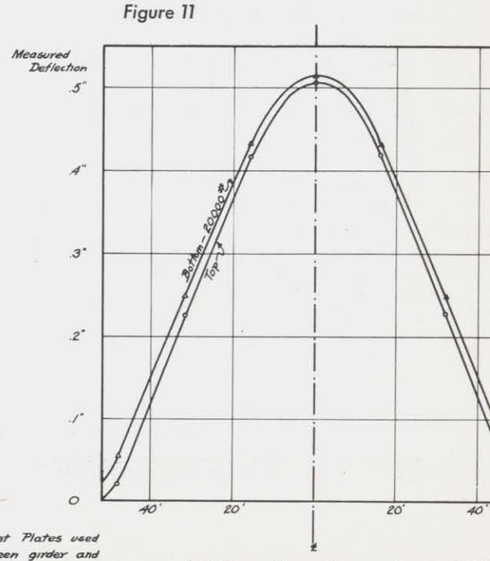

Note: Gusset Plates used between girder and end tie in this test.

LATERAL LOAD TEST ~ CRANE #84
MEASURED DEFLECTION OF GIRDERS

April

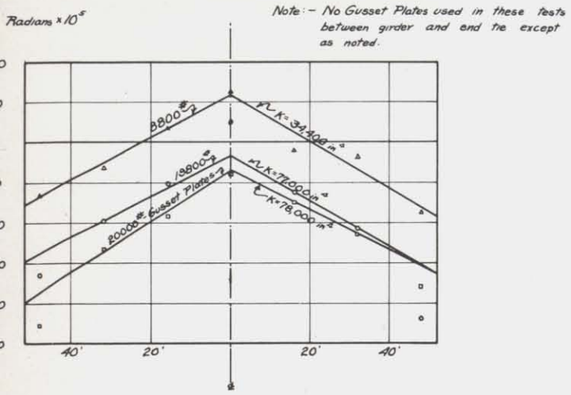

LATERAL LOAD TEST ~ CRANE #8441
MEASURED TWIST OF GIRDERS

March 30, 1940

Figure 12

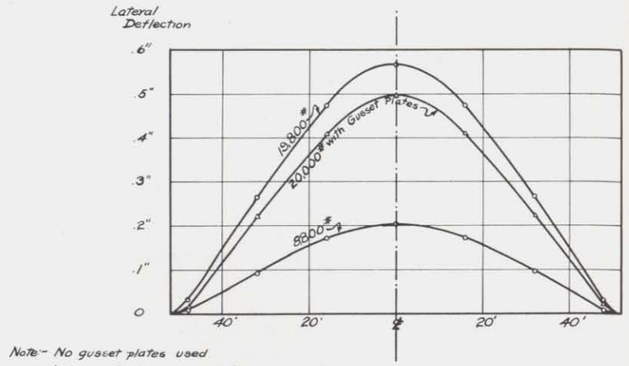

Note:- No gusset plates used between bridge girder and end tie in these tests except as noted

LATERAL LOAD TEST ~ CRANE #8441
DEFLECTION OF BRIDGE GIRDERS

Mar 30, 1940

Figure 13

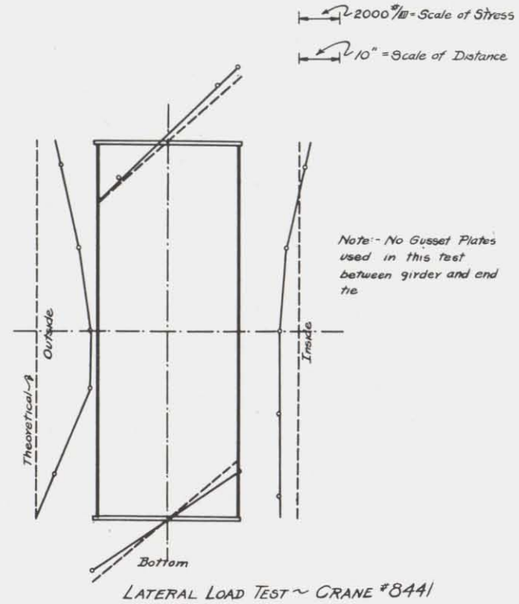

LATERAL LOAD TEST ~ CRANE #8441
STRESS DISTRIBUTION AT CENTER OF GIRDER

Mar 30, 1940

Figure 14

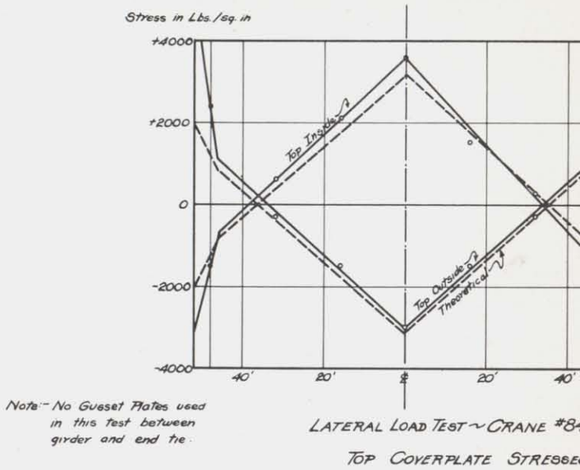

Note:- No Gusset Plates used in this test between girder and end tie

LATERAL LOAD TEST ~ CRANE #8
TOP COVERPLATE STRESSES

Mar 3

Figure 15

without the gusset plates due to the fixing effect of these plates. The fact that the deflection is greater on the bottom than on the top flange is due to slip in the end connection. The end tie was more effective in preventing slip at the top than at the bottom because the bottom of the end tie was located close to the center of rotation of the girder so that a small slip at this point would cause a large deflection on the bottom of the girder. Secondly, the bottom connection did not have as many bolts. That this slip occurred could be seen easily since the bolt holes were reamed prior to the test and they were out of line when the test was over. The resultant twist due to the slip is therefore somewhat contrary to what one might expect.

The measured twist of the girders is shown in Figure 12. The negative values are caused by the end slip. Since the measured twist is so small, the points are somewhat scattered and it is difficult to plot the correct curves. The difference between the K values of the 8800 lb. and 19,800 lb. loads is probably due to this fact. The measured values of K were found by dividing the torque by the product of the shear modulus and slope of the twist curve. Bredt's theory would give a K value of 61,000 in.^{4} However, since the twist angle is extremely small, it is believed that the difference from the theoretical is here a matter of precision. Since the twist was found by taking the difference of two sets of readings (the lateral deflection of the top and bottom flanges), whose values were very close to each other, a very small error in the measured values would give a rather large percentage error in the difference.

The lateral deflections shown in Figures 10 and 11 corrected for initial slip and twist are shown in Figure 13.

The stresses were measured on the front girder. Figure 14 shows the stress distribution at the center section of the girder and the plotted points show where the gauge lines were located. The stress distribution in the web should be noted. On the outside or compression side, very little stress is taken in the mid portion of the web. This is due either to local bending or incipient buckling of the web or perhaps to a combination of these two effects. Under lateral loads, the web acts as the compression flange of a beam and the h/t ratio of 240 for the clear depth of the web is so high that the stress is not apt to be uniform over the web cross section.

The test was repeated a number of times, similar readings were taken and the results were very inconsistent, showing that the webs were unstable at this stress. This indicates incipient buckling, since real buckling would overstress the flanges. The local bending effect was due to the fact that the welding of the diaphragms to the thin web plates caused small waves or buckles. Thus the stress caused by the test load produces bending due to eccentricity of the plate. Therefore the measured stress on one side of the web does not necessarily indicate the average stress through the thickness of the web.

Figure 15 shows the stress distribution along the top flange for the test in which no gusset plates were used. Figure 16 gives the stress distribution in the web. The irregular behavior of the web is clearly shown.

Figure 17 shows the stress distribution along the top flange when gusset plates were used. The stresses are seen to be less than those in Figure 15 which represents the same test without the gusset plates.

The stiffening effect of these gusset plates also shows up in the location of zero stress. For Figure 15 the point of zero stress averages 16¾ ft. from the end of the girder which corresponds to a fixity factor of 67 per cent. For the girder with gusset plates, the point of zero stress was 18½ ft. from the end and this corresponds to a partial fixity of 74 per cent.

The span to use in computations is a questionable point but since the full span is normally used in design, the full span of 104 ft. was used in computing the above fixity factors. However, since the moment of inertia of the girder varied at the end, the point of contraflexure for the fully fixed beam was 25 ft. from the end instead of the 26 ft. which would have been the case if the moment of inertia were constant.

It is impossible to get 100 per cent fixity since the deflection in the end tie allows the end of the bridge girder to give. In crane No. 8441, the maximum possible end fixity is reduced to 84 per cent due to frame action. Thus the efficiency of the joint when gusset plates were used was 0.74/0.84 or 88 per cent, and 0.67/0.88 or 76 per cent when no gusset plates were used.

The theoretical stresses shown in the diagrams were computed using the end fixities found from the points of contraflexure and a value of 24,300 in.^{4} for the gross horizontal moment of inertia. The check is seen to be very close. The sharp break plotted in the stress lines is based on a consideration of the change in depth of the girder section.

As an additional check, the lateral deflection was computed using 24,300 in.^{4} for the moment of inertia and the fixity factors found from the stress curves. The theoretical deflection for the first test without the gusset plates is 0.572 in. and in Figure 13 the measured deflection is 0.564 in. For the test with the gusset plates, the computed deflection was 0.516 in. which compares with a measured value of 0.500. Thus the use of the whole girder to resist the lateral forces, and the values of the fixity factors is justified by the check between the observed and computed deflections.

The stresses at the 8800 lb. load were too small to measure with precision, but the lateral deflections were measured. The center deflection of 0.205 in. measured at this load corresponds to a fixity factor of 80 per cent and a joint efficiency of 91 per cent.

The design lateral load was about 14,200 lb. The

Figure 16

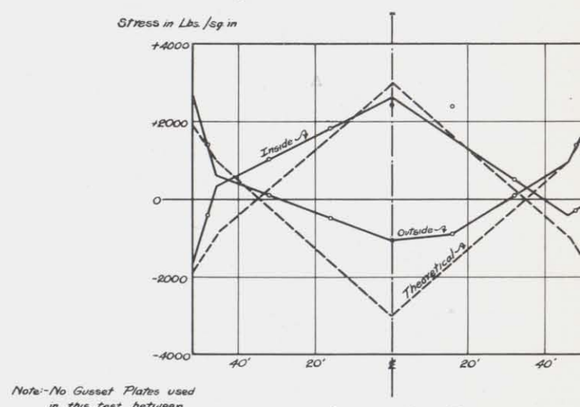

Note:-No Gusset Plates used in this test between girder and end tie

LATERAL LOAD TEST ~ CRANE #8
AVERAGE WEB STRESSES

Mar. 30

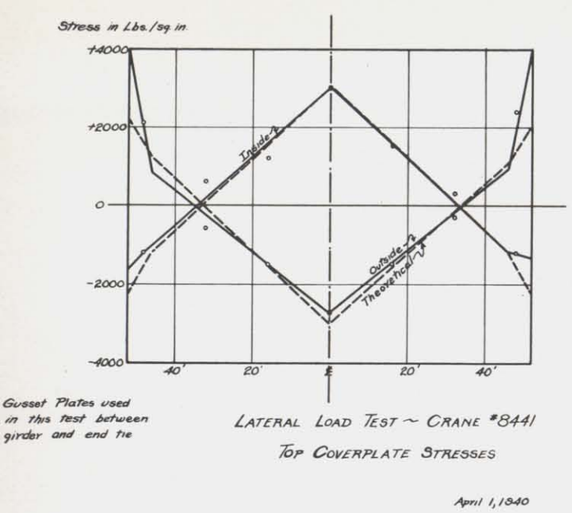

Figure 17

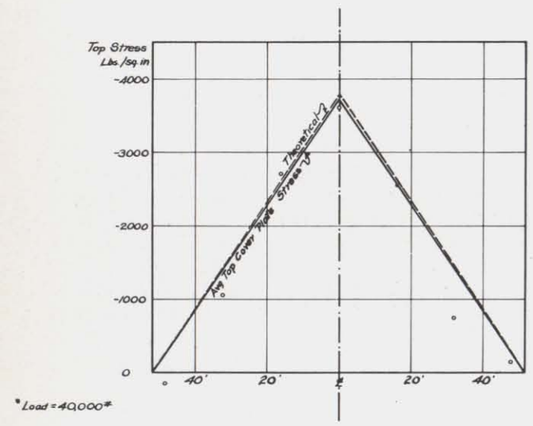

Figure 18

▲

Figure 19

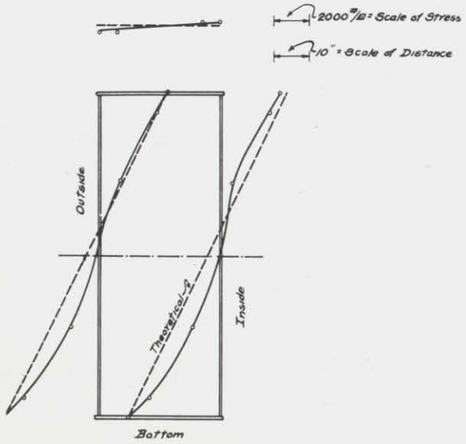

tests were therefore made at about 35 per cent overload and the stresses and deflection should be in line with what will occur when the crane is in service except as these factors are modified by the walkways, etc.

The end moments in the bridge girders caused corresponding end moments in the end ties. The stresses in the center of the end tie were found to be 3000 lb. per sq. in. at the corners of the box, which corresponds with a value of 3100 lb. per sq. in. computed from the fixed end moment. The test showed that the large manholes in the sides of the box end tie prevented the portion of the side plates in line with the manholes from carrying any stress. This was taken into account in the above computation.

The torsional moment had little effect on the end tie in comparison with the fixed end moment, since the lateral load had a small eccentricity with respect to the end tie. In this test, the twisting moment was less than 5 per cent the lateral moment.

Crane No. 8441 was also tested under vertical load. The girders were supported at the center with the ends cantilevered and the initial stress readings were taken. Then both ends were jacked up until the girders were raised off the center support and the strains measured again. This loading gave approximately the same bending moment as a load equal to the weight of the girder applied at the center of the girder.

The top coverplate stresses for this loading are shown in Figure 18. They check well with the ordinary beam theory as should be expected. Figure 19 shows the stress distribution at the center section of the girder under the action of vertical loads. The local bending in the thin web is shown by the refusal of the web to carry its full share of stress at the center line of the web while it does carry most of its share close to the flanges of the girder. This causes the curvilinear stress distribution in the webs.

The results of the tests on crane No. 8441 may be summarized as follows:

1. The whole section of the box girder resisted the lateral moment.

2. The end fixity for the girder with the gusset plates was 74 per cent for a 20,000 lb. load. The end fixity for the girder without the gusset plates was 67 per cent for a 19,800 lb. load and 80 per cent for an 8800 lb. load. This variation was due to slip in the end connection and deflection of the end tie.

4. The joint efficiency varied from 76 to 91 per cent.

5. Under vertical load, the box girder behaves as one would predict from the ordinary beam theory.

6. An h/t ratio of 240 for the clear depth of the web seems to be about the upper limit of this ratio or even somewhat above if the webs are to act as is usually assumed in design.

Crane No. 5886—The third crane tested was a fish-belly type and is sketched in Figure 20. This crane was tested with the walkway on each girder.

Figure 21 shows the lateral deflection curves of the flanges of this crane. In this case, the end deflection on the bottom is not zero and the slip caused the bottom to move outwards.

The twist of these girders is shown in Figure 22. It was rather surprising to note that the twist as measured in radians, was practically constant along the girder. However, these curves include slip. If the bottom deflection curves of Figure 21 are raised so that the end deflections are zero, the effect of slip will be eliminated. This correction results in the corrected twist curves of Figure 22. For the 20,000 lb. load the center twist as measured is 0.00118 radians and the twist computed from equation (13) in the appendix gives a theoretical value of 0.00119 radians. Similarly for the 9300 lb. load, the measured value is 0.00058 radians and the computed value is 0.00056 radians. Equation (13) is based on Bredt's value for the torsion constant. The corrected twist curves are not parallel to the original twist curves due to the variable depth of the section.

The lateral deflection of Figure 21 corrected for slip is shown in Figure 23.

Figure 24 shows the stress distribution at the center section of the girder with the plotted points indicating the location of the gauges. It should be noted that the web stresses here are much closer to the theoretical than those of crane No. 8441. The web height-thickness ratio was the same in both cases, but crane No. 5886 had a straighter web and in addition was not stressed as highly as No. 8441.

Figures 25, 26, and 27 show the measured stresses along the flanges and webs of the girders. The theoretical stress distribution is not a straight line since the cross section of the girder varies. In Figure 25, the center stress was greater than the theoretical, and in Figure 27 it was less than the theoretical, whereas the rest of the girder checked fairly well. This is probably the same effect noticed in crane No. 4683 and is due to secondary torsional stresses.

The point of contraflexure in the stress curves are at an average distance of 22 ft. from the ends of the girder, which corresponds to a fixity factor of 84 per cent.

The lateral deflection was computed using the equations in the appendix and found to be $2.10 - 1.21 = 0.89$ in. as compared with a measured value of 0.90 in. The value of 2.10 in. is the deflection which would take place if there were no end fixity, and the 1.21 in. value is the deflection due to the end moment and acts in the minus direction. The difference is the actual deflection. The importance of end fixity and of keeping the end connection tight is apparent if a laterally stiff crane is desired.

The walkways on this crane seemed to have little effect on the deflection or stresses, as the above computations were made disregarding the walkways. Strain measurements on the walkway also showed no stress. The reason for the greater effectiveness of the walkway of crane No. 4683 as compared with that of crane No. 5886 is probably due to differences in connection details. A large portion of the walkway on crane No. 5886 hung below the girder and could have no effect. Secondly, the bolts of the walkway may have been looser than in the case of crane No. 4683.

The results of the tests on crane No. 5886 may be summarized as follows:

1. The whole section of the box girder resisted the lateral moment.

2. Partial end fixity was present which reduced the lateral deflection over 50 per cent. The fixity factor was 84 per cent.

3. Secondary torsion stresses were present which

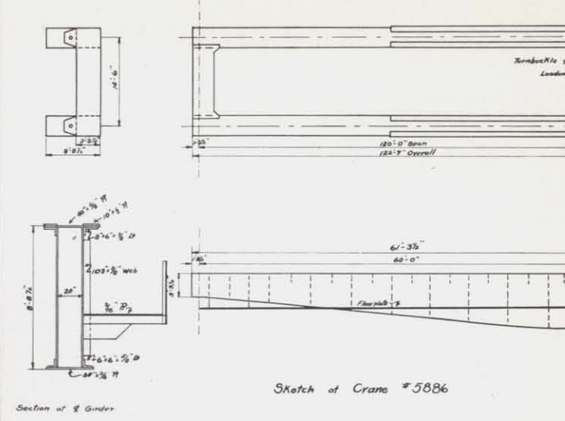

Figure 20

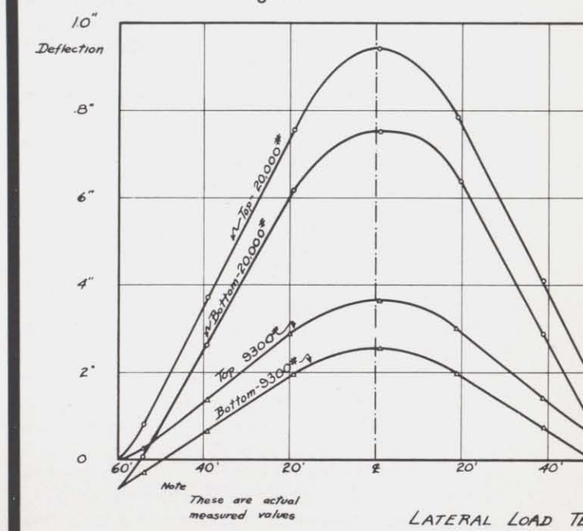

Figure 21

▲

Figure 22

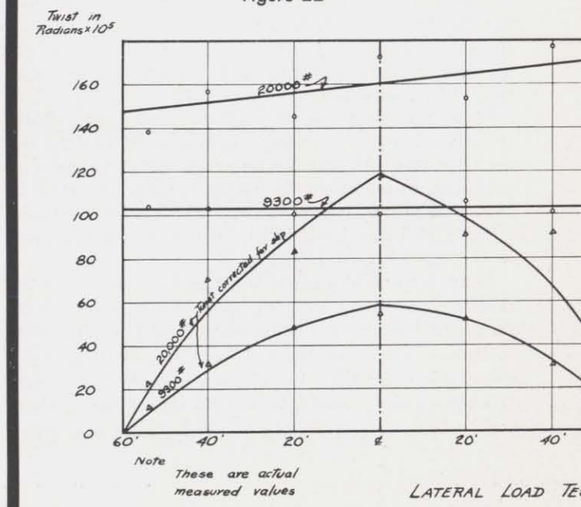

increased the top flange stresses and reduced the bottom flange stresses.

4. The walkway carried no stress and had little effect on the behavior of the girder.

DISCUSSION OF RESULTS

The main purpose of the tests was to determine what portion of a box crane girder resists lateral loads. Since three very different types of girders were tested with the same result, one may conclude that the whole section of a box girder works to resist lateral loads. Therefore it seems logical that girders should be designed on this basis, in order to correlate design procedure with actual conditions. This should result in economy, since the usual method of assuming that the top flange takes the lateral load results in computed lateral stresses which are often three to four times more than those actually present. It should also result in a safer section, since the stresses in the tension flange due to lateral load, which are normally neglected, will be allowed for in the design.

The torsional direct stresses in the usual section will be quite small and should have little effect in the normally proportioned girder. They occur only at the point where the girder is loaded and become negligible within a few feet from this section.

End fixity was present in all the tests. This fixity is normally neglected in design. This neglect is probably justifiable since end fixity will vary greatly due to detailing and design. Secondly, the play in the end connections which appears as the crane is in service would reduce any fixity present to a small degree. Every crane maintenance man is familiar with the occurrence of loose bolts and rivets in the end tie connections. It must be remembered that the tests were made on newly fabricated cranes whose joints would be tighter than normal. Thus unless the joint is designed so that no slip can take place, it should be neglected in computations. Any fixity present will be an additional safety factor and help in stiffening the girder. However, the end tie should be designed to resist the end moment since neglect of this moment may result in overstressing the end tie.

The walkway worked with the girder in one test and had no effect in another. Since the walkway also loosens in service, it is not believed that it can be taken into account in design, unless special means are taken to make it act with the girder.

With the exception of one twist curve, the elastic twist could be computed fairly closely by Bredt's theory, and it is thought that the observed variations are due primarily to precision. However, the slip occurring in the end joints may cause a twist which is large in comparison with the elastic twist. This slip would increase as the crane is used in service.

Only one test was made under vertical load, and the results checked the ordinary beam theory. There is no reason to believe that the results should be otherwise.

Two of the cranes, No. 8441 and No. 5886, had relatively thin webs, the ratio of the clear depth to the plate thickness being about 240 in each case. One of these webs which had some small initial buckles, had rather

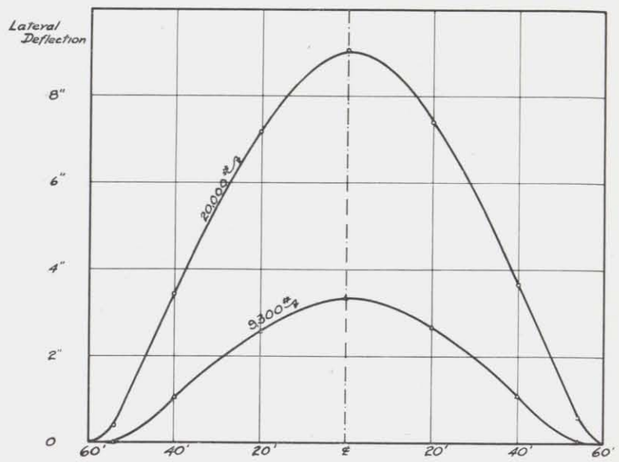

Figure 23

large bending stresses. The riveted web also had some bending stresses, but they were not as large as those in the welded web. However, before any comparison is made between the two, one should note that there was a diaphragm close to the center section of the riveted girder, whereas the center section of the welded girder was half-way between the diaphragms. This vertical

Figure 25

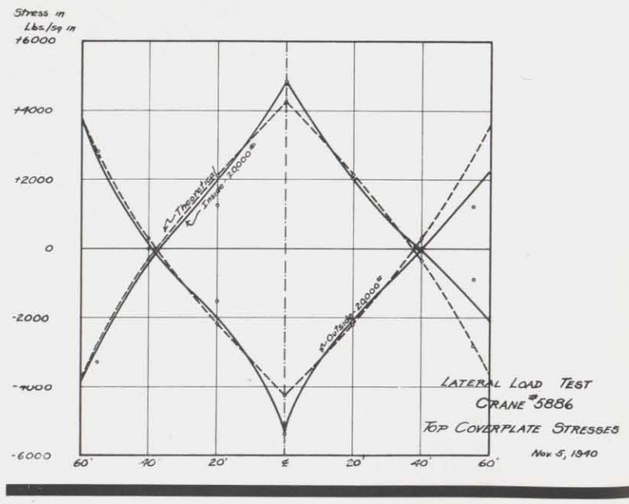

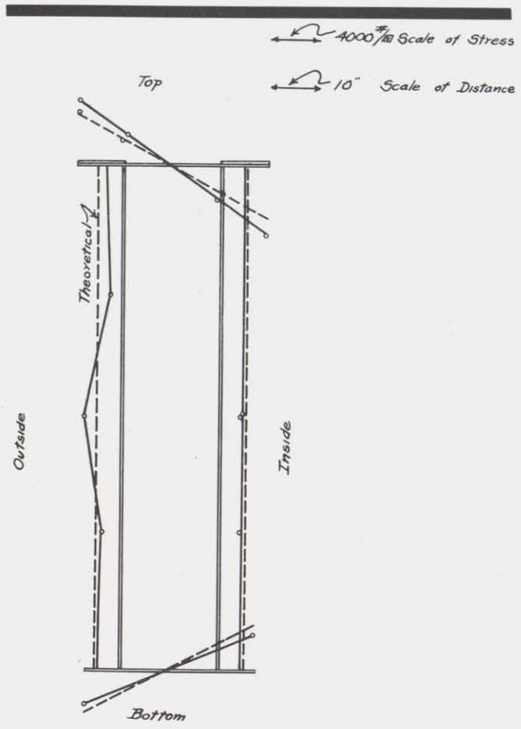

Figure 24

diaphragm would have some effect in reducing the bending stresses at the center section of the riveted girder. However, if thinner webs are to be used, it might be advisable to add longitudinal stiffeners. The above discussion applies primarily to the girder under the action of the lateral load only. In service the crane would have a vertical load in addition to the horizontal load and the combination of the two loads would usually result in a lower allowable web height-thickness ratio than if the crane were under the action of either load alone.

CONCLUSIONS

1. The results of these tests show that the whole girder section acts to resist lateral loads and should be so considered in design.

2. The stresses of a crane under vertical load can be computed by the ordinary beam theory.

3. The elastic twist of a girder can be computed approximately, by Bredt's theory. In addition to the elastic twist there is quite a bit of twist due to slip.

APPENDIX

The following formulæ were developed for fish-belly girders from the fundamental differential equation

$$E\frac{d^2y}{dx^2} = -\frac{M}{I} \qquad (1)$$

where y is the deflection of the girder at any point x measured from the end of the girder.

Since I is a variable in this equation as well as M, some assumption must be made as to the variation of I. Two sets of formulæ were derived, one in which it was assumed that I varied linearly along the girder, and second, it was assumed that I varied parabolically along the length of the girder. The first approximation is most applicable to computing the lateral moment of inertia, and the second in computing the vertical mo-

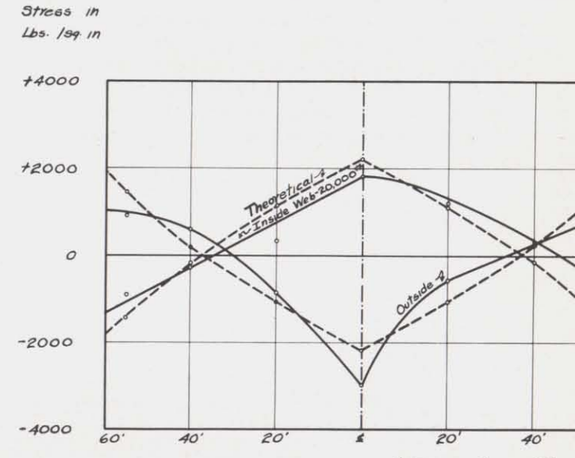

Figure 26

Figure 27

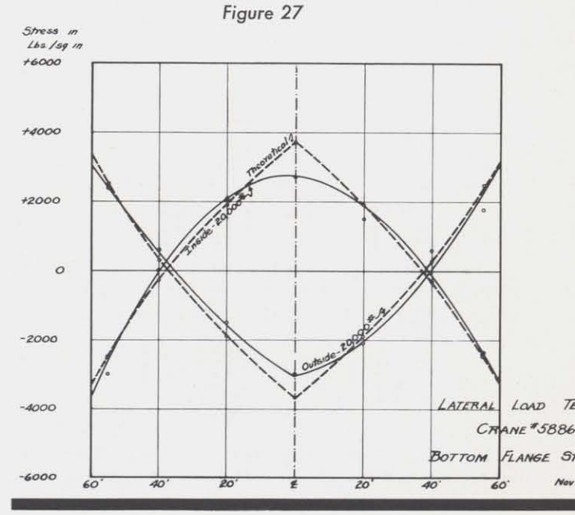

ment of inertia. For average girders they should give results which are fairly close.

The computations for deriving these formulæ are quite laborious and only the results will be given.

For a girder in which the I varies parabolically, the deflection at any point x due to a load at the center of the girder is

$$d=\frac{-Pl^2}{16EI_3}\left[x\log\left(\frac{I_1l^2}{I_3{}^4}+x^2\right)-2x+2\sqrt{\frac{I_1l^2}{4I_3}}\left(\tan^{-1}\frac{x}{\sqrt{\frac{I_1l^2}{4I_3}}}\right)-x\log\left(\frac{I_1l^2}{I_3{}^4}+\frac{l^2}{4}\right)\right] \quad \ldots\ldots(2)$$

and for the center deflection, this reduces to

$$d_c=\frac{-Pl^3}{16EI_3}\left(-1+\sqrt{\frac{1}{\frac{I_2}{I_1}-1}}\tan^{-1}\sqrt{\frac{I_2}{I_1}-1}\right) \quad \ldots\ldots(3)$$

P stands for the center load in pounds, l is the span in inches, I_1 is the gross moment of inertia at the end, I_2 is the gross moment of inertia at the center, I_3 equals I_2-I_1, and E is the modulus of elasticity. The above formulæ give the deflection for a simple beam.

The corresponding formulæ for linear variation of I are:

$$d=\frac{-Pl}{8EI_3{}^2}\left[I_3x(x-l)+I_1xl\log\left(\frac{I_1l+I_3l}{I_1l+2I_3x}\right)-\frac{I_1{}^2l^2}{2I_3}\log\left(1+\frac{2I_3x}{I_1l}\right)+I_1xl\right] \quad \ldots\ldots(4)$$

and for the center deflection

$$d_c=\frac{-Pl^3}{16EI_3}\left[-\frac{1}{2}+\frac{I_1}{I_3}-\left(\frac{I_1}{I_3}\right)^2\log\left(1+\frac{I_3}{I_1}\right)\right] \quad \ldots\ldots(5)$$

The deflections due to the end moment are given by the following formulæ where M is the end moment.

For parabolic variation of I

$$d=\frac{-Ml^2}{4EI_3}\left[\frac{2x}{l}\sqrt{\frac{I_3}{I_1}}\tan^{-1}\frac{2x}{l}\sqrt{\frac{I_3}{I_1}}-\frac{2x}{l}\sqrt{\frac{I_3}{I_1}}\tan^{-1}\sqrt{\frac{I_3}{I_1}}-\frac{1}{2}\log\left(1+\frac{4I_3x^2}{I_1l^2}\right)\right] \quad \ldots\ldots(6)$$

and for the center deflection, this reduces to

$$d_c=\left(\frac{Ml^2}{8EI_3}\right)\log\left(1+\frac{I_3}{I_1}\right) \quad \ldots\ldots(7)$$

For linear variation of I

$$d=-\frac{Ml}{2EI_3}\left[x\log\left(\frac{I_1l+2I_3x}{I_1l+I_3l}\right)-x+\frac{I_1l}{2I_3}\log\left(\frac{I_1l+2I_3x}{I_1l}\right)\right] \quad \ldots\ldots(8)$$

and for the center deflection, this reduces to

$$d_c=\frac{-Ml^2}{4EI_3}\left[-1+\frac{I_1}{I_3}\log\left(1+\frac{I_3}{I_1}\right)\right] \quad \ldots\ldots(9)$$

The fixed end moment is given by the following formula for linear variation of I. There would be no occasion to compute it in the vertical direction.

$$M=\frac{Pl}{4}\sqrt{\frac{I_1}{I_3}}\frac{\left[-1+\frac{I_1}{I_3}\log\left(1+\frac{I_3}{I_1}\right)\right]}{\tan^{-1}\sqrt{\frac{I_3}{I_1}}} \quad \ldots\ldots(10)$$

The actual fixed end moment would vary from 60 to 90 per cent of the above value depending on the end connection.

In the above equations the units must be consistent, and it is advisable to use pounds and inches. The angles are expressed in radians and the logarithms are natural logarithms to the base e and not to the base 10.

These equations require a good deal of computation for their solution, except for the deflections at the center where they are considerably simplified. The effect of varying the moment of inertia is to increase the deflection over what would take place if the whole girder section were equal to that at the center. For a number of girders which have been checked by the writer, the increase in deflection has varied from 10 to 30 per cent. Therefore for approximate computations, the following formula is suggested for the center deflection of fish-belly girders.

$$d_c=K\left[\frac{Pl^3}{48EI_c}-\frac{Ml^2}{8EI_c}\right] \quad \ldots\ldots(11)$$

I_c is the moment of inertia at the center, M is the fixed end moment which will vary from 60 to 85 per cent of the fully fixed beam depending on the connection, and K is a constant to take into account the fish-belly effect. K varies from 1.10 to 1.30, the smaller value applying to relatively flat fish-belly girders and the higher value to deep fish-belly girders. For a girder of constant section K equals 1.00.

In a fish-belly girder, the twisting moment due to a lateral load applied at the top flange is not constant but varies along the girder since the center of gravity of the girder approaches the top flange as one approaches the end.

The twist for this condition is given by the following formula, when the depth of the girder varies parabolically.

$$Y=\frac{Pl}{16b^2G}\left[\frac{b(t_2+t_1)}{2t_1t_2\sqrt{h_1h_3}}\tan^{-1}\left(\frac{2x}{l}\sqrt{\frac{h_3}{h_1}}\right)+\frac{2x}{lt_3}\right] \quad \ldots\ldots(12)$$

and the twist at the center

$$Y_c=\frac{Pl}{16b^2G}\left[\frac{b(t_2+t_1)}{2t_1t_2\sqrt{h_1h_3}}\tan^{-1}\sqrt{\frac{h_3}{h_1}}+\frac{1}{t_3}\right] \quad \ldots\ldots(13)$$

Y is the angular twist in radians, b is the distance between the web centers, G is the shear modulus, t_1 and t_2 are the cover plate thicknesses, t_3 is the web thickness, h_1 is the depth of web at the end, h_2 is the center web depth, and h_3 is the difference between the center web depth and end depth.

However, for approximate computations, we may use for the center twist

$$Y_c=\frac{Pl}{32b^2h_2G}\left[\frac{b}{t_1}+\frac{b}{t_2}+\frac{2h_2}{t_3}\right] \quad \ldots\ldots(14)$$

This formula is simply the formula for the uniform section, and its use is based upon the assumption that the resistance to twist and the applied moment at any section vary proportionately. For the crane tested, the computed value given by equation (14) is practically the same as that given by the more exact equation (13).

The twist caused by a uniform torque along this girder, such as the motor torque may be computed by the following formula.

$$Y=\frac{Ml}{4Gb^2}\left[\left(\frac{b}{t_1}+\frac{b}{t_2}\right)\frac{lx}{2h_1(h_1l^2+4h_3x^2)}+\left\{\left(\frac{b}{t_1}+\frac{b}{2}\right)\frac{1}{4h_1}+\frac{1}{t_3}\right\}\frac{1}{\sqrt{h_1h_3}}\tan^{-1}\frac{2x}{l}\sqrt{\frac{h_3}{h_1}}\right] \quad \ldots\ldots(15)$$

and the twist at the center is obtained by substituting $x=\frac{l}{2}$ in the above formula.

The above formulæ are given here as a matter of record since it was necessary to derive them in order to check the test results. Their application in practice would probably be laborious. As a matter of fact, a properly designed box girder is so stiff that there is little necessity for computing twist.

The formulæ which might have a practical application are those for lateral deflection since they are a measure of the stiffness of the crane. Also, an average crane often has a lateral deflection under the design load which is greater than the vertical deflection. Since this lateral deflection occurs in both directions, there can be no camber; and the resultant wear on shafting, bearings, etc., is more serious than that due to the vertical bending.

The above equations apply when the girders are loaded at the center, and this condition gives the maximum possible deflection very closely.

2. Lateral Load Tests on Truss I Beam Crane

▲ THIS REPORT summarizes the results of a lateral load test made on the bridge of a 175 long-ton trussed I-beam crane of 100 ft. 11 in. span. The stresses and deflections in the crane were measured for the lateral test load of 23,700 lb. The whole truss was found to resist the lateral load. Secondary stresses were present in the truss. The stresses in the crane were computed by three methods, and the computed results are compared with the measured results.

Since little is known about the behavior of trussed I-beam cranes, this test was made in order to compare actual behavior with design assumptions.

Crane No. 5879, which is a sixteen-wheel crane, was supported on the equalizer trucks during the test. The crane was tested after it had been completely assembled, but without the trolley.

The stresses were measured with a 10 in. Whittemore strain gauge which gives results accurate to about plus or minus 300 lb. per sq. in. They were measured on the girder, end ties, and on a number of the more highly stressed truss members. Since the crane was due for shipment, only a limited time was available for the test and it was impossible to take as many readings as would normally be desirable. Sketches showing some of the details of the girder and the truss members discussed in this report are given in Figures 1 and 2.

The lateral deflection of the girders was determined by means of a 0.001 in. Federal dial which measured the closure as the loading rig pulled the two girders together. The difference between the lateral deflections of the top and bottom flanges at the same section divided by the distance between the gauge points gave the twist of the girder at each section.

The load was applied by tightening a turnbuckle fastened to the top flanges of both girders at the center of the span. The load was measured by a calibrated spring which was placed in the system.

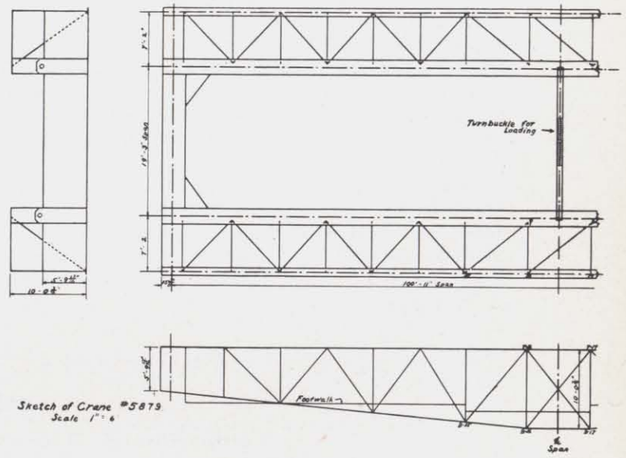

Figure 1

Figure 2

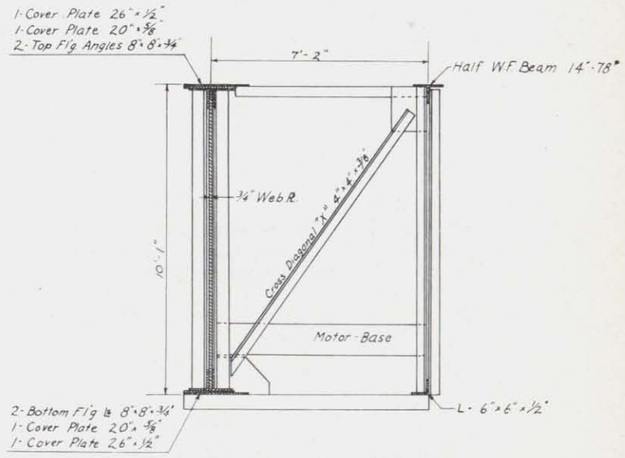

Section at ℄ of Truss Crane #5879

TEST RESULTS

The girders were loaded with a lateral load of 23,700 lb. applied on the top flange. This was the maximum capacity of the loading rig. Since the capacity of the crane was 175 long tons or about 392,000 lb., the test

load was about equivalent to a lateral load on each truss of 6 per cent of the live load capacity of the crane.

Figure 3 shows the lateral deflection of both flanges of the girder under the test load. The center line mark denotes the center of the girder span. The deflections are given in inches and are the measured deflections divided by two since the gauge gave the combined deflections of both girders.

The measured twist of the girders is shown in Figure 4.

The measured stresses due to the lateral load are shown in Figures 5, 6, and 7. Figure 5 shows the stress distribution along the top flange of the I-beam girder. The gauge lines on which these stresses were measured were located on the top coverplate 10 in. from the centerline of the I-beam. This figure shows a large bending stress at the center of the girder. The lateral load was applied at the span center and since this was not a panel point location, the I-beam transferred the load to these points. If the top flange alone is assumed to transfer the load as a continuous beam to the panel points, the computed stress will be plus or minus 2700 lb. per sq. in. Since there is a resultant tension in the girder of about 600 lb. per sq. in. due to truss action, the combined stress would be +3300 lb. per sq. in. and −2100 lb. per sq. in. The measured values are +3900 and −2700 lb. per sq. in., which are somewhat higher than the computed.

Figure 6 shows the stress distribution along the bottom flange of the I-beam. The stresses were measured on the edges of the flanges. The local bending at the load point had little effect on the bottom flange. This shows that the top flange transferred most of the load to the panel point.

In Figure 7 the average stresses of the top and bottom flanges of the girder are shown. These average stresses are a measure of the load carried by the various members. The stresses in the bottom truss are quite appreciable, and would be completely neglected in normal design procedure.

DISCUSSION OF RESULTS

In this country, truss cranes have not been as extensively used as in Europe, even though they may result in lighter cranes on long spans. Some of the reasons for this have been economic, and some have been due to a lack of data as to the stiffness and stress distribution in such cranes. This test was made to determine the latter factors and to compare actual measurements with common design assumptions. Although conclusions drawn from a single test can not be used as a basis for general conclusions, they indicate a trend. Secondly, the measurements do show how this particular crane behaved under the test load. Previous data of this type are very scarce.

Crane No. 5879 is a space frame; it is highly indeterminate, and the stresses can be found only after long, tedious computations. In addition, one side of the crane is a complete I-beam girder and little is known as to how much of the girder takes part in resisting the loads. Finally, the problem is complicated by the effect of the walkway and any end fixity which may be present.

Table I presents a comparison between the measured stresses and the stresses computed by three different

TABLE I

Comparison of Measured and Computed Stresses

Bar	Measured stress	Measured stress	Measured stress	Area	Average measured stress	Measured load, lb.	Computed stress as beam	Computed load as two separate trusses	Computed load as space frame
Top truss									
7– 8	+3900	−2700	..	90.00	+ 600	+54,000	+ 420	+53,200	+49,000
7–15	+4500	+4800	..	3.84	+4700	+18,000	..	+10,700	+13,500
7–16	+1800	+ 900	..	2.48	+1350	+ 3,400	..	+ 8,500	+ 4,400
16–17	−2100	−3600	..	11.50	−2850	−33,000	−4300	−53,200	−49,000
Side truss									
T17–B16	+ 600	−1200	..	2.48	− 300	− 750	..	...	0
T16–B16	+ 900	+1800	+1200	2.86	+1300	+ 3,700	..	...	+ 2,000
T16–B15	+ 300	+ 300	+ 900	2.48	+ 500	+ 1,240	..	...	+ 1,900
Bottom truss									
7–16	0	..	..	3.61	0	0	..	0	0
7–15	+ 900	+ 600	..	2.86	+ 750	+ 2,100	..	+ 6,000	+ 3,100
7– 8	+1200	− 600	..	90.00	+ 300	+27,000	+ 420	+29,800	+24,000
16–17	−3900	..	..	5.75	−3900	−22,500	−4300	−29,800	−24,000
15–16	−3600	..	..	5.75	−3600	−20,700	−3600	−29,800	−24,000
Diagonal *X*	−1200	−1800	− 300	5.72	−1100	− 6,300	..	− 7,200	− 7,400

TABLE II

Comparison of Measured and Computed Deflections

Location	Measured, in.	Computed as beam, in.		Computed as two trusses, in.		Computed as space framework, in.	
		No fixity	Partial fixity	No fixity	Partial fixity	No fixity	Partial fixity
Top flange center.....	0.350	0.276	0.237	0.374	0.334	0.417	0.380
Bottom flange center...	0.240	0.276	0.237	0.340	0.300	0.367	0.325

methods. Table II gives a similar comparison for them deflections. The most approximate computation method is to consider the truss as a beam. In crane No. 5879, the moment of inertia was computed by assuming the chords of the truss to be one flange of the beam and the whole I-beam to be the other flange. The computed I was 116,500 in.^{4}. The tables show that this results in a fair approximation for the stresses, and also for the deflections. However, deflections computed by this method will be low since the deflection of the structure due to the strain in the diagonals is neglected. Also this method of computation gives neither the stresses in the diagonals, nor the twist in the crane.

It should be noted in Table I that the stresses were taken on one, two, or three gauge lines on each member tested. These gauge lines were usually on the edges of the member and on the same section in every case. The tables show, however, that the stress at a section is not uniform. This variation is probably due to secondary moments in the truss. Trusses are normally considered to be pin-connected at the joints for computation purposes, whereas they are not usually so in practice. In this crane the members were welded to the gusset plates, and the chords were continuous through the truss. These secondary moments will cause bending stresses in the members, but should not appreciably affect the direct stresses. Secondly, the angles can be welded to the gusset plates on only one leg, which results in an eccentric application of the load on the member and consequent bending stresses.

Since there was some bending in the member, the measured stresses may not necessarily give the average stresses and this fact may account partly for some of the discrepancy between the computed and measured results.

In practice, a crane of the type tested is often de-

Figure 3

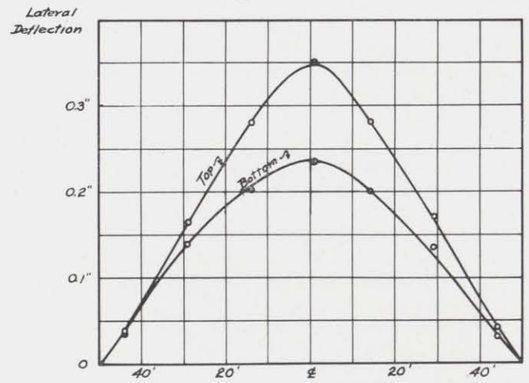

LATERAL LOAD TEST
CRANE #5879
LATERAL DEFLECTION OF GIRDER
Nov. 8, 1940

Figure 4

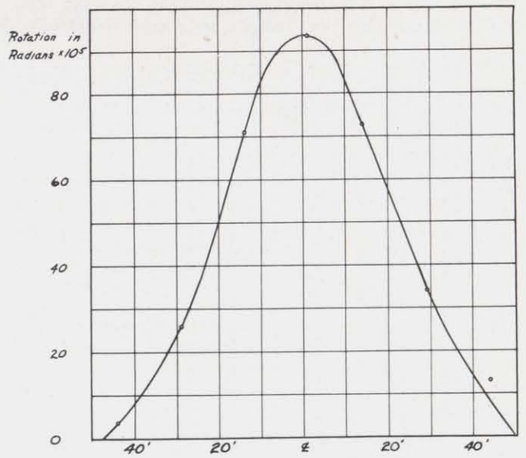

LATERAL LOAD TEST
CRANE #5879
ROTATION OF GIRDER
Nov. 8, 1940

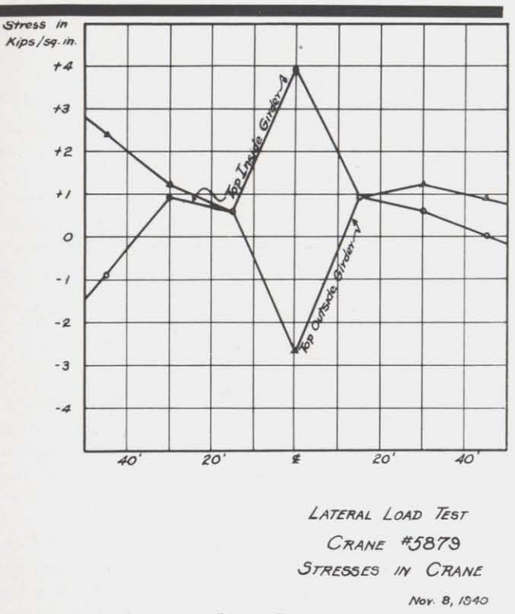

Figure 5

signed on the assumption that the top truss takes all the lateral load applied to the top flange. Some designers will split the load between the two trusses with the top truss taking the greater proportion. Figure 7 shows that the bottom truss is highly stressed due to a load on the top flange. Therefore one can not very well assume that the top chord takes all the load, and that the rest of the crane remains unstressed.

In the second method of computation, the load was split between the two trusses and each truss was analyzed as a separate truss. The method of equating deflections (*Structural Theory*—Sutherland and Bowman) was used to determine how much load was taken by each truss. In this method, the trusses are assumed to be pin-ended. It is also assumed that the center cross diagonals transfer the load from the top truss to the bottom. The diagonal is cut to obtain a statically determinate structure and is the member marked X in Figure 2. The deflections of each truss are then computed. The load taken by each truss is that which makes the relative deflection of the cut ends of the diagonal zero. In this crane, the computation showed that the top truss took 15,200 lb. and the bottom truss 8500 lb. of the applied 23,700 lb. lateral load. These results check approximately as the tables show. The method, however, neglects the effect of the side trusses and does not give the stresses in the side truss diagonals.

In the last column of the tables, the computed loads are given for the truss considered as a space frame. This computation method takes into account all the members. Two assumptions were made in the analysis. One was to split the area of the I-beam into two parts and to consider each part as one of the chords of the truss. Secondly it was assumed that only the two center cross diagonals X transferred load between the trusses. This second approximation is close since these diagonals are at the loaded panel points. When the cross-diagonals are cut, the various trusses are statically determinate for horizontal and vertical loads, and the stresses can be found by the method of deflections.

Since the structure is indeterminate, adding more area to a member does not necessarily reduce the stresses in that member. The result may be that the member will take more load. In this crane, the top chord of the outside truss had twice the area of the bottom chord. A lateral load of 100 lb. on the top chord results in a maximum force of 228 lb. in the top chord and a maximum force of 122 lb. in the bottom chord. On the other hand, if a lateral load of 100 lb. is applied on the bottom chord, there is a computed maximum force of 141 lb. in the bottom chord and 209 lb. in the top chord. In other words, the lighter the loaded truss, the more load will be transferred to the adjacent trusses. In the case of the crane tested, the computations indicate that if the top and bottom truss were made equally strong, the maximum load in the chords would be less. The trusses would have more of a tendency to take an equal portion of the load, and there would be less twist in the crane.

Figure 7 shows a slight end moment in the trusses. Stress measurements in the end tie showed that this end moment was about 20 per cent of the fully fixed end moment. Since the truss was very stiff compared with the end tie, the maximum possible end fixity which could be developed if there were no slip in the joint, was 47 per cent.

Figure 3 gives the lateral deflection of the crane. If the lateral deflection shown here is compared with that of some box girder cranes previously tested ("Lateral Load Tests on Box Girder Mill Cranes"—Madsen), and adjusted to take into account the difference in capacity and span, it is seen that the truss crane is fully as stiff. Secondly, crane No. 5879 has so little initial end fixity, it will remain almost as stiff when the end ties loosen in service. This can be seen by looking at the values for the deflection for partial fixity and no fixity in Table II. The box girders previously tested had a much higher end fixity and loosening of the end tie connection would increase the lateral deflection markedly.

The measured deflections shown in Figure 3 are less than the computed deflections given in Table II. This is most likely due to the fact that the computations are made on the basis of pin-end connections and the welded joints would stiffen the truss. Secondly, the walkway may have had some stiffening effect, particularly on the lower chord.

If the twist of the crane shown in Figure 4 is compared with the twists of the box girders previously tested, it would appear that the box girders have more resistance to twisting.

The above comparisons, however, may not be overly significant since it is very difficult in a comparison of cranes of different capacities and spans to draw any definite conclusions.

CONCLUSIONS

The measurements made in this test showed that for the crane tested:

1. The whole truss resisted the lateral load as a space frame.
2. The whole I-beam girder acted as a part of the truss.
3. The stresses computed by the three different methods gave results which were a fair approximation of the measured loads. The solution of the truss as a space frame is the only method which could be used to find the stresses in all the members.
4. When the lateral load is not applied at a panel point, the top chord must be designed to transfer the applied load to the panel points.
5. Secondary stresses were present throughout the truss.

Figure 6

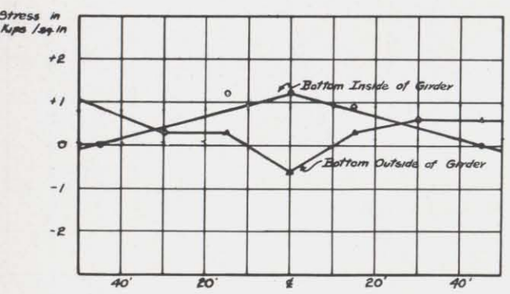

Figure 7

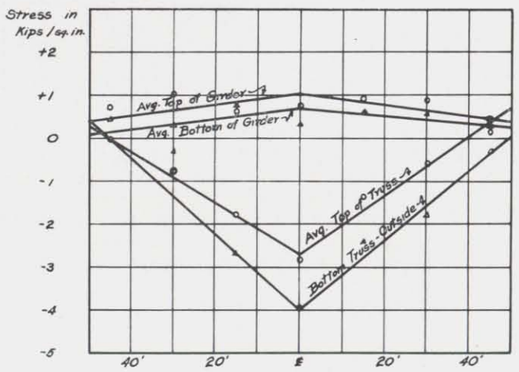

3. Dynamic Tests on Mill Cranes

▲ THIS REPORT describes the results of impact and lateral load tests on three electric overhead traveling cranes at the Bethlehem plant of the Bethlehem Steel Corporation and on the crane in the Fritz Engineering Laboratory of Lehigh University. In these tests, the stresses in the girders due to acceleration, braking, and impact, were measured with scratch gauges. It was found that the maximum lateral stress was due to braking and was about 10 per cent of the vertical live and dead load for the cranes tested. The measured impact values were quite variable. Jerk impact was found to vary from 9 to 33 per cent of the live load. Secondly, when the crane was run over wedges to simulate bad runway joints, the impact was found to vary from 56 to 100 per cent of the live load.

These tests were made in order to determine whether specification requirements for dynamic stresses in mill cranes were in accordance with those actually present in the girders of such cranes.

The dynamic stresses in cranes are of two types. One type of dynamic stress is the lateral stress due to acceleration and braking of the crane. This stress may be very large when the crane is of long span and the girders are relatively narrow. The braking stresses are usually larger than the acceleration stresses. The ratio of the braking load to the vertical load on the braked wheels may approach the value of the coefficient of friction between the crane wheel and runway rail. This maximum value may be modified by the timing of the swing of the load on the crane. If the instant of maximum swing should occur with the maximum braking force, the ratio of the maximum lateral force to the vertical force may exceed the coefficient of friction. However, in the tests made, the swing of the pendulum lagged behind the braking force. Lateral forces may also be due to other causes than those above enumerated. One such case would be the use of cranes to spot railroad cars. However, even in such cases, the maximum ratio of lateral load to vertical load should not exceed the coefficient of friction, since at this point the crane would slip on the runway rail.

Impact stresses may be due to many causes. In mill practice running the crane over bad runway joints is probably the most important cause for such stress. Impact stress will also occur when a load is jerked off the ground.

Four cranes were tested in this program. One series

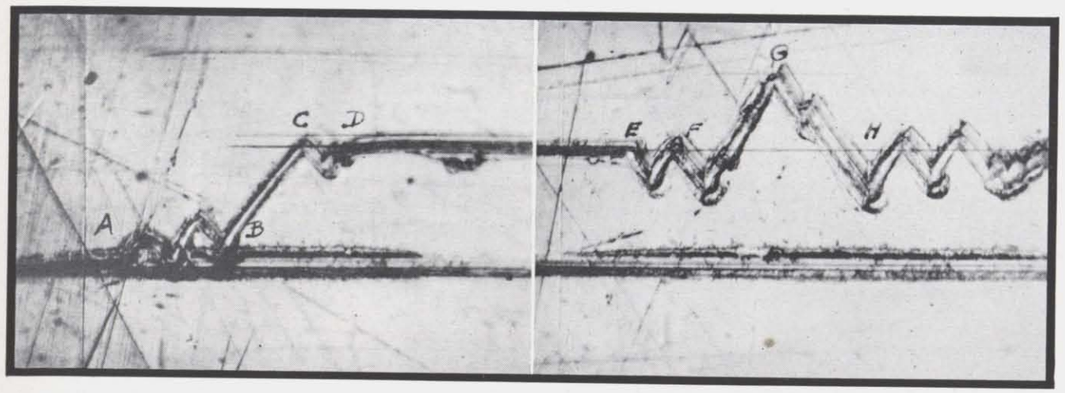

Figure 1

of tests was made on the crane located in the Fritz Engineering Laboratory. This, a 10 ton Niles crane No. 10097, has a span of 47 ft., and is a riveted fish-belly box girder. The bridge brakes are foot-operated mechanical brakes. The braking tests were made with no load on the crane due to limited clearance in the laboratory. A number of impact tests were also made on this crane. The jerk impact tests were made in the following manner. Slack was let out of the hoist. Then the slack was taken up so that the hook was moving at the maximum hoisting speed when the load was jerked off the floor. A tank of water weighing 8250 lb. was used for the load. To simulate bad joint impact, the crane was run over $\frac{3}{4}$ in. oak wedges placed under both ends of one bridge girder. Under the weight of the crane, the wedges flattened down to $\frac{9}{16}$ in. and this was assumed to be the drop of the crane. The 8250 lb. load was also used in the wedge tests and the crane was tested with 21 ft. and 14 ft. distances between the hook and hoisting drum.

Three cranes were tested at the Bethlehem plant of the Bethlehem Steel Corporation. The first crane, Bethlehem No. 430, was a new 10 ton riveted, fish-belly, box girder of 69 ft. span with hydraulic bridge brakes. Since the shop was under construction, the full length of the runway was available for test.

In the lateral tests, the load was picked up with the crane stationary. The crane was then fully accelerated until maximum speed was attained, and then the brakes were fully applied. These tests were made with a 31,000 lb. load of billets hung first as high as possible and then just high enough to clear the floor. Similar tests were made with a load of 15,500 lb. The clearance from the floor to the trolley rail of this crane was 23 ft. 9 in.

Jerk impact tests were also made on this crane. The load was raised with a jerk, and it was stopped with a jerk while being lowered.

The second crane tested at the Bethlehem plant was Bethlehem No. 410. This crane, located in the electrical shop, is a 5 ton hand-operated I-beam crane of 37 ft. 4 in. span. Lateral load tests were made on this crane using a magnet weighing 9100 lb. for the vertical load.

The third crane tested was Bethlehem No. 4. This is a 30 ton riveted, fish-belly box girder crane of 75 ft. span which is used as a skullcracker. This crane was tested to determine what impact is present as the ball is released from the magnet. A ball weighing 19,500 lb. was used in the tests and the magnet weighed 8800 lb.

The stresses in the cranes were measured by means of the De Forest scratch recording strain gauge. Since the stresses in the cranes were too small to use the gauge as manufactured, a special holder was made to increase

Figure 2

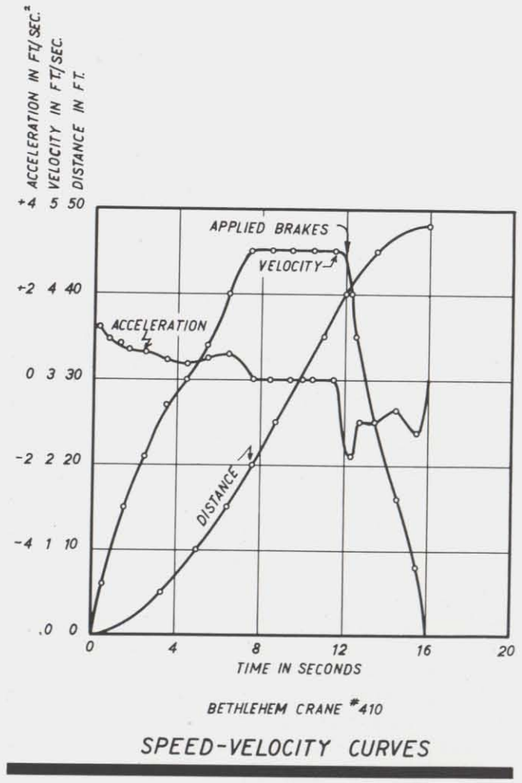

TABLE I

Lateral Load Tests

Crane	Test No.	Vertical load, lb.	Static stress, lb. per sq. in.		Maximum acceleration, ft. per sec.²	Measured deceleration, ft. per sec.²	Maximum speed, ft. per min.	Measured lateral stress, lb. per sq. in.		Computed lateral stress using 10 per cent lateral load, lb. sq. in.	Lateral load from measured braking, per cent
			Computed	Measured				Accel.	Braking		
Lab.	1	Dead load only	0	0	2.0	4.0	360	...	800	660	12.5
Beth. 410	1	9,100	2000	2050	1.2	1.8	180	800	1000	2500	5.6
Beth. 430	1	31,000	2500	1800	2.6	3.2	390	800	950	1300	10.0
Beth. 430	2	31,000	2500	1700	2.6	3.2	390	750	700	1300	10.0
Beth. 430	3	15,500	1250	1100	2.6	3.2	390	650	700	960	10.0

the gauge length to 20 in. Pictures of the strains were taken with a microscope using a magnification of 450X. Figure 1 shows such a picture. The gauges were all calibrated against a 20 in. Whittemore strain gauge. This was done in the laboratory by measuring the strains on a beam under a static bending load. In the crane tests, the gauges were mounted on both edges of the top and bottom flanges of the crane girder at the span center. The trolley was also located at the span center during the tests. Occasional difficulty was encountered with some of the gauges sticking so that no scratch was recorded, but generally enough gauges worked so that the lateral stresses could be determined. In addition each test was repeated to insure the availability of enough records to determine the dynamic stresses.

The acceleration and deceleration were determined from stop-watch readings measuring the time to one-tenth of a second. Distances were marked on the runway rail and the time at each mark was found from the stop-watch. From these measurements, the speed and acceleration can be easily determined. Figure 2 gives a picture of the acceleration and deceleration of Bethlehem, No. 410. This method is not as accurate as it should be, and in future tests it is suggested that a moving picture camera be used to photograph the stop-watch and distance marks along the rail at the same time. The acceleration and deceleration, as measured, apply only to the bridge of the crane and do not necessarily apply to the load since the motion of the load is modified by the swing.

Figure 3

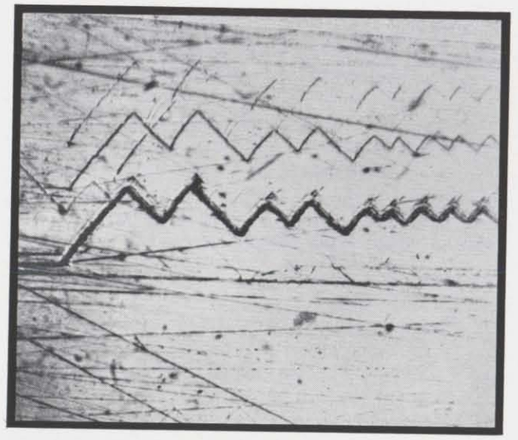

TEST RESULTS

About one hundred pictorial records of dynamic stresses were taken in this investigation. Typical records are illustrated in this report and a summary of the pertinent data is given in Tables I and II.

Table I summarizes the results of the lateral load tests on the several cranes. The columns of computed and measured static stress apply to the vertical live load. The static stresses in the tables are the arithmetical average of the tension and compression flanges. The acceleration, deceleration, and speed in the table are taken from curves similar to Figure 2. The measured lateral stresses are the arithmetical average of the readings on all the flanges, and are due to the live load and the dead load. The column of computed lateral stress is found by assuming that 10 per cent of the live load, trolley, and dead load acts laterally. The last column (lateral load from measured braking) is obtained by dividing the observed deceleration by g, the acceleration

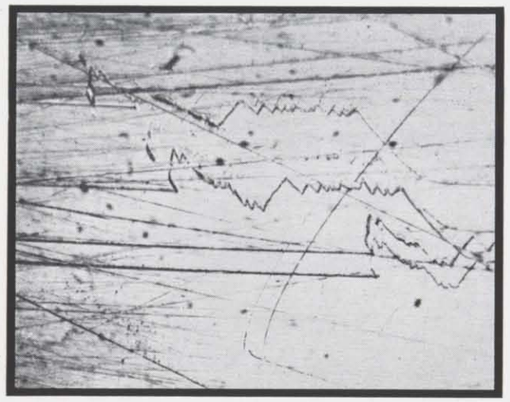

Figure 4

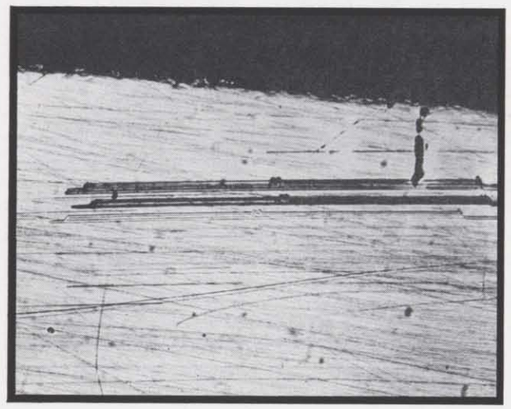

Figure 5

▲

Figure 6

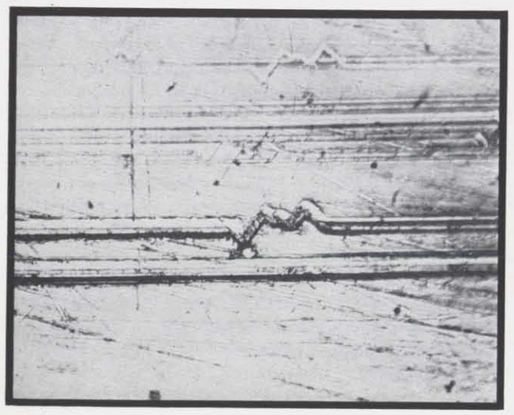

of gravity, and multiplying by 100 to get the percentage.

With the exception of the I-beam crane, the observed deceleration is about 10 per cent of gravity as shown in the last column of Table I. However, the measured stresses are somewhat less than those which correspond to the observed braking force except for the laboratory crane.

The acceleration and deceleration stresses for the I-beam crane were somewhat larger on the top flange than on the bottom flange. The average value is given in the table.

Table II gives the results of the impact tests on the various cranes. The static stress referred to in this table is that due to the live load. For the jerk impact test, this is the only force which causes an impact stress. However, when the crane is run over a bad joint or wedges as in the case of the laboratory crane, there is an impact due to the weight of the trolley and girders, in addition to the live load impact. For this reason, two columns are given for the per cent of impact, the first column is the per cent impact based on the live load, and the other is the per cent impact based on all the loads causing impact. In specifications most impact factors are based only on the live load.

The variation in the impact factor due to changing the length of the hoist is shown in tests 3 and 4 on the laboratory crane, where the impact decreased from 100 to 56 per cent of the live load with an increase in the length of the hoist.

The jerk impacts varied from 9 to 33 per cent.

Bethlehem No. 4 is a skullcracker crane, on which the impact was measured as the ball was released. The measured impact stress was 37 per cent of the weight of the ball and 25 per cent of the weight of the ball and magnet, as found from the scratch records. The center deflection was also measured in this crane with a 0.001 in. Ames dial and the impact measured from the dial was 20 per cent of the ball and magnet. This value may be a little low due to inertia of the dial. The jerk impact (not given in the table) was 12 per cent of the ball and magnet as found from the deflection.

Figure 1 shows the scratch record for one edge of the compression flange in one of the wedge impact tests. All distances in this picture are measured from the centerline of the scratch. The portion AB shows the whipping action of the hoist as the cable tightens. In BC the load is being transferred to the crane. Between C and D the jerk impact can be seen. The distance between the bottom line which is the line of zero stress and the top line DE represents the static stress. At E the crane dropped off the wedges, and the reduction in stress, while the crane is dropping is shown in this portion. Before this stress has been completely released, however, the crane hits the runway rail and point G gives the sum of the static stress plus maximum impact stress. The portion of the curve after H shows the vibrations in the crane after impact.

Some other scratch curves are given for illustration in Figures 3, 4, 5, and 6.

In Figure 3 is shown the static stress and vibration which occur when the load is picked up quickly. The variation of the vibrations about their neutral position is a measure of the jerk impact.

In Figure 4, are shown the acceleration and decelera-

TABLE II

Impact Tests

Crane	Test No.	Type of test	Load	Static stress, lb. per sq. in.		Measured impact stress, lb. per sq. in.	Impact in per cent of:		Distance from hoist drum to hook, ft.	Measured impact from deflection
				Computed	Measured		Computed live load stress	Total load acting in impact		
Lab.	2	Jerk impact	8,200	1530	....	460	33.0	33.0	21.0	...
Lab.	3	*	8,200	1530	1610	850	56.0	31.0	21.0	...
Lab.	4	*	8,200	1530	1400	1400	100.0	51.2	6.0	...
Lab.	5	Jerk impact	8,000	1500	1340	140	9.3	9.3	21.0	...
Lab.	6	Jerk impact	8,000	1500	1500	180	12.0	12.0	21.0	...
Lab.	7	Jerk impact	8,000	1500	1500	180	12.0	12.0	21.0	...
Beth. 4	1	Impact	19,500	1300	1500	475	36.6	25.0	4.0	20.0
Beth. 430	1	Jerk impact	31,000	2500	1800	550	22.0	22.0	16.0	...

*Crane run over $\frac{9}{16}$ in. wedges.

tion stresses for Bethlehem No. 430 in one of the lateral load tests.

Figure 5 is a low-power magnification of the scratch record of Bethlehem No. 430. The left portion shows the stress as the load is lifted. The center shows the acceleration and braking stresses, while the right end shows the release of stress when the load is taken off the crane. Figure 6 shows the lateral stresses of Figure 5 under a higher magnification.

DISCUSSION OF RESULTS

The column for maximum force of deceleration of Table I shows that a value of 10 per cent of the vertical load gives a fair approximation of the lateral load. However, the measured stresses for the Bethlehem cranes are somewhat less than the computed strains. One reason for this is that the computations neglected the walkway and end fixity. Since there were a walkway and end ties on these cranes, these factors probably reduced the lateral stresses. This would be particularly true for Bethlehem No. 430 which was a new crane with a tight end connection. The ratio between the observed lateral stresses and those computed for the bridge girder as a simple beam, based on the observed maximum braking force, vary from 53 to 73 per cent.

The laboratory crane which is old and has practically no end connection would be expected to show no end fixity and in this crane the measured and computed stresses were in fair agreement.

A value of 10 per cent for the lateral load would correspond to a coefficient of friction of 0.20 if one-half the bridge wheels were braked. If all the wheels were braked, the lateral force would be 20 per cent. The value of 0.20 for the coefficient of friction is one which would not be at all unlikely under actual operating conditions.

The lateral end fixity probably can not be taken into account in design, since the end connections on a crane would loosen in service, and reduce the fixity.

On the other hand, some fixity will probably be present at all times, no matter how much the end connection loosens. Any end fixity present however, will provide an additional safety factor if the crane is designed as a simple beam for the lateral load.

The fact that the maximum swing of the load and the maximum acceleration may not have occurred at the same time may also have reduced the observed stress. This can be seen in Figure 2 where it will be noted that there are two peaks in the deceleration curve. These peaks can also be seen in the acceleration and braking stresses in Figure 4. This effect is due to the fact that when the tangent of the angle of swing is greater than the coefficient of friction, the load is being decelerated more than the bridge, and when this angle is less than the coefficient of friction the load is being decelerated less than the bridge. In actual practice, however, a good crane operator will operate his brake in such a manner as to keep the swing down to a minimum.

The impact stresses caused by running the crane off wedges under both ends may represent an unduly harsh condition, if this test is to simulate bad runway joints; because bad joints under both ends of the girder are unlikely to occur at the same time. Further tests, with wedges under only one end of the bridge should be made. In the tests made, this type of impact was the most severe, and it is quite likely that it is the type of impact which should govern in design. The wedge impact tests showed also that this impact is much more severe when the load is close to the hoist drum. Since this is the position in which the load is usually placed as the crane moves down the runway, it should govern in design. Impact due to bad joints is also particularly severe, since the weight of the trolley and girders also contribute to the impact stresses, which is not the case in other types of impact. Whenever the length of hoist is great, the impact will be reduced because of the cushioning effect of the cables.

The jerk impact was a smaller factor than that due to dropping the crane off wedges. If this, then, is always the smaller factor, the design impact factor should not be a function of the hoist speed of the crane.

One interesting effect was noted in the impact test on

the skullcracker. After the switch was cut to release the ball, it took an average of 1.2 seconds before the ball left the magnet. This was apparently due to residual magnetism in the magnet even though the switch was of such a type that a reverse current was applied.

CONCLUSIONS

The dynamic tests discussed in this report indicate that for the cranes tested:

1. The maximum lateral force on a crane was due to braking and was approximately 10 per cent of the vertical forces.
2. Some end fixity was present which reduced the stresses due to the lateral force. However, this fixity probably can not be counted on in design and the full value of 10 per cent for the lateral load should be used in design.
3. Jerk impact, as measured, varied from 9 to 33 per cent.
4. The impact due to running the crane off wedges to simulate bad joints was quite large. For the tests made, values of 56 and 100 per cent of the live load were measured. More tests on this factor are needed.
5. The closer the load is to the hoist drum, the greater will be the impact.

4. Torsional Properties of Fabricated I Beam and Box Sections

▲ THIS REPORT gives the results of a series of torsion tests on riveted and welded I-beams, and riveted and welded box girders. Due to the slipping which occurs in the seams, the fabricated girders were neither as strong nor as rigid as the equivalent girder section without longitudinal seams.

On the basis of the tests which were made, it was found that a riveted section was about one-third as stiff in torsion as a section in which no slipping occurs. Design methods for computing the stresses and twists of built-up girders are included in this report.

The stresses and twist in a hollow tube may be predicted fairly accurately by the theoretical formulæ proposed by R. Bredt. These formulæ state that the average shear stress in the walls of the tube due to torque is:

$$\tau = \frac{M}{2At}$$

The angle of twist per unit length is:

$$\Theta = \frac{M}{GJ}$$

τ is the shearing stress in pounds per square inch, M is the twisting moment in inch-pounds, t is the wall thickness of the tube, A is the area bounded by the center lines of the tube walls, G is the shear modulus (about 11,500,000 lb. per in.^{2} for steel), and J is the torsional constant in in.^{4}.

J is analogous to the polar moment of inertia and for a hollow tube:

$$J = \frac{4A}{\Sigma \frac{s}{t}}$$

where s and t are the length and thickness of each side.

The above formulæ apply to hollow tubes of all shapes which are bounded by one single line. The formulæ are approximate, but give close results when the thickness of the tube wall is small in comparison with the distance of the wall from the center of gravity of the tube. For crane girders this approximation is usually small.

The formulæ are derived for one piece tubes, thus they do not necessarily apply to built-up sections since slipping may occur along the longitudinal seams. The torsional strength of a built-up section, loosely bolted together, would be only the sum of the strengths of the individual pieces. This sum is but a fraction of the

Figure 2

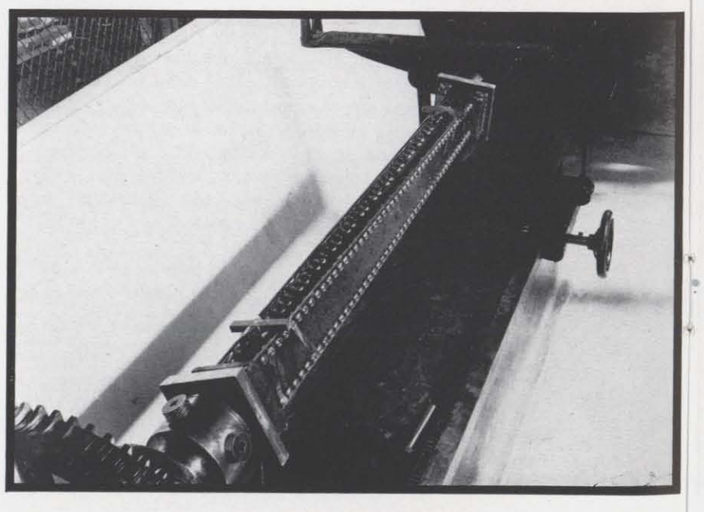

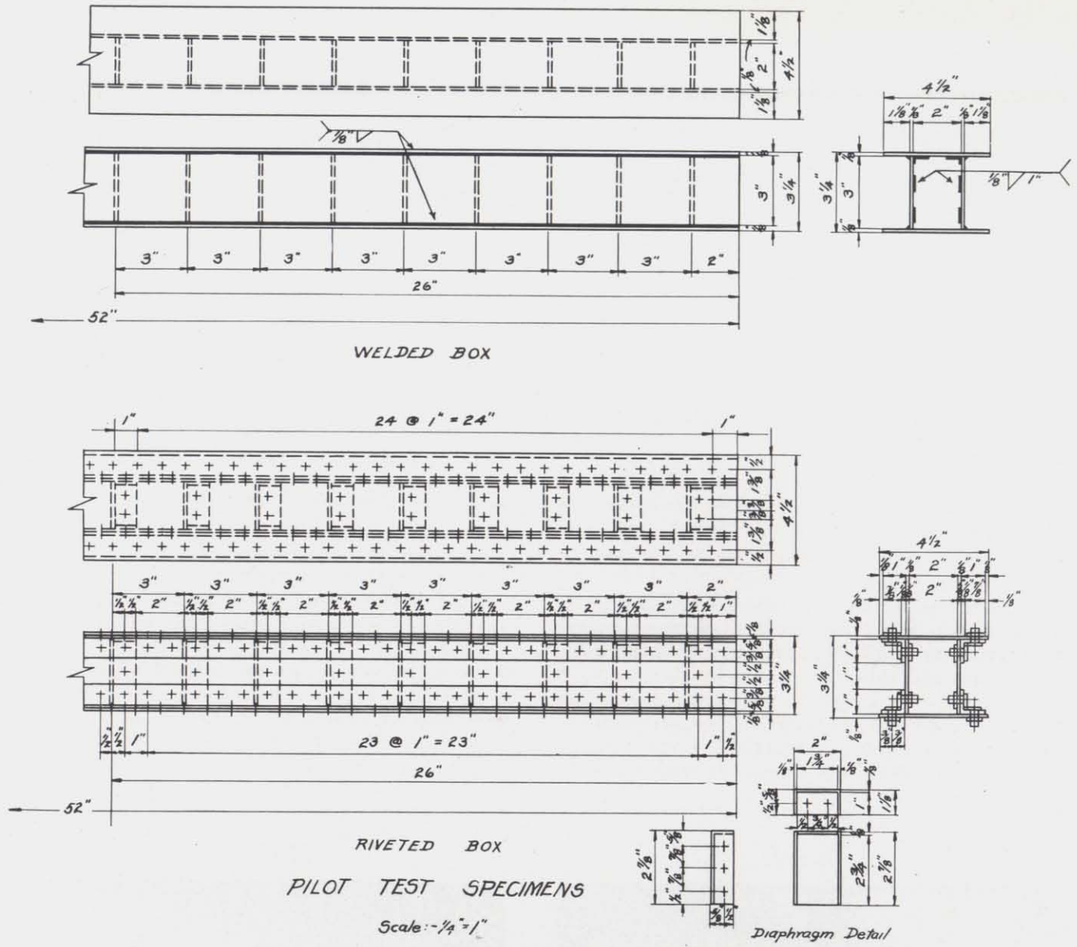

Figure 1

▲

Figure 3

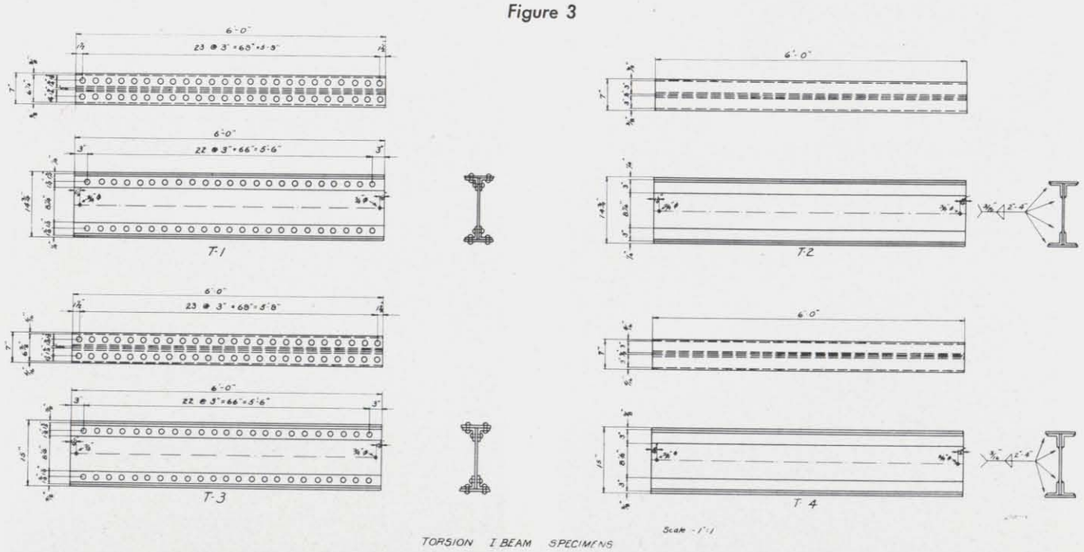

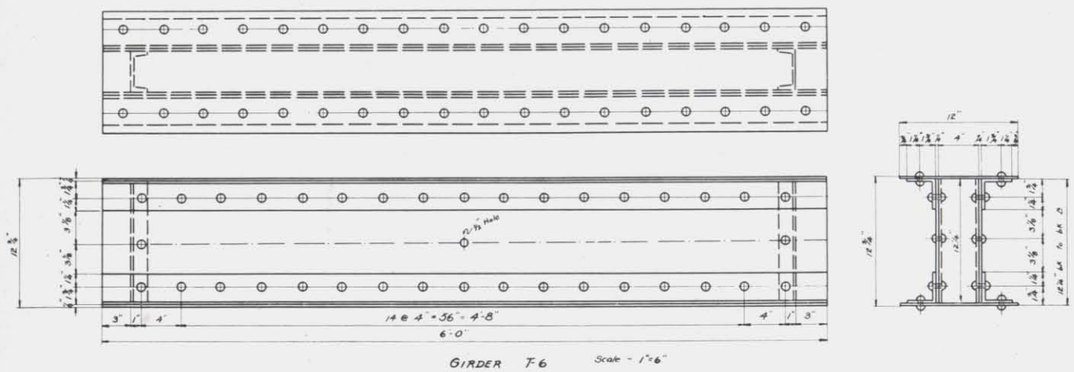

Figure 4

strength of the section as a tube. In a continuously welded section, on the other hand, no slipping can occur along the seams and the twisting strength should equal that of the solid tube as predicted by the theory. A built-up riveted or tightly bolted section should have properties somewhat less favorable than the welded or solid tube since a limited amount of slip may occur.

This series of tests was made to determine how the actual behavior of built-up box sections compared with that of one-piece sections. In addition, built-up I-beams were also tested to compare their behavior with solid I-beams, for which rational methods of analysis are available. ("Structural Beams in Torsion," Inge Lyse and Bruce G. Johnston, *Transactions A.S.C.E.*, 1936, p. 1389; *Bethlehem Manual of Steel Construction*, p. 279.)

Pilot tests were made on a series of small 2 by 3 in.

Figure 5

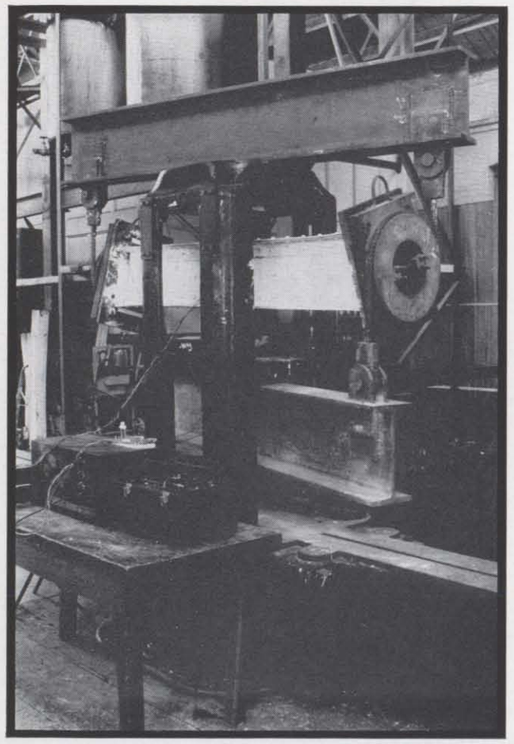

Figure 6

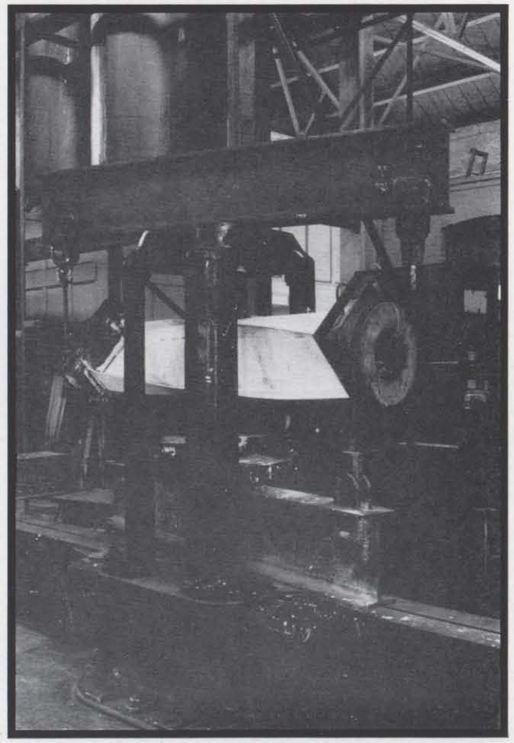

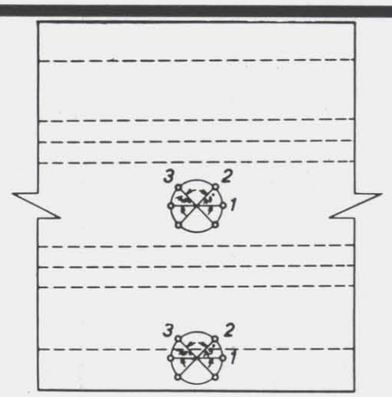

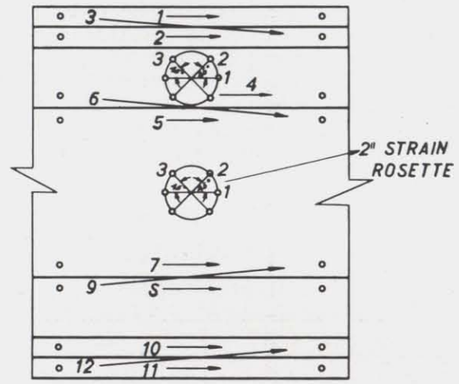

LOCATION OF STRAIN GAGE LINES

Figure 7

▲

Figure 8

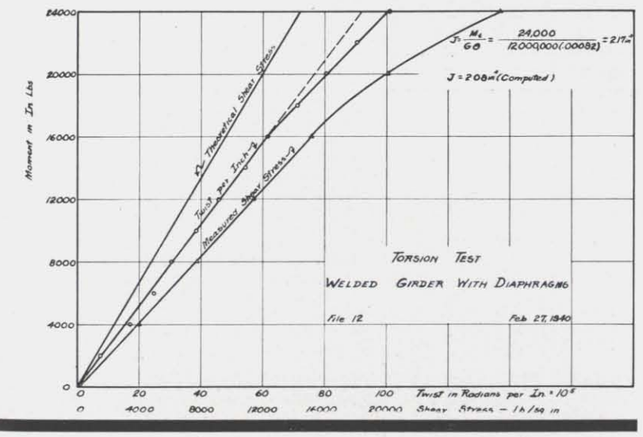

box sections, 50 in. long and made of $\frac{1}{8}$ in. plate. The sections consisted of welded and bolted boxes as shown in the drawing of Figure 1. These boxes were tested in a torsion machine of 24,000 in.-lb. capacity. Figure 2 shows a picture of the bolted box being twisted in the testing machine.

The bolted girders were made to simulate the action of a riveted girder by using $\frac{3}{8}$ in. bolts which fitted tightly in the holes. Tests were made on the bolted girder with the diaphragms fastened on one, two, and three sides, and with diaphragm spacings varying from 3 to 48 in.

Pilot torsion tests were also made on two welded boxes, one had diaphragms as shown in Figure 1, the other had no diaphragms. Three tests were made on the box with the diaphragms. It was first tested with the section shown in Figure 1, then it was tested with flange angles welded to the box to make the section similar to a riveted section. Finally, the top plate and angle were burned off, leaving a plain rectangular box, and the torsional constant was again found.

The welded box in the pilot test behaved as the theory predicted, so further torsion tests were not deemed necessary on the welded sections. However, the twist and the stresses in the bolted box were so much higher than that predicted by theory, it was thought advisable to make additional tests on riveted sections. Tests were made, therefore, on four I-beam and three box sections. The details of the I-beams are shown in Figure 3. The details of the box girder called T-6 is shown in Figure 4. The other box girders were similar to T-6 except for the diaphragms. T-5 had no diaphragms and T-7 had four diaphragms equally spaced. The riveted girders were fabricated with $\frac{1}{2}$ in. rivets, which were designed to take the longitudinal shear of the girders under a concentrated center load.

Since these specimens were too large to be tested in an ordinary torsion machine, they were loaded by a special rig attached to a 300,000 lb. Olsen machine. ("Torsion Testing Machine of 750,000 Inch-pound Capacity," Bruce G. Johnston, *Engineering News-Record*, Vol. 114, No. 9, p. 310, February 28, 1935.) Figures 5 and 6 show the details of the load rig and also show girders T-2 and T-6 being tested. The girders were free to warp at the ends except as the warping might be influenced by frictional forces at the ends.

The twist in the girders was measured by means of level bars. The strains, from which the stresses were determined, were measured with a 2 in. Olsen and a 10 in. Whittemore strain gauge on the outside of the boxes and both sides of the I-beams. The strains were measured longitudinally along the girder and on strain rosettes located on the webs and flange. The shear stresses were found from the strain rosettes. So far as the author knows, very few tests have been made in which the stresses have been measured in box beams under torsional loads. ("Torsion of Rectangular Tubes," William Hovgaard, *Journal of Applied Mechanics*, September 1937, p. A-131.)

The slip in the seams of the girder was measured by the Whittemore gauge with one end of the gauge on one side of the seam and the other end on the other side of the seam. The locations of the gauge lines are

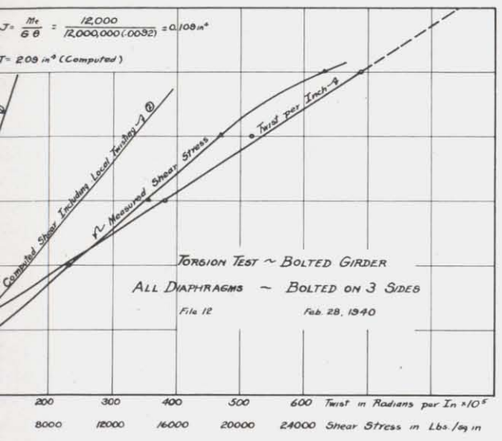

Figure 9

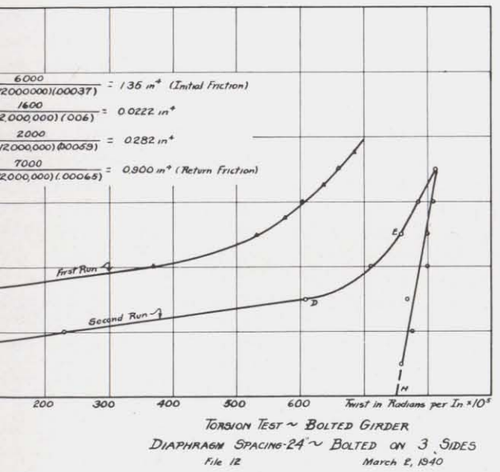

Figure 10

▲

Figure 11

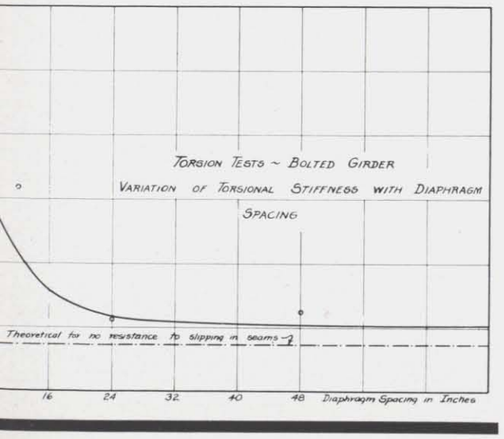

shown in Figure 7. The gauge lines marked 3, 6, 9, and 12 are a measure of the slip when corrected for the actual strain in the elements themselves.

TEST RESULTS

Pilot Tests—Table I presents the results of the twisting tests on the pilot specimens. The torsion constants of the welded boxes agree with the theoretical values of 2.09 in.⁴. The flange angles and outstanding portion of the coverplate have little effect on the results. Neither did the diaphragms have any appreciable effect, since in these girders no slipping occurred to bring the diaphragms into action.

The values of the torsion constants, as shown in Table I, are quite variable for the bolted girder. They are much less than that given by Bredt's theory for a box. This is due to the slipping which occurred along the seams of these girders. As the table shows, the diaphragms had an important effect on the twisting of the beam. When the diaphragms were fastened on three sides, they were much more effective than when fastened on two sides. Secondly, increasing the number of diaphragms, when bolted on three sides, increased the stiffness of the girders.

Figure 8 gives the results of the torsion test on the welded box. The outside stresses, as measured, are

TABLE I

Welded Girder

Measured values of J in.⁴	Remarks on test
2.17	3 in. diaphragm spacing
2.25	3 in. diaphragm spacing (Flange angles added)
2.03	3 in. diaphragm spacing (Flange angles cut off)
2.09	No diaphragms
2.09	Theoretical value by Bredt's theory

Bolted Girder

Measured values of J in.⁴			Remarks on test
Slipping	Built-up	Friction	
.0391	.242	...	3 in. diaphragm spacing Diaphragms bolted on 1 side
.0393	.445	...	3 in. diaphragm spacing Diaphragms bolted on 2 sides
.1090	...	...	3 in. diaphragm spacing Diaphragms bolted on 3 sides
.0647	.180	...	6 in. diaphragm spacing Diaphragms bolted on 3 sides
.0639	.229	...	12 in. diaphragm spacing Diaphragms bolted on 3 sides
.0222	.282	1.35	24 in. diaphragm spacing Diaphragms bolted on 3 sides
.0250	.131	1.32	48 in. diaphragm spacing Diaphragms bolted on 3 sides
.0204	.264	1.02	No diaphragms
.0146	...	...	Theoretical value for freely slipping bolts

TABLE II

Girder	Twist, Θ in radians per in.	Shear in web		Shear in flange		Direct stress in web, 4 in. from center line		Direct stress, edge of flange		
		Measured	Computed $\tau=tG\Theta$	Measured	Computed $\tau=tG\Theta$	Measured	Computed	Angle, measured	Cover plate, measured	Computed*
T-1	.0057	16,800	17,100	26,600	34,200	−12,600	−10,300	+11,500	+16,400	+12,500
T-2	.0040	12,800	12,000	16,000	24,000	− 3,600	− 4,900	+ 9,500	+ 6,000	+ 6,000
T-3	.0024	13,400	10,800	16,000	21,600	− 1,800	− 1,800	+ 3,200	+ 3,700	+ 2,100
T-4	.0014	6,200	6,300	7,600	12,600	− 1,200	− 600	+ 800	+ 700	+ 600

All values given for torque load of 40,000 in.-lb.

*Formula for direct stress at edge of flange:

$$f=E\Theta^2\left[\frac{h^2}{8}+\frac{w^2}{8}-\frac{th^3+6h^2tt'+2t'w^3+2t''h^3-16t''a^3}{24(ht+2t'w+ht''-4at'')}\right]$$

Formula for direct stress in web:

$$f=E\Theta^2\left[\frac{y^2}{2}-\frac{th^3+6h^2tt'+2t'w^3}{24(ht+2t'w)}\right]$$

h = height of web
t = web thickness
t' = flange plate thickness
w = width of flange
t'' = thickness of flange angie
a = distance to bottom of flange angle
y = distance to point in web where stress is computed
Θ = angle of twist in radians

about 60 per cent grester than the theoretical average as computed by Bredt's theory. The twist checks closely. Figure 9 gives a similar curve for a bolted girder. Two computed shear stresses are shown in this figure. The lower stress curve marked 1 is that given by Bredt's theory, while the higher value marked 2, includes the shear stress due to the twisting of each side of the box. This second factor is small for a box with no slip and can be safely neglected. It is large, however, in the present case.

Figure 10 gives the results of the torsion test on the bolted girder with the diaphragms spaced at 24 in. It shows in detail the action of the girder. When the girder is first twisted, as shown in the curve marked "First Run," the box is initially very stiff due to the friction of the seams. However, as the load is increased, the joints slip, and the friction is gradually broken. The portion of the curve marked *CD* shows the twist which takes place while the bolts are slipping. Most of the total twist occurs in this range. At point *D*, the bolts start to bear and the portion of the curve beyond *D* shows the increased resistance to slip which results. At point *F*, the load was released, and the section *FH* on the curve shows the effect of the return friction in preventing the girder from untwisting. If the testing machine had been of such a type that the box could have been twisted in the reverse direction, it is expected that the resultant curve would have a large hysteresis loop.

Figure 11 shows the variation in the torsional stiffness as the number of diaphragms is increased.

I-Beam Tests—The test results on the I-beams were quite similar. T-1 and T-2 were identical in section but T-2 was welded and T-1 was riveted. T-3 and T-4 were similar to T-1 and T-2 except that the sections of the former were ⅜ in. thick, and the sections of the latter were ¼ in. thick.

Since T-2 and T-4 were welded, less slip could occur. Therefore, the stresses and twists in these girders should be less than those of girders T-1 and T-3.

Figure 12 compares the twists of the four I-beam girders under a torque load. The rotation given is the average of the rotation of the flanges and the webs except for T-3 for which the top twist is given. The top twist of T-3 is somewhat less than the average, since the web usually twisted a little more than the flange. The values for the torsion constants are appreciably less than the theoretical values for the equivalent solid I-beam.

Figure 13 gives the magnitudes of the shear stresses in the web and coverplate of the four I-beam girders. This figure shows that in the same girder section, as for example T-3 and T-4, the measured stresses in the riveted section are about twice that of the welded section. This is the result of the greater twist of the riveted girder. The shear stresses in the flange are greater than those in the web. Theoretically, disregarding stress concentrations, the flange shearing stresses should be twice the web stresses for the girders tested since the flange is twice as thick as the web.

Table II gives a comparison of computed and measured stresses for the 40,000 in.-lb. load. The shear stresses were computed by the formula $\tau=tG\Theta$, where τ is the shearing stress, and t is the thickness of the section considered. This formula comes directly from the formulæ for twist and stress of a narrow rectangular section. The web stresses check closely as shown by the

table. The flange stresses are larger than the web stresses but smaller than the theoretical. This shows that some slippage is taking place and that the full thickness of the flange can not be assumed to be acting as a unit.

Figure 14 gives curves for the variation of the slip with the twist and the moment for girders T-1 and T-2. Similar results were obtained for T-3 and T-4. The slip given is the total of the slips in all the seams around the girder. It should be noted that for T-1, the twist is proportional to the slip. The slips for T-2 are much smaller than for T-1. The values for T-2 are not actually slips since the seam was welded, but since the welding was intermittent, the welds are strained higher than the adjacent plates and this results in a relative strain between the plates.

Secondary longitudinal direct stresses are set up in a twisted I-section or box as a result of the tendency of the fibers farthest from the center of twist to be lengthened. In Figure 15 are plotted the curves of direct stress in T-1 as actually measured. Table II gives a comparison between computed values of the stress and the measured values at the 40,000 in.-lb. load. These stresses are quite appreciable. The formula for the direct stress in the I-beam was derived in a manner

Figure 12

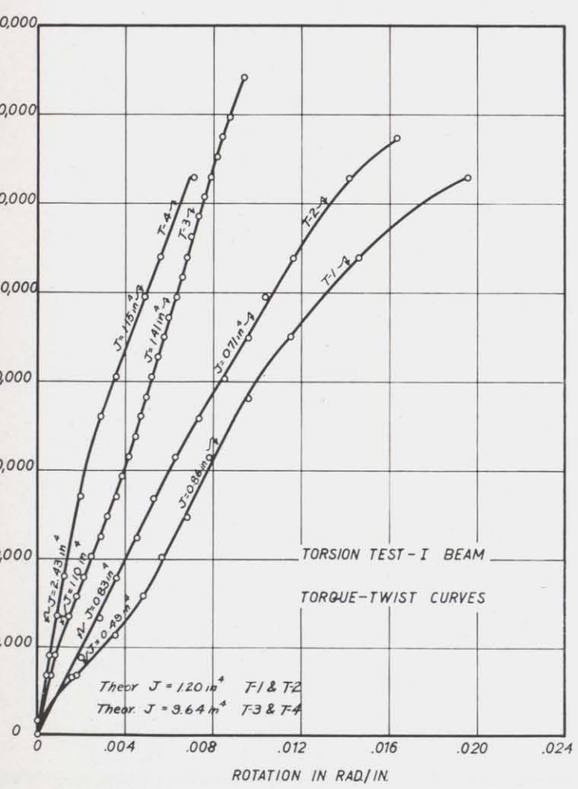

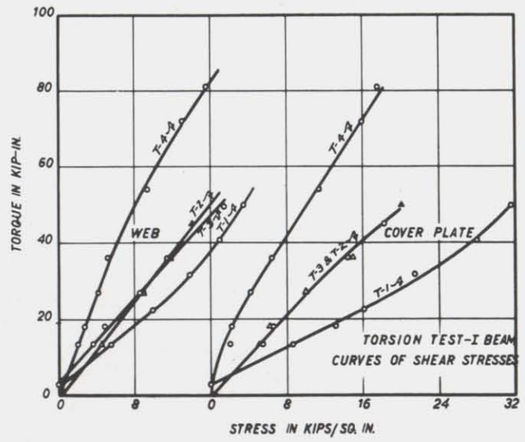

Figure 13

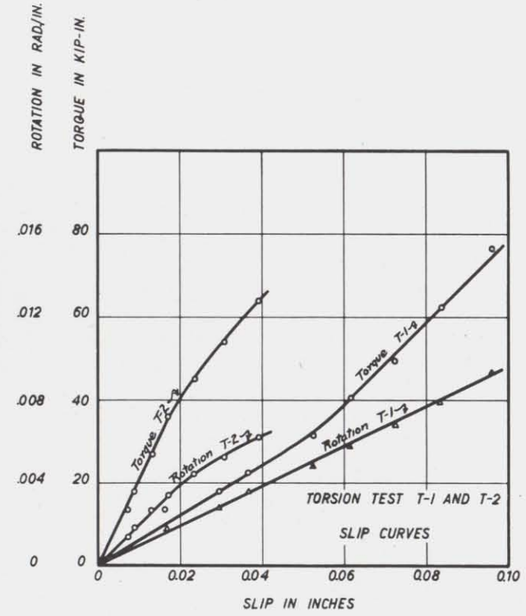

Figure 14

▲

Figure 15

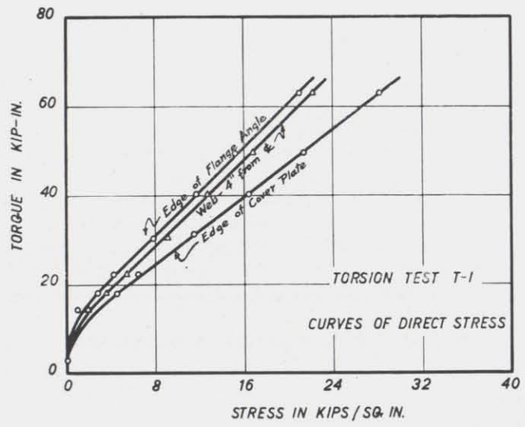

similar to that which Timoshenko uses for the rectangle in torsion (*Strength of Materials*, vol. 1, S. Timoshenko). It should be noted that the stress increases with the square of the twist. Since the built-up beam twists more than the solid beam, these direct stresses are much more important than in the solid beam. The computed stress in the webs checks fairly well with the theory but the stresses in the flange do not check as well. This is probably due to the slipping which occurs, as indicated by the fact that the stresses at the edge of the cover plate and at the edge of the flange angle are quite different, showing a relative slip.

Box Girder Tests—The three box girders were alike except for diaphragm spacing. T-5 had no diaphragms, T-6 had one diaphragm in each end, and T-7 had four diaphragms equally spaced. After T-7 had been tested the first time, the seams were welded with intermittent welds to prevent slippage and the girder retested. This test was called W-T-7.

Very little difference was found in the tests on the three boxes, so apparently the diaphragms were of little effect in the elastic range. These diaphragms were riveted only to the webs as is the usual practice, and thus are relatively ineffective in preventing slip. Since the results for all girders are so very much alike, the test results will be given only for T-6.

In Figure 16 is plotted the twist of the box as the moment was increased. Figure 17 gives curves showing the measured slip and measured stresses in the box.

The measured shears in the flange and web are fairly close to the theoretical. The theoretical shear curve marked 1 is the stress as found from Bredt's formula. The other theoretical curve marked 2 is the sum of the stress from Bredt's theory and the stress due to the twisting of the elements of the box.

The shear curves are computed from the strain rosette data and are the shears acting on the cross-section of the girder perpendicular to the longitudinal axis. The rosettes in the portion of the webs and flanges forming the box showed that the direct stresses on these cross-sectional planes were negligible.

In the rosettes on the outstanding portions of the cover plates and flange angles outside the box section, the measured shear stresses were less than the theoretical shear stresses in the box. The direct stresses determined by these rosettes were appreciable, showing that these sections were not subjected to pure shear.

The direct stress at the edge of the flange as shown in Figure 17 is appreciable for high loads, but in the working range this stress is zero. This stress is a secondary stress and increases with the square of the twist.

The stress in the diaphragm is rather large. This stress was taken on a gauge line 45 degrees with the horizontal since it was thought that the slip in the

Figure 16

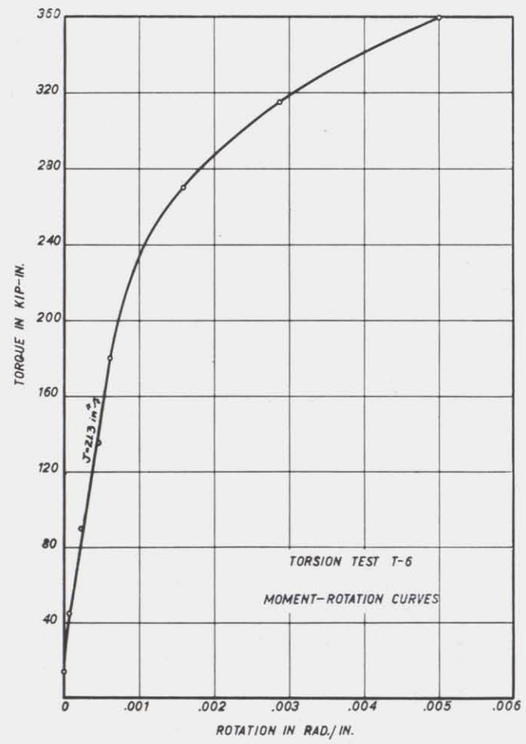

Figure 17

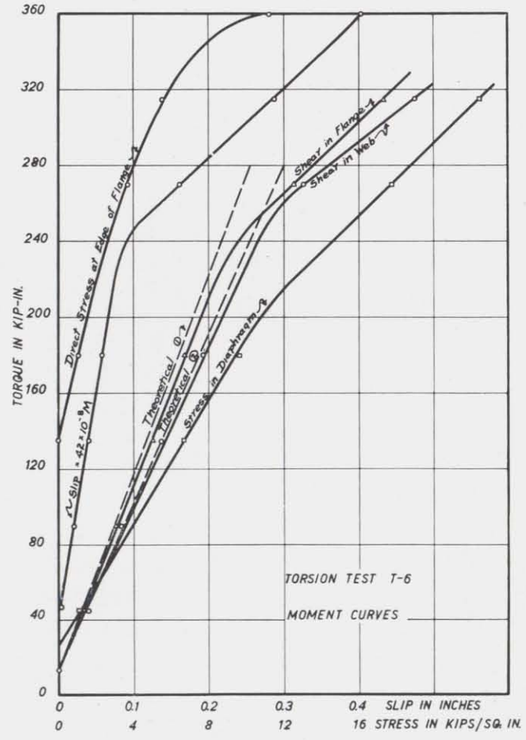

girder would stress the diaphragm with a twisting moment. However, this measured stress is much larger than any which were computed.

The slip in the girder is quite appreciable. The slip did not start with the initial torque but at a torque load of about 45,000 in.-lb. If an initial tension of 32,000 lb. per sq. in. is assumed in the rivets and a coefficient of friction of 0.2 is assumed to be acting between the plates, the load at which slippage will occur is 44,000 in.-lb.

In making these tests, one has to be careful that the torque is applied equally to the whole girder section. The test on T-5 was made with the torque applied to the webs. Figure 18 shows that the top flange and web did not twist equally. The average rotation, however, is about the same as that for T-6 and T-7.

The test results for T-7 after the seams were welded are shown in Figure 19. It is seen that this girder is then much stiffer. The shear curves also check the theoretical computed from Bredt's formulæ, because there was no added twist due to slip.

DISCUSSION OF RESULTS

Pilot Tests—The pilot tests on the box girders showed that the actual twist in a welded box agreed with the theoretical, and that Bredt's formula gives a good value for the torsional constant. These tests also showed that the flange angles, and outstanding edges of the cover plate had little effect on the torsional constant.

The shear stresses on the outside of the box were about 60 per cent greater than the theoretical average value from Bredt's formula. This may be due to the eccentric application of the load through the fillet weld. Since the plate is thin, and the box section very small, this effect is emphasized in this test, and it would be picked up by the comparatively long 2 in. gauge length of the strain gauge. This effect was not noticed in the larger specimens, and it may be a peculiarity of the small specimen.

The pilot tests on the bolted girders probably have no practical significance by themselves. Their chief value is that they exaggerate and emphasize the effects due to slipping in the seams of a riveted girder. As shown by Figure 11, the torsional stiffness of the girder approaches that of the sum of the component parts as the restraints to slipping are removed.

I-Beam Tests—The shear and twist of a long narrow rectangle are given by the formula

$$\tau = \frac{3M}{bc^2}$$

$$\text{and } \Theta = \frac{3M}{bc^3G}$$

$$\text{and } \tau = cG\Theta$$

Figure 18

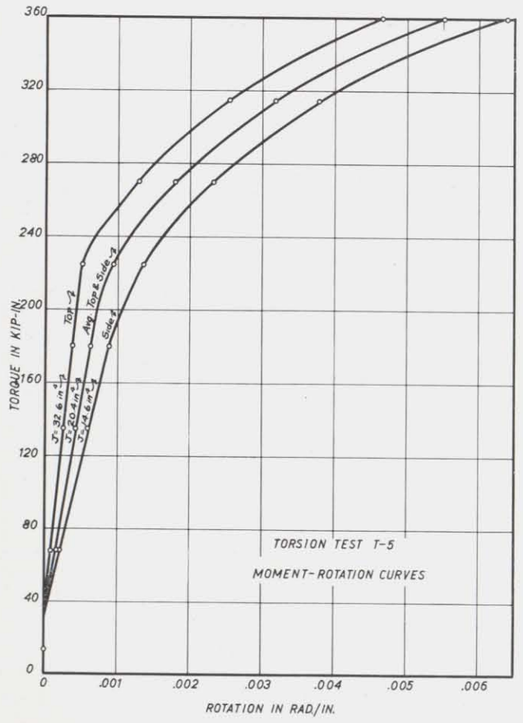

Figure 19

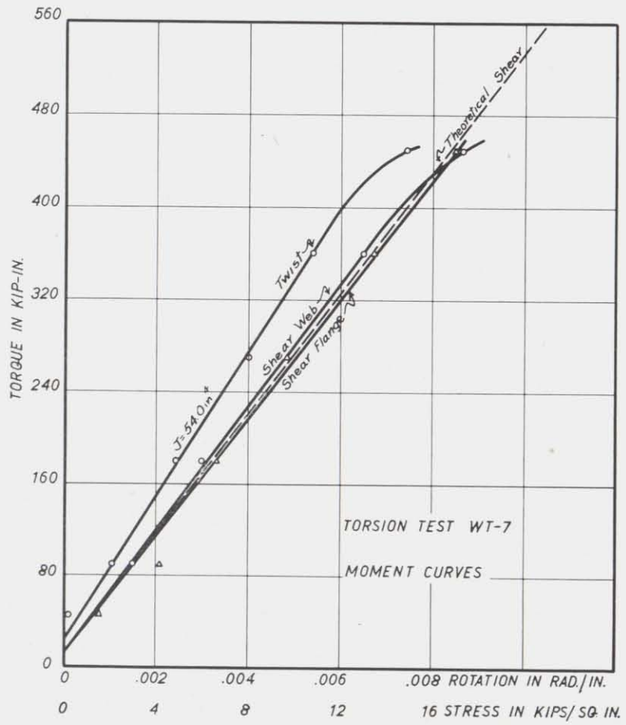

where τ is the shear stress, Θ is the angle of twist in radians per inch, b is the width of the rectangle, and c is the thickness of the rectangle. Since an I-beam is composed of a number of rectangles, an approximate solution for the torsional stresses and twist can be made by dividing the I-beam into a number of rectangles and summing up the sections. However, since the plate thickness enters into the formulæ as square and cube terms, it becomes a question as to what thickness to use when several rectangles are put together. Figure 20a gives a diagrammatic idea of the shear stress distribution when slipping is allowed to occur freely. Figure 20b gives a similar picture for the solid girder in which no slipping occurs. The increased strength due to the greater effective moment arm of the shear stress is apparent. For a riveted girder where some slipping takes place the resultant stress distribution falls between the two distributions shown in Figures 20a and 20b.

In Table III are given the computed torsional constants of the various girders tested. Two values are given, one is computed assuming free slippage and the other is computed on the basis of no slippage. The measured torsional constants for the riveted girders average a little more than one-third of those for the equivalent solid section. The welded girders average 68 per cent. The welded I-beam girders do not have a factor of 100 per cent, since, although the weld does prevent slipping at the toe of the angle, relative strain can occur at the corners of the angles.

For design computations, if a value of the torsion constant of one-third the solid section is used, the computed angles of twist should be fairly close to the actual values. To compute the stresses, these values of Θ should be used in the formulæ. As shown in Table II, the computed stresses are close enough for design purposes. There is little need to go into any refinements in the calculations since the behavior of the girder will depend largely on the slip. Since this slip depends on many factors, and is relatively unpredictable, the behavior of the girders may be quite variable.

The direct stresses shown in Table II are quite large. Since the direct stresses increase with the square of the twist, and the twist of the riveted girder is three times that of the solid girder, these direct stresses will be nine

TABLE III

Girder	Computed J, in.		Ratio Col. 1 / Col. 2	Measured J, in.⁴	Ratio Col. 4 / Col. 1	Ratio Col. 4 / Col. 2
	Sum of individual parts	Solid beam				
	1	2	3	4	5	6
T-1	.26	1.20	.22	.49	1.89	.41
T-2	.26	1.20	.22	.83	3.20	.69
T-3	.88	3.64	.24	1.10	1.25	.30
T-4	.88	3.64	.24	2.43	2.76	.67
T-5	.38	57.80	.01	20.40	53.70	.35
T-6	.38	57.80	.01	21.30	56.00	.37
T-7	.38	57.80	.01	20.30	53.50	.35
WT-7*	.38	57.80	.01	54.00	142.00	.94

*Girder T-7 with intermittent welds on seams to prevent slipping.

Figure 20

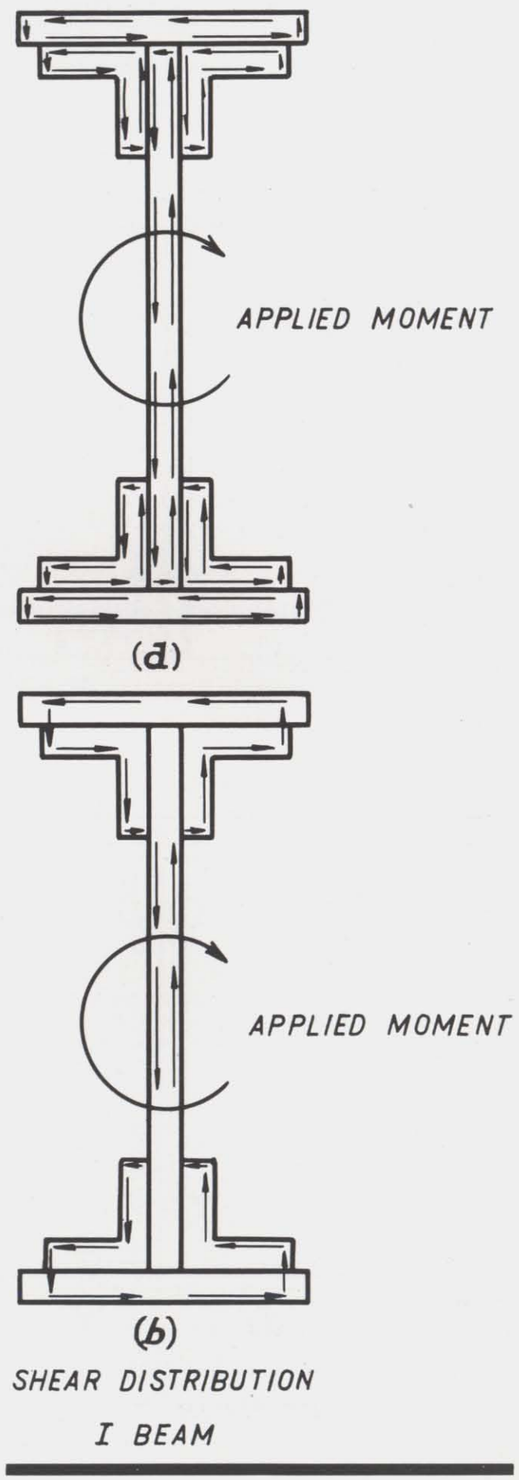

times those in the solid girder. The direct stresses are secondary stresses and therefore have little effect on the ultimate load-carrying capacity of the girder. However, a permanent twist will result in the girder, if these stresses exceed the yield point.

Tests of Box Girders—The tests on the riveted girders showed that they behaved about as predicted by Bredt's formula, except as this is modified by slip. Table II shows that the torsion constant is about one-third that which is predicted by Bredt's theory. In computing this torsion constant, one must remember that the built-up rectangular section is not a box but a figure more like an H-beam since the stress in the flange must travel outside the box section to the rivet and back again before it is transferred to the web. Figure 21a shows the section acting in the stress transfer. The dotted line shows the edges of the section used to compute A in Bredt's formula. Figure 21a also gives a diagrammatic picture of the shear stress transfer in a box section where slipping is allowed to occur. Figure 21b shows the shear stress transfer when no slipping occurs. The reason for the effectiveness of the box section is obvious when one notices the large effective moment arm of the shear stress.

Figure 21

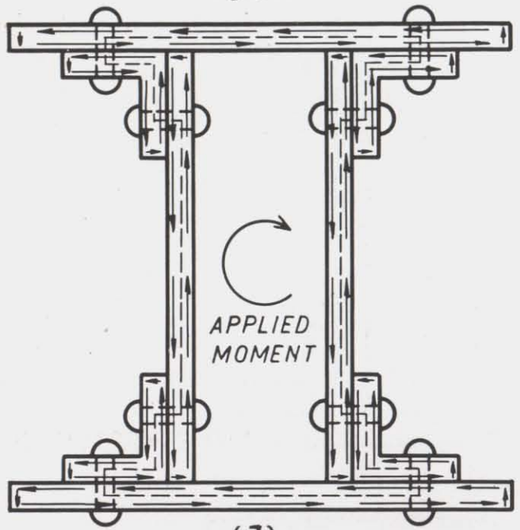

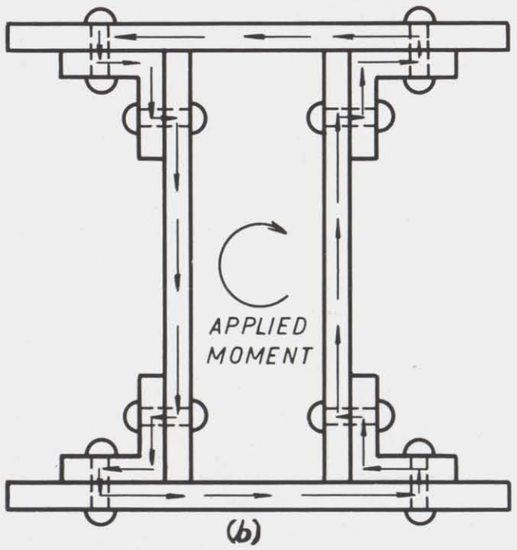

SHEAR DISTRIBUTION
BOX GIRDER

The shear curves for Figure 17 show that Bredt's theory gives a fair approximation for the average shear stress, and this computation can be made more exact by adding the stress due to the twist of the sides of the box. Bredt's theory assumes that the shear stress is constant through the thickness of the box, and when the thickness of a wall is small in comparison with the distance of the plate to the center of gravity of the box, this approximation is small. Actually, the stress increases from the inside of the box wall to the outside. The correction added to the average shear as given by Bredt's formula gives the maximum stress on the outside of the box. Since the riveted box twists more than the solid box, the correction is larger for the riveted box. In Figure 19 this correction is negligible since the welded box did not slip resulting in a smaller angle of rotation.

The direct secondary stress in the box as shown by Figure 17 can be safely neglected in the working range.

The stress in the diaphragms was larger than expected. It may have been affected by local bending and readjustments. The direct stresses for the welded girder were much less than those for the riveted girder.

The measured slip in the joints as given in the curves is the total of the slip in all the seams. The actual slip in any one corner of the box is the plotted slip divided by four. It can be shown (N.A.C.A. Report No. 502, "A Theory for Primary Failure of Straight Centrally-loaded Columns") for a box with free slipping seams (no rivets or welds) that the longitudinal motion or warping of any point in the box section is the product of the x and y coördinates of the point multiplied by the angle of twist Θ when slipping occurs in all the seams. Since in the same corner, the web and the flange warp in opposite directions, the relative slip is equal to twice this product. Thus the relative slip in the corner of a box of height h and width w would be $wh\Theta/2$. When the box is riveted, the actual slip is less than the computed value above, and this actual slip is a measure of the torsional constant. For the gauge lines on which slip was measured in the test, the relative slip for loose seams is 42Θ. For girder T-6 the measured slip for the straight line portions of the slip curve is $10.5M(10)^{-8}$ for one seam.

Then the twist angle is given by:

$$\Theta = \frac{M}{GJ\ (\text{no slip})} + \Theta\ (\text{due to slip})$$

or $$\Theta = \frac{M}{GJ} + \frac{10.5M(10)^{-8}G}{42G}$$

$$= \frac{M}{G}\left(\frac{1}{57.8} + \frac{1}{33.3}\right) = \frac{M}{G}\left(\frac{1}{21.2}\right)$$

The value of 21.2 is the effective torsion constant, and provides a check on the value computed directly from the curve. This check is not absolutely independent, since the value of Θ is inherent in the second term.

CONCLUSIONS

The torsion tests herein reported indicate that the following results may be concluded.

1. Fabricated I-beam and box sections do not behave the same as the equivalent solid sections.
2. The slip which occurs in the seams of built-up sections is appreciable under torsional loading and increases the twist and stresses of such sections markedly.
3. The torsional constant of the riveted built-up I and box sections tested in this program was about one-third that of the equivalent solid section.
4. If the twist angle Θ is computed using the reduced value of the torsional constant, shear stresses computed from this value will agree fairly well with the actual values for I-beams.
5. Direct secondary stresses are quite large in the built-up I section and may be important.
6. Direct secondary stresses are small in a box section when stressed in the working range.
7. The direct stresses vary with the square of the angle of twist.
8. Bredt's theory gives good approximate values for the shear stress in box sections.
9. In applying Bredt's theory to a fabricated box section, one must be careful to use the section bounded by the stress path. This will not be a rectangular section when the corners are formed by riveted angles.
10. Built-up welded I-beams fabricated with flange angles had a torsion constant two-thirds that of the equivalent solid section.
11. Built-up welded box girders had a torsional constant close to that predicted by Bredt's theory.
12. The outstanding legs and parts of a fabricated box section not included in the box have little effect on the torsional properties of the section.

5. Box Girder Buckling Tests

▲ THIS REPORT describes the results of three series of buckling tests on a number of box girders.

The first series of tests investigated the length-width of box or l/b ratio of the girders. This series was divided into two parts. In the first part, the girders were loaded with a vertical load only, and in the second part the girders were loaded with both a vertical load and a lateral load applied to the top flange. The lateral load caused a lateral moment which was 10 per cent of the vertical moment. Both riveted and welded girders were tested with l/b ratios varying from 110 to 60. In no test was there any sign of lateral buckling, and all the girders failed because of local yielding.

The second series investigated the coverplate width-thickness or w/t ratio of the girders. This series was also divided into two parts. In the first part, the girders were loaded on the top flange at diaphragm points, and in the second part, the girders were loaded through a rail at a point half-way between the diaphragm points. Welded girders were tested with w/t ratios varying from 32 to 96. The ultimate strength of the girders and the buckling strengths are given in this report.

The third series investigated the web height-thickness or h/t ratio of the girders. Welded girders were tested with h/t ratios varying from 320 to 144. The girders with the h/t ratio of 320 had a horizontal stiffener. The buckling loads of the web plates were computed by Southwell's method and the loads at which buckles could first be noticed are given in this report.

In this investigation, tests were conducted to determine the buckling strength of the component parts of box girders, and the buckling strength of the girders as a whole. Since the present tendency of design is to use higher allowable design stresses, a more exact knowledge of buckling loads is necessary. This is particularly true when high-tensile steel is to be used. The buckling strength of a structure in the elastic range does not depend on the strength of the steel but on the form and the modulus of elasticity. A more precise knowledge of buckling is therefore necessary when high-tensile steel is used in order to take advantage of the higher strength of such steel.

The allowable thickness ratios in many box girder specifications have been taken from bridge specifications such as the A.R.E.A. Specifications for Steel Railway Bridges. These bridge specifications were primarily written for I-beams and do not necessarily apply to box girders. Since the edges of the plates forming box girders are usually held more rigidly than the edges of the plates in I-beams the plates forming the box girder should not buckle as easily.

In addition, the maximum allowable compression stresses in a box girder are usually much too low. They have been taken from old I-beam formulæ which do not apply. The beam in a bending test must twist if lateral buckling due to bending occurs. Such buckling may occur rather easily in I-beams which are relatively weak in torsion. Box crane girders of normal proportions are

very rigid in torsion and this type of buckling can not occur.

Three series of girder tests were made in this investigation.

In Table A is given a summary of the pertinent data of the tests and test girders. The following is a more extended description of these tests.

l/b Ratio Tests—The first series of tests investigated the unsupported length-width ratios of the girders. Welded girders G-1, G-2, G-3, G-4 with l/b ratios of 80, 60, 40, and 30, and riveted girders G-15 and G-16 with l/b ratios of 58.2 and 29.1 respectively, were subjected to bending tests. These girders were loaded symmetrically about their centerline by two vertical loads placed at distances 5 ft. from each end. The l/b ratios given above are the ratios for the unsupported spans between the load points. The total overall span-width ratios were 110, 90, 70, and 60 for the welded girders and 78 and 61 for the riveted girders.

A high-tensile steel girder G-17 was included in the above series. This girder is a duplicate of G-4 except that it was made of Mayari-R steel.

In Figure 1 are shown the essential details of the girders tested in the l/b series. These girders were supported on rollers at each end and were loaded through rollers located 5 ft. from each end. Figure 2 is a picture of G-2 in the testing machine. Since the girders were loaded through rollers, there was very little restraint offered the test beam at the load points.

In order to simulate design practice with regard to lateral load allowances, four of the above girders were tested with a lateral load applied to the top flange at the span center in addition to the vertical load. The lateral load was of such a magnitude that the lateral

TABLE A

Series; purpose of test	Girders tested	Variable: Clear span	Variable: Overall span	How tested description	Material		Measurements
		l/b ratio					
1. Length-width ratios Initial tests	G- 1	80	110	Symmetrical vertical loads placed at distances 5 ft. from ends.	Welded	Carbon steel	Stresses: 10 in. W. S. G. Vertical deflection: Strings and mirror Lateral deflection: 0.001 Federal dial
	G- 2	60	90		Welded		
	G- 3	40	70		Welded		
	G- 4	30	60		Welded		
	G-15	58	78		Riveted		
	G-16	29	61		Riveted		
	G-17	30	60		*		
Retests	G- 2a	60	90	Vertical load plus lateral load applied to top flange.			
	G- 3a	40	70				
	G- 4a	30	60				
	G-17a	30	60				
		w/t ratio					
2. Spacing of webs Width-thickness ratios of cover plates Initial tests	G- 5	32		Girders 18 ft. long. Loaded with symmetrical vertical loads on diaphragms at third-points.	Welded	Carbon steel	Stresses: 10 in. W. S. G. Deflections: Vertical—Ames dials Lateral—Ames dials
	G- 6	48			Welded		
	G- 7	64			Welded		
	G- 8	80			Welded		
	G- 9	96			Welded		
	G-18	64			*		
Retests	G- 5a			Girders loaded through rail by vertical loads at points half-way between diaphragms.			
	G- 6a						
	G- 7a						
	G- 8a						
	G-18a						
		h/t ratio					
3. Height-thickness ratio of web	G-10	320		Girders are 18 ft. long. All girders loaded by two vertical loads at one-third points.	Welded	Carbon steel	Stresses: 10 in. W. S. G. Deflections: Vertical—Ames dials Lateral—Ames dials
	G-11	192			Welded		
	G-12	176			Welded		
	G-13	160			Welded		
	G-14	144			Welded		

*Welded Mayari-R steel

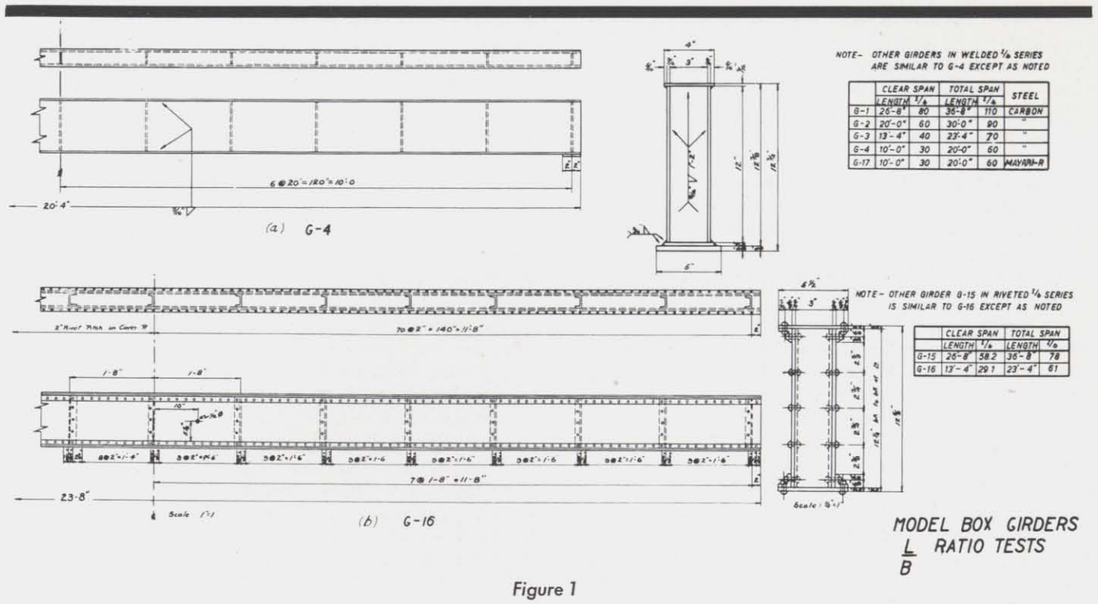

Figure 1

moment at the span center was 10 per cent of the vertical moment. The retests were made on girders G-4, G-3, G-2, and G-17, and the retest specimens are denoted in this report with the letter "a" following the girder number, as for example G-4a. Figure 3 shows a picture of girder G-4a in the testing machine.

Figure 3 →

▲

Figure 2

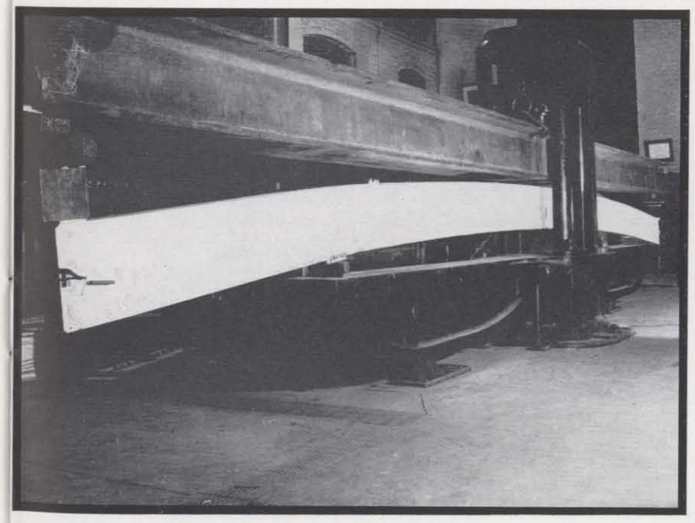

In the first tests, the girders had been loaded to their ultimate load and failure occurred with excessive deflection and local buckling. These girders had to be restraightened for the retests. This was done by turning the girders upside down in the testing machine and applying load until the girders were straight and the buckles had disappeared. The first loading and the straightening process probably affected the yield point of the steel but should have had little effect on the other

properties. The retests were made with the girders in the upside down position.

The stresses in the girders were measured on a number of gauge lines at the span center with a 10 in. Whittemore strain gauge. The vertical deflection was measured on both sides of the girder by the stretched wire and scale method. The lateral deflections of both the top and bottom flanges of the girder were measured with a 0.001 in. Federal dial attached to a portable arm 10 ft. long. The lateral load on the girders was applied by tightening a nut on the lateral load rod, and the magnitude of the lateral load was determined from the strain in the rod.

w/t Ratio Tests—The second series of tests investigated the spacing of the webs, and the width-thickness ratio of the cover plate. These girders were 18 ft. long and loaded with symmetrical vertical loads on the diaphragms at the third-points. The girders in this series were G-5, G-6, G-7, G-8, G-9, with width-thickness ratios for the coverplate of 32, 48, 64, 80, and 96 respectively. Girder G-9 had a longitudinal stiffener along the center line of the coverplate. A high-tensile girder G-18 made of Mayari-R steel, was also tested in this series. This girder is a duplicate of G-7. Figure 4a shows the details of the girders in this series.

Retests were made on four girders in this series identified as G-5a, G-6a, G-7a, and G-8a. Since the girders are loaded through a trolley rail in actual practice, the retests were made to determine whether the coverplate was appreciably weaker when loaded through a rail at a point half-way between the diaphragms. The rail would have a tendency to stiffen the coverplate which would strengthen the coverplate, whereas the wheel load half-way between the diaphragms would stress the coverplate and thus weaken it.

To simulate the rail a 3 in., 5.7 lb. I-section was used in these retests. Girder G-5a was loaded with a single concentrated load at the span center which point is half-way between two diaphragms. Girders G-6a, G-7a, G-8a, and G-18a were loaded through the rail at two points, each 2 ft. from the span center. These load points are also half-way between diaphragms.

The girders had been fabricated with the diaphragms welded to the top flange and webs, thus leaving a space between the diaphragm and bottom flange. Therefore in the retests, the diaphragms probably offered no support to the rail, since the girders were upside down in the retests and the load was applied to what had been the bottom flange.

The deflections of the girders in this series were measured with Ames dials. The stresses were measured with a 10 in. Whittemore strain gauge. The local bending and buckling of the top coverplate was measured with a small contact dial measuring to 0.001 in. over a grid of very small squares for a distance of 12 in. on each side of the center line.

h/t Ratio Tests—In the third series of tests, the height-thickness ratio of the web was investigated. The girders in this series were G-10, G-11, G-12, G-13, and G-14. These girders had web height-thickness ratios of 320, 192, 176, 160 and 144 respectively. The girder with the height-thickness ratio of 320 had a longitudinal stiffener the whole length of the girder at a distance about one-fourth of the way down from the compression flange. Figure 4b shows the details of these girders. These girders were loaded at the third-points so that there was pure bending moment with no shear in the center third of the beam. There were no diaphragms in the center third of the girder. In the sections of the beam between the load point and the end support, there were vertical diaphragms and also a longitudinal stiffener along the center line of the web to prevent shear buckling and to assure failure in the center third of the beam.

Figure 4

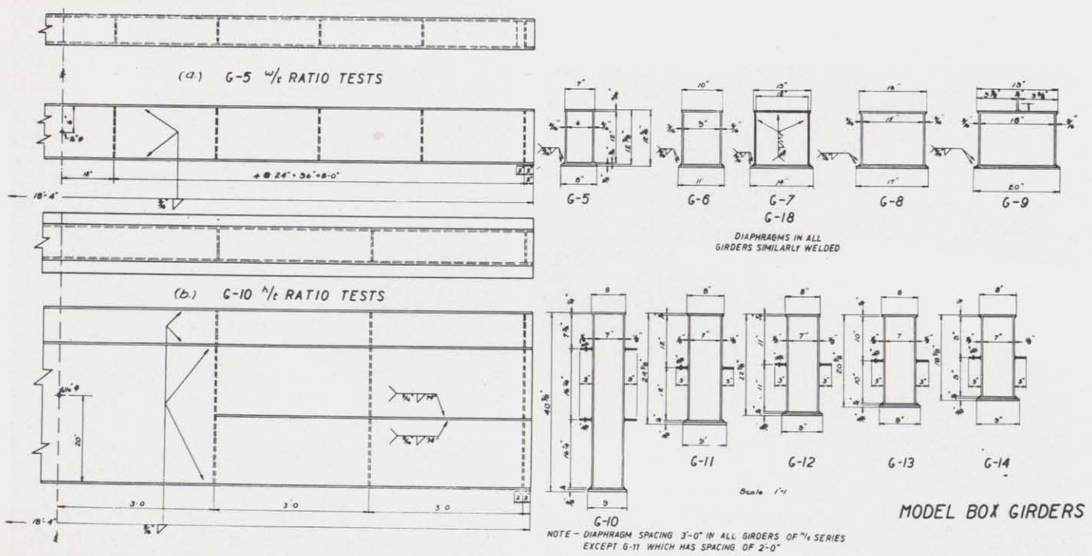

TABLE I

l/b Ratio Tests—Vertical Load Only

1 Girder	2 Theoretical buckling moment, kip-in.	3 Maximum vertical load, kips	4 Maximum applied moment, kip-in.	5 Net vertical moment of inertia, in.^{4}	6 Vertical section modulus, in.^{3}	7 Maximum computed stress, M/S, kips per sq. in.	8 Maximum computed stress, parabolic distribution, kips per sq. in.	9 Average yield point of flange material, kips per sq. in.	10 Unsupported l/b	11 Allowable stress formula, kips per sq. in.	12 Total l/b	13 Allowable stress formula, kips per sq. in.
G- 1	2700	35.0	1050	112.9	18.2	57.8	48.2	44.9	80.0	0	110	0
G- 2	3300	31.5	945	114.0	18.4	51.3	42.7	42.4	60.0	7.4	90	0
G- 3	4240	33.3	1000	114.0	18.4	54.4	45.2	44.7	40.0	13.3	70	3.6
G- 4	4970	32.3	965	117.5	18.9	51.1	42.6	42.7	30.0	15.4	60	7.4
G-15	2480	11.3	1240	151.5	22.0	56.3	42.8	42.0	58.2	4.8	78	0
					26.3	47.3						
G-16	2860	40.1	1200	147.8	21.4	56.0	42.8	45.9	29.1	14.7	61	8.0
					25.6	47.0						
G-17	4970	46.0	1380	117.0	18.9	73.1	60.8	63.2	30.0	21.3	60	4.0

Girder G-10 was tested twice. It was first loaded to 169,000 lb. at which load the loading beam started to fail. Then, most of the longitudinal stiffener was burned off until it extended only about an inch from the web. The girder was retested and then failed at a load of 118,000 lb.

The stresses in these tests were measured in the girder with a 10 in. Whittemore strain gauge. The vertical deflections of the girder were measured with Ames dials and the local lateral buckling of the web was also measured with Ames dials. The location of the points where the lateral deflection was measured can be seen in the figures showing the lateral deflection of the girders.

The stresses in the diaphragms were measured in many of these tests with strain rosettes. The stresses on the inside of the plates of the box girders were also measured. These strain rosettes were read on an electric gauge.

Remarks on Buckling Theory—In determining buckling strength, it is sometimes difficult to define the buckling load, since buckling is primarily a mathematical concept based on assumptions which are often different from actual conditions. The buckling of a column is defined as the load which causes excessive lateral deflection, when the column is perfectly straight, the load perfectly centered, and all strains perfectly elastic. For long slender columns, these conditions can be approximated by test and the test loads will be fairly close to the theoretical. Theoretically there is no lateral deflection until the buckling load is reached. Actually in practice, no column is perfectly straight and some lateral deflection occurs even at low loads. This lateral deflection increases more rapidly than the load, and the column may approach but never attain its true buckling value.

The same criterion applies to the buckling of plates. The problem is here more difficult than the problem of the column, since a plate in a structure is relatively more crooked than a column. In addition, in many structures such as box girders, the remaining portion of the structure restrains the component plates from buckling. When the web buckles, for example, the flanges prevent excessive lateral deflection, and thus the webs will hold the buckling load while additional load applied to the beam is taken by the flanges. Similarly, if the flange buckles, the box girder acts as a U-beam and the webs take the additional load until they too buckle. Thus normally, the box girder as usually designed, will not fail until both the web and flanges buckle. The load at which this occurs will depend upon the proportions of the webs and flanges. Since the plates in the girder are not perfectly straight, some local lateral deflection will occur at very low loads.

There is a method, originally proposed by Southwell (*Proceedings Royal Society*, Vol. 135, 1932, p. 601; N.A.C.A. Tech. Notes 658, E. E. Lundquist), by which the theoretical buckling load can be computed from the lateral deflection readings. This method was applied to finding the buckling loads in the l/b series and the h/t series but was not applicable to the w/t series due to the variable eccentricity on the plate caused by the deflection of the beam.

In all these tests, an attempt was made to design the girders so that the failure would be influenced primarily by the variable being investigated. In other words, in the girders with the variable h/t ratio, the flanges were made thick enough so that failure would not occur in the top flange. However, in many of the girders, the yield point was reached before the buckling load, and then the girders failed as a unit.

TEST RESULTS

l/b Ratio Tests—Table I gives the test results for this series. With the exception of G-15 all girders were loaded symmetrically with two vertical loads spaced 5 ft. from each end. G-15 was loaded with a center load since the supporting beam was not strong enough for the other type of loading. As can be seen in the table, all the welded carbon steel girders failed at about the same load. Both riveted girders failed under the same bending moment. The alloy steel girder failed at a load

TABLE II

l/b Ratio Tests—Vertical Load Plus Lateral Load

1 Girder	2 Maximum applied vertical moment, kip-in.	3 Vertical section modulus, in.³	4 Maximum applied lateral moment, kip-in.	5 Lateral section modulus, in.³	6 Maximum computed vertical stress = M/S, kips per sq. in.	7 Maximum computed lateral stress = M/S, kips per sq. in.	8 Total maximum computed stress, kips per sq. in.	9 Total computed stress parabolic distribution, kips per sq. in.	10 Average yield point flange, kips per sq. in.
G- 2a	885	18.4	82.0	6.1	48.2	13.4	61.6	51.2	42.4
G- 3a	940	18.4	94.5	6.1	51.2	15.5	66.7	55.5	44.7
G- 4a	935	18.9	94.5	6.2	49.6	15.2	64.8	54.0	42.7
G-17a	1285	18.9	122.0	6.2	68.0	19.7	87.7	73.0	63.2

which was in proportion to the yield point. Evidently the length of span did not influence the strengths of the girders tested.

Column 7 gives the stresses in the girder based on the common beam formula. Since the computed stresses are higher than the yield point of the material, these stresses are not true stresses. Column 9 gives the yield points of the steel as determined from tensile coupons. This yield point was about 42,000 to 45,000 lbs. per sq. in. and therefore the stress distribution of the beams is not linear nor does the beam formula apply above this stress. If the resisting load in the box is assumed to vary parabolically, the stresses will be five-sixths that of the ordinary beam formula. Column 8 gives these stresses, and they are seen to check very well with the yield point of the material as determined from the tension test. This is evident when comparing the values of column 8 with column 9.

It should be pointed out that the assumption of parabolic distribution for these tests is an empirical one and may not apply to girders of different cross-sectional proportions. The important fact is that the girders carried greater moment than that which would be predicted by using the yield-point stress of the material in the ordinary beam formula.

Column 13 gives the allowable stress in the compression flange of the girders using the total span in the common specification formula:

$$fc = 18{,}000 - (0.35)\left(\frac{l}{r}\right)^2$$

These stresses are much less than those present at the ultimate load. The computed allowable stresses by this formula are appreciably higher than those given by most other specification formulæ. Column 11 gives the stresses computed by this formula on the basis of the unsupported span. These stresses are higher than those given in column 13, but in most crane design the total span is used in this computation.

In column 2 is given the theoretical buckling moment of each girder as computed by the stability formulæ derived by Timoshenko (*Theory of Elastic Stability*, Stephen Timoshenko, p. 242; N.A.C.A. Technical Note No. 601, "The Lateral Instability of Deep Rectangular Beams," C. Dumont and H. N. Hill). With the exception of G-15, these moments were computed assuming that a constant moment acted along the whole girder. This assumption will give buckling moments which are smaller than the actual buckling moments. For the longer girders the approximation is small. The formula, by which these moments are computed is:

$$M_{cr} = \frac{\pi\sqrt{B_1 C}}{l}$$

M is the buckling moment in inch-pounds.
l is the span length in inches.
B_1 is the lateral rigidity and equals the lateral moment of inertia I_2 times the modulus of elasticity E,
C is the torsional rigidity and equals J the torsional constant times G the modulus of shear.

The buckling moment of G-15 was computed from the formula:

$$P_{crit} = \frac{16.93\sqrt{B_1 C}}{l^2}$$

where P_{crit} is the buckling load. This last formula applies to a beam loaded at the center, and thus should give close results for a crane when the trolley is at the center.

These formulæ give buckling loads much higher than those given by most design formulæ, because the above formulæ take into account the torsional strength of the girders. Since box girders are so strong in torsion, neglecting this factor seriously underestimates the strength of such girders. In I-beams where torsional strength is relatively small, this neglect does not result in such a large error.

In computing the strength of the riveted girders, the value of the torsion constant was multiplied by one-third to take into account the effect of rivet slip (*Torsional Properties of Fabricated I-Beam and Box Sections*, I. E. Madsen).

These buckling formulæ apply only in the elastic range. Since the theoretical buckling loads corresponded to stresses far above the yield point, the girders failed due to yielding of the steel.

The ultimate loads of the girders with the 10 per cent lateral moment are given in Table II. These ultimate loads are almost as large as those for the tests in which no lateral load was present. If the lateral stress is added to the vertical stress, the maximum stresses in these tests are greater than those in the vertical load tests. However, since these computed stresses are above the yield point, the formulæ do not apply. The stresses based on parabolic distribution of the resisting bending force are larger than the yield point as shown in Table II. It is uncertain, however, that these yield-point values apply, after the cold-working the girders were subjected to in the straightening process.

In this report, plotted curves of test results will be reported for the tests on girder G-2 and G-2a. The results for the other girders in this series are very similar.

Figure 5 gives a number of curves which show the behavior of this girder under the vertical test load. Curves for the center vertical and lateral deflection, and the stresses in the compression flange, tension flange, and at the center line of the girder are given in this figure.

Up to a load of about eight kips, the stresses and deflection were linear and checked the theoretical.

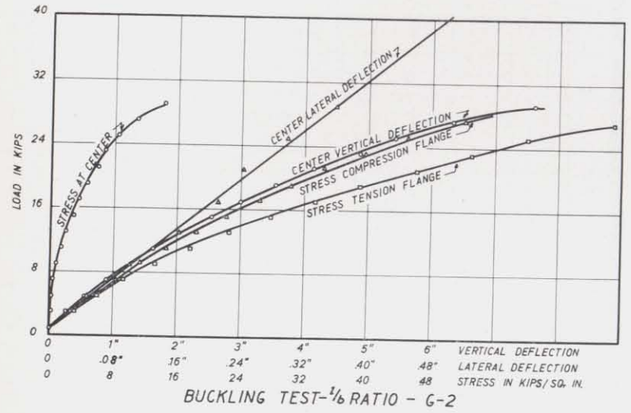

Figure 5

▲

Figure 6

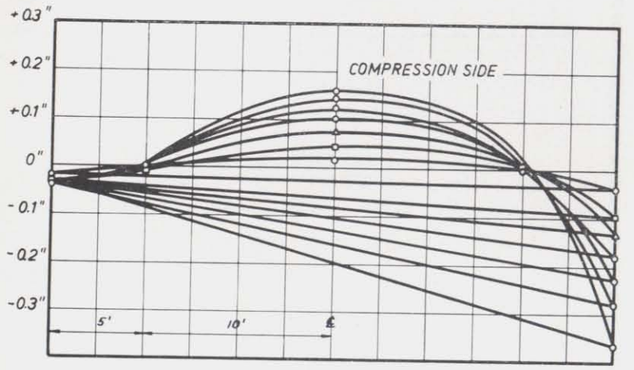

Above this load, the stresses and deflection increased somewhat more rapidly than the load. It should be noticed that the compression stress above this load is less than the tension stress and the difference becomes relatively greater. This is rather unusual, for the stresses in both the tension and compression flanges should have been the same, since the girder section was symmetrical and had no holes.

The effect is believed due to internal welding stresses. After the flanges are welded to the webs, there is an initial yield-point tension in the weld metal and the material next to it. Then as the load is applied to the beam, the material on the tension flange which is at the yield point refuses to take more stress. The weld metal on the compression flange, which has yield-point tension, takes compression however, and the resultant stresses are the same as those present in an unsymmetrical beam with a portion of the tension flange missing. The resultant stress distribution is similar to that in a riveted girder.

As the tension increases in the tension flange, the material adjacent to the welds, which is close to the yield point, becomes ineffective, resulting in less effective flange area, and moving the apparent neutral axis still closer to the compression flange. This is shown in Figure 5 by the curve showing the stress at the center of the girder. Since the initial tension is an internal stress, there must be an initial compression to balance this tension. The internal compression stress is spread out on a much larger area than the tension stress and consequently the compression stress is much lower than the tension stress, so this area does not go out of action at the lower loads. If the girders are stressed above the yield point, the internal stresses are largely relieved, and this will be shown in the curves for G-2a where the measured values of the tension and compression stresses were practically alike.

This effect of the shifting of the neutral axis was noticed in all the girders, though in no case was the effect larger than in G-2, and in most cases, it was smaller. The effect was usually greater than the net section effect in the riveted girders.

One curve which should be noted is the curve for the center lateral deflection. This curve is a straight line. If there were any tendency for lateral buckling, this curve would show increasing deflections for the same load increments, as the load was increased.

The measured lateral deflection is due to the fact that the girders were fabricated with the usual structural tolerances, and the top and bottom flanges were not perfectly parallel. The measured lateral deflection here corresponds to a lateral load of 0.01 the vertical load.

The lateral deflections, as measured on the compression flange, are shown in Figure 6. The measured lateral deflections on the tension flange were practically the same. This shows that no twist occurred in the test. The lateral deflection plotted in Figure 5 is the average of the tension and compression measurements.

In Figure 7, the stress distribution at the center of the girder is shown at three loads. The neutral axis moved towards the compression flange as the load was increased. The strain gauge measurements showed that the straight line strain distribution remained linear up to the ultimate load. This was true in all the girders

except those of the h/t series in which the webs buckled.

Figure 8 shows curves for the deflection and the stresses in girder G-2a. The stresses are the average stresses in the flange. Since there was a lateral load, the stresses varied from one flange edge to the other. The stress values in both the tension and compression flanges are about equal as can be seen in the figure. This shows that the internal stress condition shown by the test on G-2 had been relieved. The stresses and also the deflection are linear up through the proportional limit.

The lateral deflection curve at the center is plotted against the lateral moment. The measured lateral deflection is practically as large as the vertical deflection,

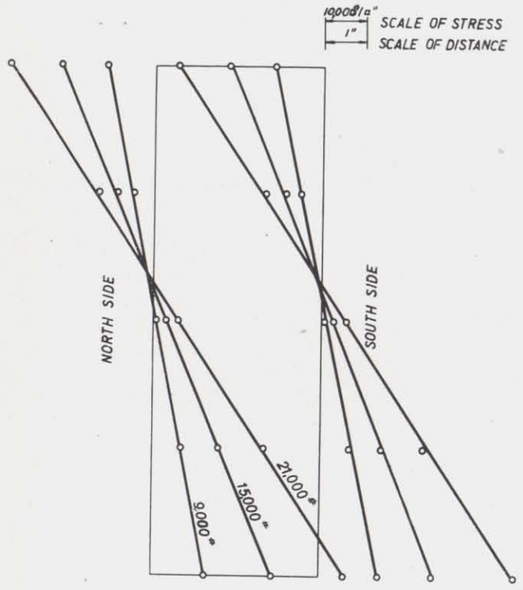

BUCKLING TEST-1/6 RATIO
G-2-STRESS DISTRIBUTION

Figure 7

and is the average of the readings on the tension and compression flanges. The deflection on the compression flange was about 5 per cent greater than that on the bottom flange showing that the lateral load, which was applied to the top flange, caused some twist.

In Figure 9, are shown the curves of the lateral deflection of the top flange, as they were actually measured. The points where the curves cross the zero line are the points where the vertical load was applied.

w/t Ratio Tests—The results of the w/t test series are summarized in Table III. Column 2 gives the maximum loads and column 3 gives the maximum moments applied to the girders when failure occurred. The computed maximum stress based on the common beam

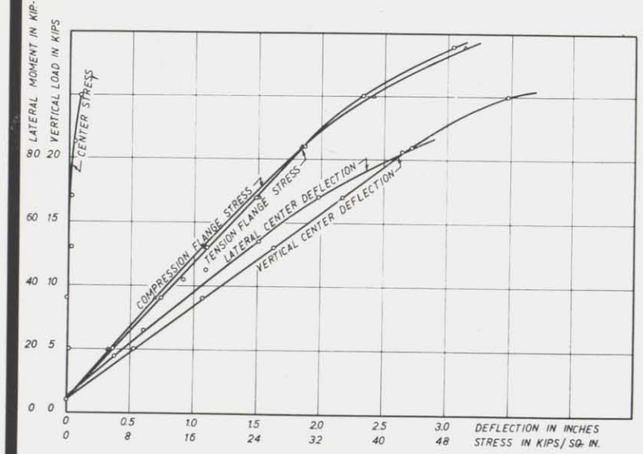

BUCKLING TEST-1/6 RATIO
G-2A

Figure 8

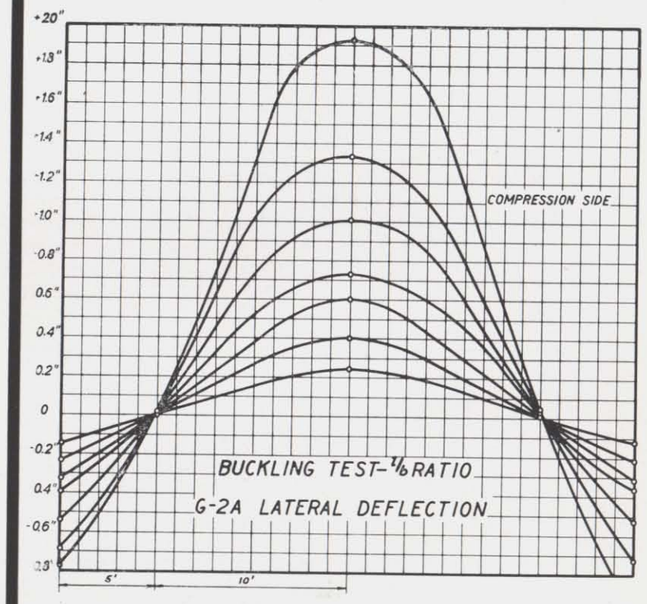

Figure 9

▲

Figure 10

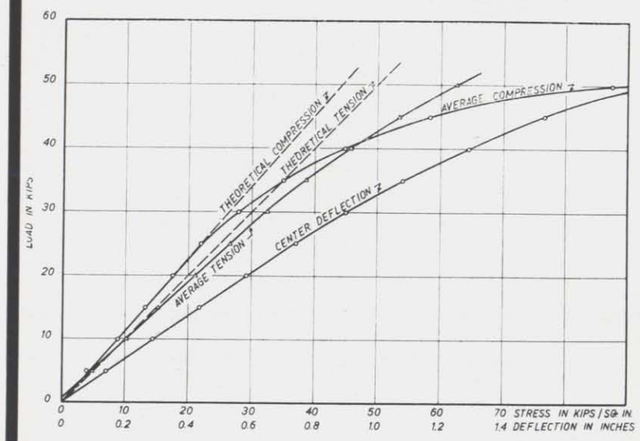

BUCKLING TEST-w/t RATIO G-18

theory is given in column 6. For the girders without the rail, the maximum computed stress is less than the yield point with the exception of girder G-5. This shows that buckling must have contributed to the failure of the girders. The buckling of the cover plate in most of the girders tested in this series may have occurred long before the girder failed as a whole.

Column 9 gives the theoretical buckling stress of the girders as developed by Timoshenko assuming the edges of the plates to be simply supported. The measured stresses in the flange plates when they buckled are given in columns 10 and 11. These stresses are appreciably smaller than the theoretical.

As stated in the introduction, the buckling loads for the girders in this series are difficult to determine. Two criteria were used to determine the buckling stresses. The buckling loads given in column 10 were determined from stress curves, similar to those in Figure 10 for girder G-18. In this figure which is typical of this series, the compression stress is less than the tension stress at the lower loads. This is due to the initial tension stress in the girder caused by welding stresses discussed in the previous section. At the higher loads, the compression stresses increase more rapidly than the tension stresses, and become greater than the tension stresses at a load of 40,000 lb. for girder G-18. The load at which the compression stress begins to increase more rapidly than the tension stress is about 26,000 lb. and this was taken as the buckling load of the compression flange. This load was taken as the buckling load because at this load, the compression flange ceases to be fully effective (due to buckling) and the neutral axis begins to approach the tension flange. The stress in the compression flange then increases more rapidly than that in the

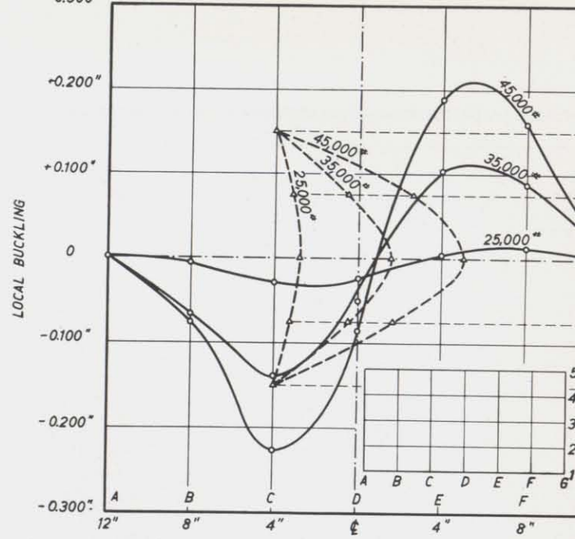

COVER PLATE BUCKLING
G-18

Figure 11

tension flange. The center deflection shown in Figure 10 also leaves the straight line at this load which also shows that the girder becomes less effective at this point.

The theoretical compression and tension curves in Figure 10 were computed on the basis that the weld metal and the material adjacent to it were at an initial

TABLE III

w/t Ratio Tests

1 Girder	2 Maximum load, kips	3 Maximum applied moment, kip-in.	4 Vertical moment of inertia, in.⁴	5 Vertical section modulus, in.³	6 Computed maximum stress, M/S, kips per sq. in.	7 Yield point material, kips per sq. in.	8 w/t	9 Theoretical buckling stress, free edge, kips per sq. in.	10 Stress at which flange plate buckled from stresses, kips per sq. in.	11 Stress at which flange plate buckled from lateral measurements, kips sq. in.	12 Compressive welding stress in flange, kips per sq. in.	13 Internal stress + average measured buckling stress, kips sq. in.
G- 5	32.1	1160	156.4	25.2	46.0	41.4	32	106.0	..	..	17.7	..
G- 6	35.9	1290	197.4	31.9	40.5	40.9	48	47.0	27.0	25.0	10.0	36.0
G- 7	35.9	1290	241.5	39.0	33.1	38.0	64	27.4	18.0	18.0	6.4	24.4
G- 8	37.2	1340	294.8	47.5	28.2	39.4	80	16.9	9.0	8.0	4.8	13.3
G- 9	60.4	2170	347.7	44.9 60.5 55.4	−48.3 −36.0 +39.2	41.5	96	11.7 or 47.0	32.0	32.0	12.0	44.0
G-18	51.3	1850	238.7	38.5	48.0	61.4	64	27.4	22.0	24.0	6.4	29.4
G- 5a	24.7	1330	156.4	25.2	52.7	41.4	32	..	20.0	..	..	..
G- 6a	32.5	1360	197.4	31.9	42.7	40.9	48	..	30.0	..	..	..
G- 7a	33.5	1410	241.5	39.0	36.2	38.0	64	..	24.0	..	..	..
G- 8a*	23.3	980	294.8	47.5	20.4	39.4	80	..	8.0	..	..	..
G-18a	48.9	2060	238.7	38.5	53.3	61.4	64	..	..	..	..	..

*Girder buckled at point where it had buckled in first test.

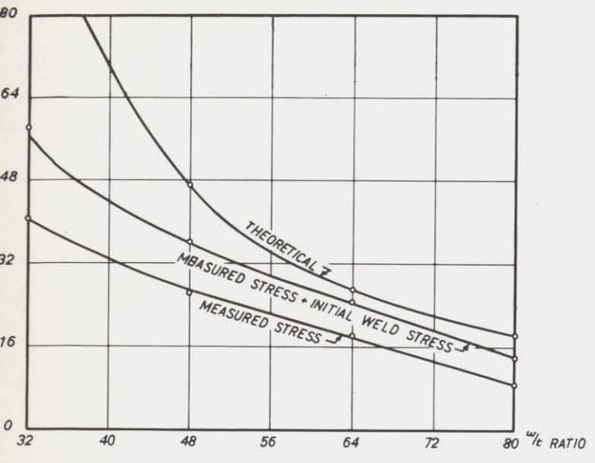

BUCKLING STRESSES — w/t RATIO SERIES

Figure 12

yield-point stress of 60,000 lb. This results in the net section effect previously mentioned. The resultant compressive welding stress in the flanges necessary to balance the initial tension stresses are given in column 12. Column 13 gives the sum of the initial welding stress plus the measured buckling stress. This stress approximates the theoretical buckling stress of column 9.

The second criterion for determining the buckling deflections was derived from measured local buckling deflections similar to those shown in Figure 11. These values also check the values found in the first method. The load at which the flange plate had buckled a distance equal to one-sixth the plate thickness, was taken as the buckling load. When the local buckling exceeds this value, the compression force passes outside the kern point of the plate, the maximum compressive stress in the plate is then more than twice the average and tension is also present on the other side of the plate. The compressive stress early reaches its yield point at these points of maximum buckling, local plastic yielding occurs, and there is a redistribution of stress. It is probably due to this fact that the Southwell method could not be used to determine the buckling loads in this series, with the exception of G-18, whose yield point was enough higher than the other girders' so that enough buckling readings could be taken below the yield point to determine the buckling stress. This value was 32,000 lb. per sq. in., which compares with the values in columns 9 and 13 for this girder.

The compression flange plates in a box girder are subjected to a more severe buckling condition than the plates in a column. This is due to the fact that as the girder deflects under vertical load, the cover plates are curved and thus the compression stress is eccentrically applied. Local deflection results and a true buckling stress can not be determined. Figure 11 shows the lateral buckling at three loads and the small insert shows the points where the deflection readings were taken. Lines A and G are diaphragm locations. The flange plate buckled in a double wave longitudinally along the girder as shown by the solid curves for line 3 between the diaphragms. Between the webs, the girder deflects in a single wave, as shown by the dotted curves which give the deflections for line C.

The flanges of the test girders buckled at lower loads than predicted by theory, and it is thought that this is due to internal welding stresses. Girder G-5 showed no sign of cover-plate buckling but yielded first as a unit with no local buckling.

In Figure 12, is plotted a curve showing how the measured buckling stresses varied with the w/t ratio. The curve of measured stresses plus welding stresses is also given. This second curve is fairly close to the theoretical.

Girder G-9 as shown by Table III, failed at a higher stress than the other girders, even though it had a higher w/t ratio. The reason for the added strength was the longitudinal stiffener on the compression flange of this girder. The stiffener should have increased the strength of the plate to one having a w/t ratio of 48, and this it did. This girder failed when the stiffener reached its yield point, thus rendering the stiffener ineffective. The three values for the section modulus given in column 5 for this girder are the values for the edge of the stiffener, the compression flange, and the tension flange.

The primary object of the retests in the w/t series

Figure 13

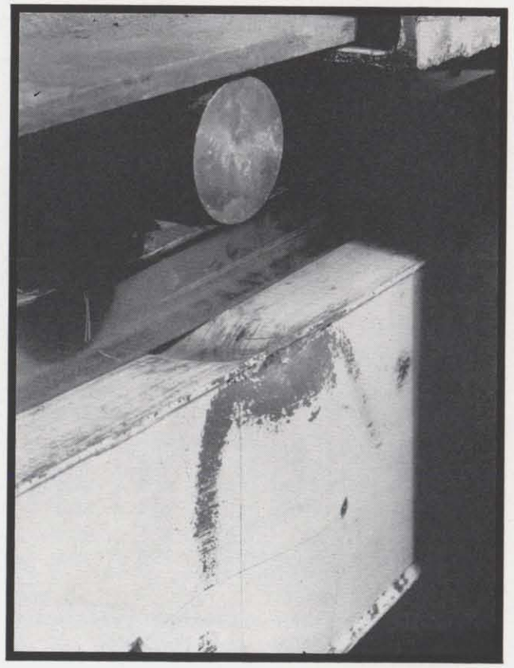

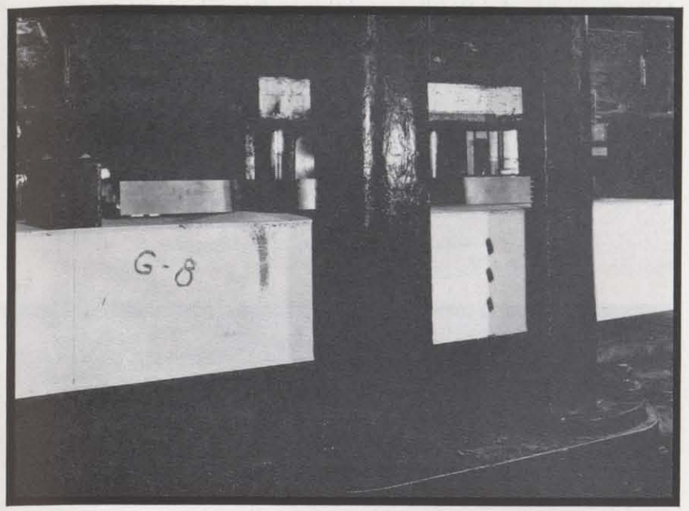

Figure 14

was to determine if loading the girder through the rail would weaken the girder. As is shown in Table III, every girder with the exception of G-8a failed at a greater bending moment than in the first test. Girder G-8a could not be fully straightened from the first test and this probably accounts for its low strength value in the retests.

The measured buckling stresses of the girders in the retests were greater than in the original tests except for G-5a. Local yielding of the rail under the load occurred in this girder and probably lowered the buckling value. With the exception of G-5a, the rail was just laid on the girder and was not fastened to it. It acted as a stiffener by preventing the cover plate from buckling upwards. Since the buckles could only occur downwards, the effect was the same as if the edges of the plate were fixed perpendicular to the cross section of the beam. Loading the girder through the rail caused local bending stress in the flange plate which will be discussed later.

Figure 13 is a picture showing how girder G-6a failed in this series. This picture shows that both the flange and web buckled at the ultimate load. The cover plate necessarily had to buckle inwards with the edges of the buckle perpendicular to the length acting as fixed edges. This picture also shows the details of the loading in the retests.

Figure 14 on the other hand shows the details of the failure when the girders were not loaded through the rail. The difference in the buckles in this picture and in the preceding picture are evident, since in Figure 14 the buckles are alternately up and down.

Figure 15 is a picture showing some of the details of the test set-up for girder G-5.

h/t Ratio Tests—The results of the third series of tests, the h/t series, are given in Table IV. The second column gives the maximum loads taken by the girders and the third column gives the maximum moments. Column 6 gives the maximum computed stress as computed by the usual beam formula. With the exception of G-10, these stresses are less than the yield point. However, the actual measured stresses in these girders were at the yield point just prior to failure. The beam formula does not give true values at the higher loads since at these loads the webs had buckled and transferred some of their load to the flanges.

Column 9 gives the theoretical buckling load for the girders with the computations based on free edges. Column 10 gives the measured buckling stress as determined from Southwell's method. This stress is the stress at which the webs would have buckled had they

TABLE IV

h/t Ratio Tests

1 Girder	2 Maximum load, kips	3 Maximum applied moment, kip-in.	4 Vertical moment of inertia, in.^{4}	5 Vertical section modulus, in.^{3}	6 Computed maximum stress, M/S, kips per sq. in.	7 Average yield point, kips per sq. in.	8 h/t	9 Theoretical buckling stress free edge, kips per sq. in.	10 Measured buckling stress, Southwell, kips per sq. in.	11 Measured buckling stress from lateral deflection, kips per sq. in.	12 Measured buckling stress from stress curves	13 Average of columns 11 and 12, kips per sq. in.
G-10	169.0	6090	2953	146.0	41.7	37.3	320	33.2	43.0	..	..	..
G-10a	118.0	4250	2953	146.0	29.1	37.3	320	33.2 6.4*	..	..	..	..
G-11	65.4	2350	876	71.5	32.9	39.4	192	17.6	27.6	19.0	18.0	18.5
G-12	63.3	2280	717	64.3	35.4	37.4	176	21.0	31.0	20.0	20.0	20.0
G-13	56.4	2030	577	56.3	36.0	37.8	160	25.0	34.0	25.0	22.0	23.5
G-14	50.7	1820	456	49.3	36.9	38.7	144	31.3	39.0	29.2	26.0	27.6

*This value computed assuming no stiffener.

been perfectly straight and the material perfectly elastic.

However, the webs were not perfectly straight, there was some eccentricity, so that the webs buckled at lower loads than that given by Southwell's method. Columns 11 and 12 give the measured buckling stresses determined by two methods and column 13 gives the average of column 11 and column 12.

The buckling stress given by Southwell's method is greater than the theoretical buckling stress based on free edges given in column 10. This shows that the edges were not free and that the true buckling stress is

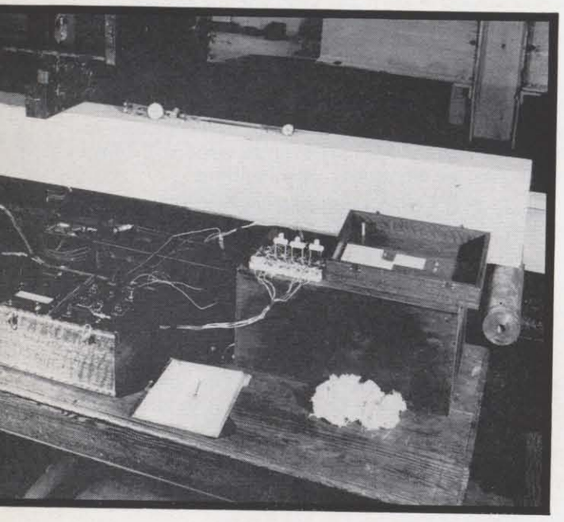

Figure 15

greater than that computed on the basis of free edges. This is shown in Figure 16, which shows the buckling in a vertical plane. The curves on the left side are for the north web and those on the right side are for the south web. The fact that the curves have a point of contraflexure at the bottom shows that there was partial fixity along the edge of the plate.

Figure 17 gives curves for the web buckling along the length of the girder, in the middle third of the girder. This section which had bending stress only and no shear, buckled into five waves in a 6 ft. length. This shows why vertical stiffeners are of little value in preventing buckling due to bending, since they can have little effect unless their spacing is less than the wave length of the buckles. Otherwise the plate would buckle between the stiffeners. Such a spacing of vertical stiffeners is uneconomical.

All girders with the exception of G-10 buckled in a manner similar to that shown in Figure 17. G-10 deflected into a single wave in the 6 ft. length of the center panel, showing that the effect of the horizontal stiffener was to increase the wave length of the buckle. This is the usual effect of longitudinal stiffeners. Girder G-10 was not loaded to failure and the maximum load given for this girder in Table IV is the maximum load which was applied to the girder.

In girder G-10a, where most of the longitudinal stiffener had been burnt off, the web buckled into three waves in the middle panel. Figure 18 gives a picture of this girder after failure.

The buckling criteria applied to the other girders were not used on G-10 or G-10a, since it was thought that the presence of the longitudinal stiffener made the criteria inapplicable. The buckling stress of G-10a was the stress of 29,000 lb. per sq. in., which was present

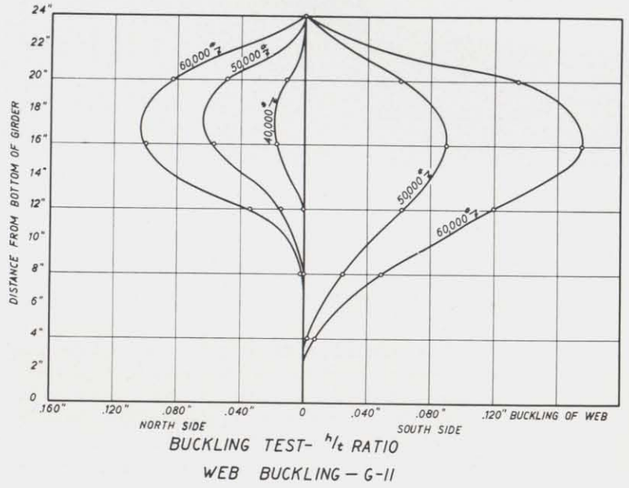

BUCKLING TEST- h/t RATIO

WEB BUCKLING – G-11

Figure 16

▲

Figure 17

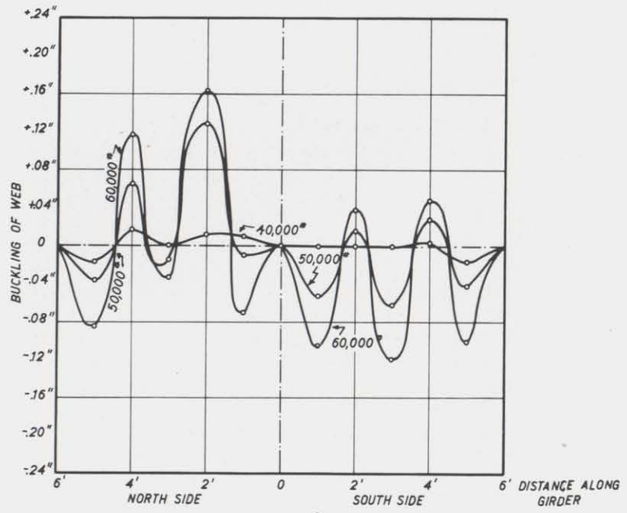

BUCKLING TEST- h/t RATIO

WEB BUCKLING – G-11

when the girder buckled. This girder failed very suddenly, whereas all the other girders failed gradually. In girder G-10, which was not taken to its buckling load, the stress criteria never indicated buckling, while the buckling stress, determined from a lateral deflection of 0.02 in., was only about 2000 lb. per sq. in. This lateral deflection, which is the distance to the kern of the $\frac{1}{8}$ in. plate, does not apply to the stiffener-plate combination.

It is believed that the stress criteria for buckling is better than the lateral deflection criteria. In plates with very large height-thickness ratios, the load could pass outside the kern point so that tension would be

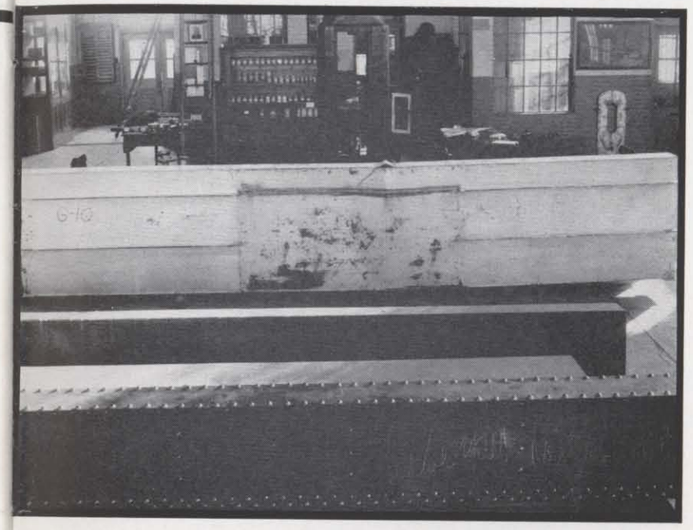

Figure 18

present, and the compression stress would still remain within the elastic limit. However, the proportions of the plates were such with the exception of G-10, that when the deflection had exceeded the kern distance, the maximum stress had exceeded the yield point.

Figure 19 shows the stress curves for G-11 and one can easily determine from the compression curve where the web started to become ineffective. The deflection curves for this girder also broke away from the straight line at this load.

In Figure 20 are plotted the buckling stresses for the various h/t ratios of the web plates. In the right side of the figure the buckling stresses are plotted against the h/t ratio and the result is a curve. In the left side of the figure, the stresses are plotted against $(t/h)^2$ and the resulting curves are straight lines. The left figure is more useful in extrapolating for results outside the test range. Three curves are plotted in this figure, the measured buckling stress by Southwell's method, the theoretical buckling stress assuming free edges and the actual measured buckling stress. The weakening effect of small waves in the plate is quite evident when comparing the measured buckling stress with the stress by Southwell's method. It is also quite probable that there may have been initial compressive stresses in the plate due to the welding which would have contributed to the low buckling values.

The theoretical deflections, including the shear deflection, were computed for the girders in this series and compared with the measured values of the straight line portion of the deflection curve. The ratio between the measured deflections and the theoretical varied from 1.26 in the case of G-10 to 0.99 in the case of G-14. Apparently the lack of straightness or initial waves in

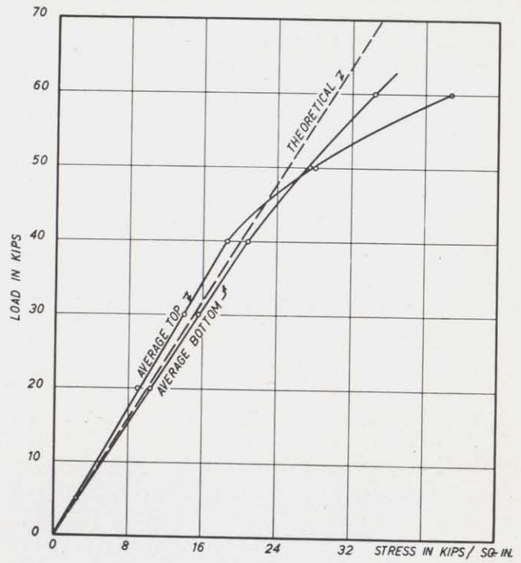

BUCKLING TEST- h/t RATIO

STRESSES G-11

Figure 19

▲

Figure 20

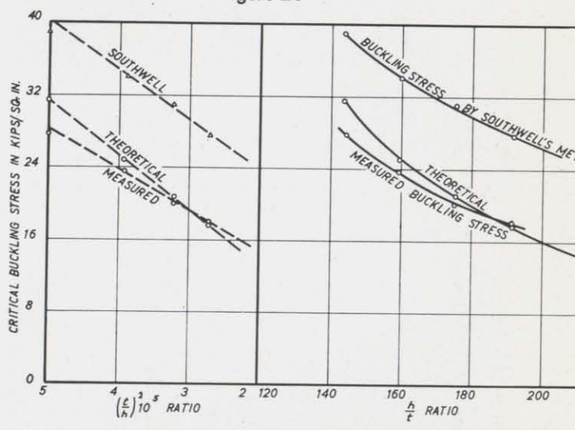

BUCKLING STRESSES – h/t RATIO SERIES

the thin web plates decreased the effective modulus of elasticity and thus increased the deflection.

Miscellaneous Tests—The stresses on a number of diaphragms were measured by means of strain rosettes in which the strains were read on the electric gauge. For the girders in the l/b series, no stresses were measured on the diaphragms in the bending tests except when the load was placed directly over the diaphragm. When this was done, the maximum stress measured was 1000 lb. per sq. in. in one corner of the diaphragm for a 3000 lb. load. The area of the diaphragm was 0.75 sq. in.

For G-7, the stresses on a vertical line on one side of the upper corner of an unloaded diaphragm increased by 110 lb. per sq. in. for every 5000 lb. load increment up to 20,000 lb. At this load, the cover plate buckled and then the stress in the diaphragm increased by +1300 lb. per sq. in. for every 5000 lb. load increment up to the ultimate load. The buckling of the cover plate applied a moment to the diaphragm and the bending force set up in the diaphragm reduced the buckling of the cover plate.

Strain rosette readings were also taken on the inside of the cover plate in girders G-5 and G-18. Table V summarizes the results of these tests.

In test No. 2 on G-5, the girder was loaded at the span center by a concentrated load through a 2 in. square steel block on the center of the cover plate. Such a load introduces bending stresses both in the longitudinal direction of the girder and in the cross direction between the webs. The cross stresses given in column 3 are the greater since the span is shorter in this direction. Column 4 gives the longitudinal bending stress. This longitudinal bending stress in the cover plate is additional to the direct compressive stresses in the flange caused by the bending of the whole girder. The stress given in column 4 consists only of the bending stress. It can be seen from columns 5 and 6 that the proportions of the cross bending stress to the longitudinal bending stress is inversely proportional to the ratio of the distance between the webs and the diaphragm spacing when the load is applied half-way between the diaphragms. In column 7 the computed cross stress is given for a concentrated load applied to the plate. This stress is computed from a semi-empirical formula:

$$f=\frac{M}{4SL}$$

where f is the average cross bending stress in pounds per square inch.

M is the fixed end cross bending moment in inch-pounds.

TABLE V

Plate Stresses

1 Girder	2 Test	3 Cross stress kips per sq. in.	4 Longitudinal stress, kips sq. in.	5 Ratio Col. 5 / Col. 6	6 Ratio cross span to longitudinal span	7 Computed cross stress, kips per sq. in.	8 Applied load, lb.	9 Per cent of load taken by plate	10 Remarks
									Concentrated load placed:
G- 5*	1	+ 6.0	+2.0	.33	.25	+ 8.0	500	80	At center-line on 1 in. square longitudinal bar.
G- 5	2	+ 5.6	+1.3	.23	.25	+ 5.7	355	98	At center-line of girder on 2 in. block on center of cover plate.
G- 5	3	+ 2.4	+0.5	.21	.25	+ 3.4	640	70	6 in. from diaphragm on 2 in. sq. block.
G- 5	4	+ 0.7	0	...	.25	+ 2.0	370	35	6 in. from diaphragm on 1 in. longitudinal bar.
G- 5	5	+ 5.1	+1.2	.24	.25	+ 63.3	4020	8	On 3 in. 5.7 lb. I-beam at center-line of girder.
G- 5	6	+ 6.6	+0.1	...	.25	+126.0	8000	5	On 3 in. 5.7 lb. I-beam 6 in. from diaphragm.
G- 5	7	+22.0	+4.8	.25	.25	+ 63.3	4020	35	On 2⅜ in. I-beam at center-line of girder.
G-18†	1	+ 8.7	..	...	1.00	+ 7.9	490	110	On 2 in. square block directly over gauge.
G-18	2	+ 5.7	..	...	1.00	+ 4.3	800	130	On 2 in. square block at center-line of girder.
G-18	3	+ 6.3	..	...	1.00	+ 4.3	800	146	At center-line of girder on 1 in. square longitudinal bar.
G-18	4	+ 3.0	..	...	1.00	+ 9.5	590	32	On 1 in. square bar directly over gauge.

*Location of stress reading—Center of cover plate at center-line of girder.
†Location of stress reading—Center of cover plate 6 in. from center-line.

S is the section modulus of the plate per inch of plate.

L is the clear span between the webs.

This formula has been derived on the basis of a parabolic distribution of bending moment ("Structural Behavior of Battledeck Floor Systems," I. Lyse and I. E. Madsen, *Trans. A.S.C.E.*, 1939, p. 264). The maximum stress directly under the concentrated load is three times the average value given above.

When the load is applied to the center through a light rail as in test 1 on G-5, some of the load was transferred to the diaphragms and some of the load was spread a longer distance over the plate resulting in a lower maximum stress. When the load was applied to a heavier rail as in test 7, only 35 per cent of the load was taken by the plate, and when the load was taken by a still heavier rail as in test 5, only 8 per cent of the load was taken by the plate. The other tests show that the maximum stress occurs at the load point, when the load is placed half-way between the diaphragms.

These tests show that the bending stress in the plate can be made quite small by using a stiff rail and by spacing the diaphragms closely together. In order to determine the proportion of the load taken by the plate and rail, the deflections of both must be computed and the loads taken by each will be in proportion to the loads which will cause equal deflection in the rail and plate.

Column 9 gives a comparison between the resisting force or stress in the plate at the point where the stresses are measured, and the stresses which would be present there if the load had been applied to this point as a concentrated load. The value of 146 per cent for test 3 of G-18 merely shows that the bar distributed the load so that the stresses at the gauge point which is 6 in. from the load point, are higher than they would have been if the bar had distributed no stress. In other words, the rail distributes the load.

DISCUSSION OF RESULTS

l/b Ratio Tests—The l/b ratio tests show conclusively that within usual limits of crane design, there is no reason to use a compressive design stress lower than the tension design stress, if the girder is proportioned so that local buckling does not occur in the flange plate. In addition, any local buckling which may occur, does not depend on the span of the crane, so there is no reason in this case, to make a larger reduction in design stress for a long span crane than for a short span crane.

The box portion of the girders tested had a width-depth ratio of one-fourth. This is in line with common practice in crane construction for riveted girders, and is probably smaller than normal proportions for welded girders. The thickness ratios for the webs and flanges in actual cranes may be about three times those in the model girders. However, girders with such ratios would fail due to local web or flange plate buckling rather than buckling of the girder as a whole.

In addition, the torsional constant and the moment of inertia of the girder increase with the square of the dimensions of the girder. Thus when these factors are all considered, full size crane girders will be relatively stronger than the model girders as far as lateral buckling is concerned. In cranes where there is a good end connection between the girder and the end tie, some lateral end fixity is present, and this further reduces the possibility of lateral buckling of the girder as a whole.

Lateral load applied to the girders will lower the buckling load, but for girders with the proportions tested, this effect is not appreciable. The fact that the lateral load did not weaken the girders is borne out by the retests of the l/b series.

The test results show that a maximum allowable l/b ratio of at least 110 for welded girders and 80 for riveted girders could be used without reducing the allowable compressive stresses. Since these ratios are far greater than any used in present practice, it may be advisable to lower this limit to 60 for the allowable l/b. A higher ratio than this will probably be uneconomical, since such proportions result in a low lateral section modulus and consequent high lateral stresses.

In designing boxes of unusual proportions where there may be some doubt as to the lateral strength of the girder, it would be advisable to check the buckling load by the stability formula for the concentrated load at the center of the beam.

$$P_{crit}=\frac{16.93\sqrt{B_1C}}{l^2}$$

In using this formula, the computed torsion constants

Figure 21

of riveted girders must be reduced by a factor of one-third.

The l/b ratio tests are probably the most important in this whole girder program, since they show where design stresses for box girders may be safely increased, provided proper precautions against local buckling are observed. Such an increase should result in appreciable saving.

Figure 21 is a picture which shows the details of the failure of girder G-1, which girder had the longest l/b ratio. The failure is seen to be local buckling of the compression flange with no signs of lateral buckling.

In discussing this series, it should be noted that the stress curves, such as those in Figure 5, are not actual stresses above the yield point, but rather represent strains.

The tests in this series also confirm the fact that the strain distribution in the girders remained linear over the cross section above the yield point.

The shift in the neutral axis due to the weld stresses was an interesting phenomenon. These stresses might be relieved by annealing or by stressing the girders above the yield point. However, the first method is impracticable and the second method would not occur in service. Where buckling is not a factor, these internal stresses have no appreciable harmful effect.

w/t Ratio Tests—In welding thin plates it is necessary to keep the heat at a minimum, for otherwise the plates may buckle without the application of external load. It follows then, that the welding process may leave internal stresses which are not large enough themselves to cause buckling, but which will cause an apparent low buckling stress, when the girder is loaded. Whether the internal weld stresses will contribute to buckling or not will depend on the location and size of the welds. In a box girder, the tension due to the welds in the corners of the box cause compression stresses in all four plates, since the sum of the internal stresses must equal zero for equilibrium. These stresses will lower the buckling values of the compression flange and web plates.

Since the internal stresses can not exceed the yield point, elastic buckling can never occur if the theoretical buckling stress of the plate is equal to twice the yield strength of the plate. This condition was true in girder G-5 where there was no indication of plate buckling. In the other girders buckling could occur.

It is believed that the difference between the theoretical and buckling stresses in the w/t test series was primarily due to internal weld stresses. These stresses were much larger in the test models than they would be in actual crane girders, since the model sections had a larger proportion of weld metal than is usually used in actual construction. This is due to the fact that the girders had minimum practical size welds.

The weld stresses as computed in the tables are based on the area of the weld metal and the relative proportions of the flanges and webs. They were not actually measured in the girders, but the data by which they were computed were determined from the shift in the neutral axis, and from pilot models in which the internal stresses due to welding were measured with a 10 in. Whittemore strain gauge. These computed stresses may be somewhat in error quantitatively but should represent actual conditions qualitatively. In riveted girders, these stresses would not occur.

The criteria used to determine the buckling stresses may not be strictly correct mathematically, but it is felt that they define the very practical point where the plates cease to be fully effective due to excessive lateral deflection.

The buckling stresses, measured in this series, were less than the theoretical values as shown in Figure 12, but in larger girders where internal weld stresses are much smaller, or in riveted girders, the theoretical values for buckling stress should be close to the actual values. It is believed that these theoretical values can be used safely in design. This is particularly true when the load is applied to the girder through a rail, since the rail acts as a stiffener to the girder.

The rails must be large enough to transfer most of the load to the diaphragms, or otherwise bending stresses in the cover plate will weaken the cover plate.

When an adequate stiffener is applied to the flange plate, the w/t ratio of the plate can be taken as the distance between the web and stiffener. This was borne out by the test on G-9.

The alloy steel girder was somewhat stronger than the same carbon steel girder, since local yielding due to small buckles in the plate occurred more rapidly in the carbon steel girder than in the alloy steel girder.

h/t Ratio Tests—One of the standard references on stability is "Theory of Elastic Stability" by S. Timoshenko. Some of this material is in a form which is inconvenient for the use of the designer. A recent paper by L. S. Moisseiff and F. Lienhard ("Theory of Elastic Stability Applied to Structural Design," *Proceedings, A.S.C.E.*, January 1940) is an attempt to correlate stability theory so that the designer may use it conveniently. Most of the following theory comes from this paper. The general formula for buckling of plates is:

$$\sigma_{crit} = K \frac{\pi^2 E \zeta}{12\left[1-\left(\frac{l}{m}\right)^2\right]}\left(\frac{t}{d}\right)^2$$

in which t = the thickness of the plate.
d = the width of the plate.
$\frac{1}{m}$ = Poisson's ratio.
σ_{crit} = the buckling stress.
E = the modulus of elasticity.
K = a constant which depends on the dimension of the plate, the end conditions, and the kind of stress.
ζ = the modulus factor, a value by which E is multiplied when the stress exceeds the elastic range.

For plates with simply-supported edges and subjected to pure compression, the value of K is 4. For plates with simply supported edges, in pure bending, the value of K is 24.

For freely supported plates, subjected to a combination of pure compression and bending, the value of K is given by the empirical equation:

$$K = \alpha^3 + 3\alpha^2 + 4$$

The value of α is given by the equation:

$$\sigma_y = \sigma_o\left(1-\alpha\frac{y}{d}\right)$$

in which y = the distance of stress from the edge.
σ_o = unit stress at $y = 0$, the upper or lower edge of the plate.
σ_y = unit stress at a distance y from edge.

When a crane girder is subjected to both lateral and vertical loads, the web plates are subjected to both a compressive and bending stress and the allowable stress must be computed from the above formulæ. Since the combination of vertical and lateral loads results in a lower buckling stress for the same h/t ratio, this factor should govern in setting the allowable h/t ratio.

The test girders in this series subjected the webs to pure bending only. As is shown by the values of Table IV, and the curves of Figure 20, the measured buckling stresses agree fairly well with the theoretical. The computed theoretical stress was based on simply-supported edges, but no account was taken of the ζ factor which reduces the theoretical buckling stress at stresses above the elastic limit (Table 3, "Theory of Elastic Stability Applied to Structural Design," L. S. Moisseiff and F. Lienhard, *Proceedings, A.S.C.E.*, 1940). If this factor is taken into account, the theoretical stresses check the measured stresses very closely.

The measured buckling stress by Southwell's method showed that there was some partial fixity on the edges of the plate. However, the small waves in the plate and possibly the welding stresses reduced the buckling stress to the simply-supported edge value. For a maximum fibre stress of 18,000 lb. per sq. in. and a safety factor of 1.83, the ratio between 33,000 and 18,000, the maximum allowable h/t ratio is about 144. If the girder is subjected to lateral moments as well as vertical moments, this ratio should be still less.

Apparently h/t ratios used in present cranes are too high if design stresses are to be increased. These ratios have not caused any trouble in the older cranes since the maximum compressive design stresses in these cranes seldom exceed 12,000 lb. per sq. in. Furthermore, the webs of these cranes may sometimes buckle slightly in service with no damage at low design stresses. As was shown in Table IV, there is a large margin between the load at which the web buckled and the load at which the girder failed. For this reason, a relatively smaller factor of safety can be used in web design. If high web-thickness ratios are to be used with high stresses, longitudinal stiffeners should prove economical. The effectiveness of longitudinal stiffeners was clearly demonstrated by girder G-10. The paper by Moisseiff and Lienhard also gives data relative to such design procedure.

Miscellaneous Tests—When the load was applied directly to the flange plate of a box girder, the load was transferred to the webs by cross bending in the flange plate. There is also a longitudinal bending stress in the flange plate which is inversely proportional to the diaphragm spacing and the distance between the webs. This longitudinal stress will reduce the buckling strength of the flange plate appreciably. For this reason, it is essential that crane girders have rails that are strong enough to transfer the wheel load to the adjacent diaphragms and are sufficiently stiff so that the rail will not deflect enough to transfer appreciable bending stresses to the cover plate.

CONCLUSIONS

The box girder tests made in this investigation lead to the following conclusions:

1. Box girders of the proportions tested will fail at stresses as computed by the ordinary beam formula, which are about 20 per cent higher than the yield point of the material, unless local buckling first occurs.
2. For the girders tested, there was no tendency for lateral buckling to occur, even when the girders were loaded with both a vertical load and a 10 per cent lateral load applied to the top flange.
3. For welded girders with l/b ratios up to 110, and riveted girders with l/b ratios up to 80, it is not necessary to reduce the allowable compressive design stress.
4. The strain distribution of the girders was linear over the cross section of the girder up to the ultimate load.
5. There was a shift of the neutral axis towards the compression side of welded girders as the load was applied, apparently caused by welding stresses.
6. Internal weld stresses lowered the buckling strength of the model girders. These stresses may be small in full-size cranes.
7. The buckling stress of the cover plate of a crane box girder can be closely computed from the theoretical buckling formula or the curve in Figure 12, which assumes simply-supported edges for the plate.
8. The rail of a crane acts as a stiffener on the cover plate.
9. The allowable w/t ratio should be computed using the distance between the stiffeners when stiffeners are used. The stiffener must be rigid enough so that it will not buckle.
10. The alloy steel girder was somewhat stronger than the carbon steel girder because it did not yield locally as rapidly as the carbon steel girder.
11. The buckling stress of webs subjected to pure bending can be determined from the theoretical buckling formula using the K for free edges. These values, disregarding ζ are given in Figure 20. If the girder web is subjected to both compression and bending, the values in Figure 20 for the h/t ratio should be reduced.
12. The present allowable h/t ratios must be reduced if design stresses are to be increased.
13. Longitudinal web stiffeners are very effective in preventing buckling of the web. For high h/t ratios, consideration should be given to the use of such stiffeners.
14. Vertical stiffeners are of little use in preventing compression web buckling.
15. A smaller factor of safety may be permissible in computing plate thickness ratios since there is a great deal of reserve strength in the girders after the plates buckle.
16. The stress in the unloaded diaphragms of the girders in the bend tests was negligible. The stresses in the loaded diaphragms were small.
17. The diaphragms reduced the buckling deflection when the flange plates buckled in a girder. When this type of buckling occurred, a small stress was present in the diaphragm.
18. Crane girders must have rails stiff enough to transfer the wheel load to the diaphragms without causing appreciable stresses in the cover plate. Otherwise the strength of the cover plate will be reduced.